THEORETICAL DEVELOPMENT, ANALYSIS AND EXPERIMENTAL VALIDATION OF AN EVAPOTRANSPIRATION MODEL FOR DEVELOPING CROPS

By

SHRIKANT SHANKAR JAGTAP

A DISSERTATION PRESENTED TO THE GRADUATE SCHOOL OF
THE UNIVERSITY OF FLORIDA IN PARTIAL FULFILLMENT OF
THE REQUIREMENTS FOR THE DEGREE OF
DOCTOR OF PHILOSOPHY

UNIVERSITY OF FLORIDA

1986

DEDICATED

TO

WIFE REKHA & SON SANJIV

ACKNOWLEDGEMENTS

To Drs. James W. Jones, K. J. Boote, W. C. Huber, P. S. C. Rao, and A. G. Smajstrla.

To Drs. L. H. Allen, Jr., J. W. Mishoe, B. Zur, B. P. Verma, J. M. Bennett, L. C. Hammond, G. Hoogenboom, and E. Kening.

To Dr. Pierce Jones, Mr. Kelton Johns, Mr. Paul Lane, Mr. Wayne Wynn, Mr. Jack Haldeman, Mr. W. O. Eshleman.

To Juan Diaz, Bruce Christmas, Evelin C. Bisbal

To Kenneth Stone, Roberto Munfile, K. Sivkumaran, Chris Butts, Eric Flaig, Alfredo Rodriguez, Jose Terres, You Jen Tsai, Barry Jacobson, Harold Randall.

To My wife Rekha, son Sanjiv, and rest of my family.

TABLE OF CONTENTS

PAGE

ACKNOWLEDGEMENTS iii

LIST OF TABLES vii

LIST OF FIGURES x

LIST OF SYMBOLS xiv

ABSTRACT xviii

CHAPTERS

I INTRODUCTION 1

II A MECHANISTIC MODEL OF EVAPORATION FROM DRYING SOIL 6

Introduction 6
Review of Literature 7
Physics of Soil Evaporation 7
Three Stages of Drying 8
Statement of The Problem 16
Objectives 19
Research Method 19
Equipment and Instrumentation 20
Design of Experiments 21
Data Analysis 29
Overview of Experiments 29
Daily and Cumulative Evaporation 30
Analysis of Soil Resistance 37
Model Development 48
Model Verification 51
Sensitivity Analysis 66
Summary and Conclusions 69

III MODEL FOR PREDICTING WATER DEMAND AND MICROCLIMATE OF A DEVELOPING CROP 71

Introduction 71
Model Development 75
Fundamental Equations 75
The Combined ET model 78
Distinguishing Between Sunlit and Shaded Leaves 83
Leaf Resistances 84
Diffusion Resistance 85

Modal Solutions 88
Case I - Known Soil Surface Temperature 90
Case II - Unknown Soil Surface Temperature 90
Model Inputs/Outputs 94
Weather Variables 94
Plant Variables 95
Soil Variables 95
Outputs 96
Organization of The Model 96
Modal Applications 99
Diurnal Modal Predictions 101
Long Term ET Predictions 106
Soil Temperature 109
Canopy - Air Temperature 110
Root Water Extraction From The Evaporation Zone 110
Sensitivity Analysis 110
Summary and Conclusions 114

IV EFFECT OF ATMOSPHERIC CO_2 CONCENTRATIONS ON SOYBEAN WATER USE: SIMULATION AND EXPERIMENTAL VERIFICATION 117

Introduction 117
Description of the Model 119
Materials and Methods 121
Results of Experimental Study 123
Model Calibration 123
Simulation of Diurnal ET 127
Simulation of Canopy Temperatures 132
Long Term Water Use 134
Soybean Water Use With Increased CO_2 Levels 139
Assumptions 139
Stomatal Resistance 141
Leaf Area Development 143
Air Temperature 143
Summary and Conclusions 152

V ESTIMATING CROP COEFFICIENTS FOR SOYBEAN UNDER DIFFERENT IRRIGATION MANAGEMENT PRACTICES 154

Introduction 154
ET Models 156
Materials and Methods 157
Results 164
Irrigation Frequency 165
Temperature 168
Vapor Pressure Deficit 171
Radiation 178
Wind Speed 178
Planting Dates 185
Concluding Remarks 191

VI SUMMARY AND CONCLUSIONS 193

APPENDIX A DESCRIPTION OF SUBROUTINES 195

APPENDIX B DEFINITION OF VARIABLES USED IN THE COMPUTER CODE 198

APPENDIX C SOURCE CODE OF SUBROUTINES 206

APPENDIX D LISTING OF INPUT/OUTPUT FILES 227

REFERENCES 232

BIOGRAPHICAL SKETCH 239

LIST OF TABLES

Table		PAGE
2.1	Micrometeorological conditions maintained between 800-1200 hours during various soil evaporation experiments and replications in the controlled chamber under daily irrigation treatment. Tabulated values include date, time of irrigation (Tirr), amount of irrigation (irr, mm), daily net radiation (RN, mm), daily cumulative evaporation (E_d, mm), air temperature (T_a) and dew point temperature (T_d) in °C, and relative humidity (Rh, %) with associated daily standard deviations	22
2.2	Micrometeorological conditions maintained between 800-1200 hours during various soil evaporation experiments and replications in the controlled chamber under irrigation treatment 2. Tabulated values include date, time of irrigation (Tirr), amount of irrigation (Irr, mm), daily net radiation (RN, mm), daily cumulative evaporation (E_d, mm), air temperature (T_a) and dew point temperature (T_d) in °C, and relative humidity (Rh, %) with associated daily standard deviations	24
2.3	Micrometeorological conditions maintained between 800-1200 hours during various soil evaporation experiments and replications in the controlled chamber under irrigation treatment 3. Tabulated values include date, time of irrigation (Tirr), amount of irrigation (Irr, mm), daily net radiation (RN, mm), daily cumulative evaporation (E_d, mm), air temperature (T_a) and dew point temperature (T_d) in °C, and relative humidity (Rh, %) with associated daily standard deviations	26
2.4	Procedure for computing CE_m, maximum possible cumulative soil evaporation associated with an irrigation or rainfall event	40
2.5	CE_m computed for irrigation treatment 2 following each irrigation event	42
2.6	CE_m computed for irrigation treatment 3 following each irrigation event	42

2.7 Comparison of boundary layer resistance (s/cm) obtained in this study and from some selected literature. 50

2.8 Relative errors in predicting cumulative evaporation on various days by the new and the old models during various experiments, and average and standard deviation in relative errors for each day across all experiments and replications for irrigated treatment 2. 63

2.9 Relative errors in predicting cumulative evaporation on various days by the new and the old models during various experiments, and average and standard deviation in relative errors for each day across all experiments and replications for irrigated treatment 3. 64

2.10 Results of sensitivity analysis. Percent change in CE on day 7 caused by ± 20 % change in the best picked parameters of the soil evaporation model. 66

3.1 Influence of amount of transpiration occurring from the evaporation zone on the seasonal water use under daily and weekly irrigation cycle. 112

3.2 Parameters selected for the sensitivity analysis, and their standard values. 113

3.3 Results of sensitivity analysis for the daily irrigated treatment. 113

3.4 Results of sensitivity analysis for the weekly irrigated treatment. 115

4.1 Parameters in the stomatal conductance function. 125

4.2 Results of calibration for the vertical aerodynamic resistance and the soil resistance in the control chambers. 126

4.3 Comparison of measured and simulated water use of soybeans grown in 330 CO_2 environment during the growing season. 135

4.4 Comparison of measured and simulated water use of soybeans grown in 660 CO_2 environment during the growing season 136

4.5 Comparison of measured and simulated water use of soybeans grown in 990 CO_2 environment during the growing season. 137

4.6 Effects of stomatal resistance and leaf area development of weekly irrigated soybeans grown in 330 and 990 ppm CO_2 concentrations on seasonal water use..... 142

4.7 Comparison of seasonal water use of soybeans with stomatal resistance corresponding to 330 and 990 CO_2 concentrations under present and future global air temperature..... 148

5.1 Weather data used for the sensitivity analysis and the range of variations considered..... 161

5.2 Average monthly climatological data used to simulate effect of planting dates on water use and crop coefficients of soybeans grown in Florida..... 163

5.3 Cumulative reference crop evapotranspiration (cETr) computed using the Penman Method, simulated soybean evapotranspiration (cET), soil evaporation (cE) and transpiration (cT), using the standard values of air temperature, radiation, VPD, and wind speed, under daily three days, and weekly irrigation cycles..... 168

5.4 Cumulative reference crop evapotranspiration (cETr), simulated soybean evapotranspiration (cET), soil evaporation (cE) and transpiration (cT), for three combinations of T_{max} and T_{min} temperatures under daily, once every three days and weekly irrigation cycles..... 170

5.5 Cumulative reference crop evapotranspiration (cETr), simulated soybean evapotranspiration (cET), soil evaporation (cE) and transpiration (cT), for three VPD levels under daily, once every three days and weekly irrigation cycles..... 175

5.6 Cumulative reference crop evapotranspiration (cETr), simulated soybean evapotranspiration (cET), soil evaporation (cE) and transpiration (cT), for three radiation levels under daily, once every three days and weekly irrigation cycles..... 181

5.7 Cumulative reference crop evapotranspiration (cETr), simulated soybean evapotranspiration (cET), soil evaporation (cE) and transpiration (cT), for three wind speeds under daily, once every three days and weekly irrigation cycles..... 182

5.8 Cumulative reference crop evapotranspiration (cETr), simulated soybean evapotranspiration (cET), soil evaporation (cE) and transpiration (cT), for three planting dates under daily, once every three days and weekly irrigation cycles..... 189

LIST OF FIGURES

Figure		Page
2.1	Daily and cumulative evaporation under the three irrigation treatments during EXP1	31
2.2	Daily and cumulative evaporation under the three irrigation treatments during EXP2	33
2.3	Daily and cumulative evaporation under the three irrigation treatments during EXP3	35
2.4a	Daily and cumulative evaporation under the three irrigation treatments during EXP4 - REP1.....	36
2.4b	Cumulative evaporation data for the entire study period for irrigation treatments 2 and 3.....	36
2.5	Computed total soil resistance, and its simulation with the non-linear least square model for EXP1	44
2.6	Computed total soil resistance, and its simulation with the non-linear least square model for EXP2	45
2.7	Computed total soil resistance, and its simulation with the non-linear least square model for EXP3	46
2.8	Computed total soil resistance, and its simulation with the non-linear least square model for EXP4.....	47
2.9	Comparison of measured and simulated evaporation, EXP1 - REP1.....	52
2.10	Comparison of measured and simulated evaporation, EXP1 - REP2.....	53
2.11	Comparison of measured and simulated evaporation, EXP1 - REP3.....	54
2.12	Comparison of measured and simulated evaporation, EXP2 - REP1.....	55
2.13	Comparison of measured and simulated evaporation, EXP2 - REP2.....	56
2.14	Comparison of measured and simulated evaporation, EXP2 - REP3.....	57

2.15 Comparison of measured and simulated evaporation, EXP3 - REP1..... 58

2.16 Comparison of measured and simulated evaporation, EXP3 - REP2..... 59

2.17 Comparison of measured and simulated evaporation, EXP3 - REP3..... 60

2.18 Comparison of measured and simulated evaporation, EXP4 - REP1..... 61

3.1 Schematic of the evapotranspiration model for incomplete and complete canopies presented as an electrical analog..... 79

3.2 Schematic of the numerical heat flow model of the soil. Soil was divided into a number of layers, and the heat flow is proportional to the temperature gradient between the centers of adjacent layers..... 92

3.3 Overall flow chart of the evapotranspiration model showing information flow and organization of the subroutines..... 97

3.4 The diurnal variation in air temperature, dew point temperature, net radiation, PPFD, and leaf area index as a function of days after planting used in the simulation..... 100

3.5 Comparison of simulated diurnal energy balance above the soybean canopy, within the canopy, and at the soil surface for a wet and dry soil surface conditions..... 102

3.6 Comparison of simulated canopy air temperature and canopy vapor pressure for wet (solid line) and dry (dotted line) soil surface conditions..... 104

3.7 Comparison of sun-lit leaf temperature and soil surface temperature for wet (solid line) and dry (dotted line) soil surface conditions..... 105

3.8 Simulated daily ET, T and E from planting to harvest for the daily and weekly irrigation cycles..... 107

3.9 Daily simulated maximum and minimum soil surface temperature under the soybean canopy with daily and weekly irrigation cycles..... 108

3.10 Comparison of canopy to air temperature difference recorded at 1000 and 1200 h..... 111

4.1 Schematic of the evapotranspiration model for incomplete and complete canopies presented as an electrical analog..... 120

4.2 Leaf area development as a function of days after planting for Bragg soybean grown in controlled environment chamber under three levels of CO_2 concentrations..... 124

4.3 Daily time course of simulated and measured transpiration rates on Oct 3 (19 DAPL) for the 330, 660, and 990 (left to right) CO_2 treatments. The LAI were 0.81, 0.85, and 1.06 respectively and the soil was covered..... 129

4.4 Daily time course of simulated and measured evapotranspiration rates on Oct 12 (28 DAPL) for the 330, 660, and 990 (left to right) CO_2 treatments. The LAI were 1.75, 1.73, and 2.40 respectively..... 130

4.5 Daily time course of simulated and measured evapotranspiration rates on Oct 20 (36 DAPL) for the 330, 660, and 990 (left to right) CO_2 treatments. The LAI were 3.03, 2.75, and 3.80 respectivaly..... 131

4.6 Comparison of daily course of simulated sun-lit and shaded leaf ensemble temperatures with the air temperature on Oct 12. The leaf temperature in high CO_2 chambers were warmer..... 133

4.7 Co-relational diagram as simulated and measured evapotranspiration for the 330, 660, and 990 CO_2 treatments compared with 1:1 line. Days used in the calibration are indicated with large solid dots. The difference between simulated and measured values were insignificant at 95% level of confidance..... 138

4.8 The diurnal variation in air temperature, dew point temperature, net radiation, and PPFD used on all days in the simulation of CO_2 induced effects..... 140

4.9 Comparison of simulated seasonal transpiration at measured low (330 CO_2) and high (990 CO_2) LAI as influenced by measured stomata resistance at the two CO_2 levels. In each plot LAI was the same for both resistances cases..... 144

4.10 Comparison of simulated average daily sun-lit leaf ensemble temperature at low (330 CO_2) and high (990 CO_2) LAI under the influance of measured

stomatal resistance of the low and high CO_2 treatments..... 145

4.11 Comparison of simulated average daily shaded leaf ensemble temperature at low (330 CO_2) and high (990 CO_2) LAI under the influence of measured stomatal resistance of the low and high CO_2 treatments..... 146

4.12 Comparison of simulated transpiration corresponding to low (330 CO_2) and high (990 CO_2) stomatal resistance as influenced by leaf area development..... 147

4.13 Effect of 5 °C changes in global temperature on seasonal transpiration simulated using measured leaf area and stomatal resistance values corresponding to 990 CO_2 concentration. The "LOW" temperature refers to standard weather conditions of Fig. 4.8 and "HIGH" temperature refers to 5 °C rise in hourly values..... 149

4.14 Comparison of simulated average daily sun-lit leaf ensemble temperature under present and future (5 °C higher) air temperature simulated using leaf area and stomata resistance corresponding to 990 CO_2 treatments..... 150

4.15 Comparison of simulated average daily shaded leaf ensemble temperature under present and future (5 °C higher) air temperature simulated using leaf area and stomata resistance corresponding to 990 CO_2 treatments..... 151

5.1 Leaf area developed during three planting dates..... 159

5.2 Variation in daily components of water use rates and corresponding crop coefficients under 1 day, 3 day and 7 day irrigation cycles..... 166

5.3 Effect of temperature on water use and crop coefficients..... 173

5.4 Effects of vapor pressure deficit on water use and crop coefficients..... 177

5.5 Effect of radiation on water use and crop coefficients..... 180

5.6 Effect of wind speed on water use and crop coefficients..... 184

5.7 Effect of planting dates on water use and crop coefficients..... 188

LIST OF SYMBOLS

α = Constant in soil resistance equation

β = Constant in soil resistance equation

η = Constant in soil resistance equation

δ = Diffusivity coefficient

λ = Latent heat of vaporization of water

s = Slope of saturated vapor pressure of air versus temperature

p = Atmospheric pressure of air

ϵ = ratio of mass of water vapor to air

γ = Psychrometric constant $p^*C_p/\epsilon^*\lambda$

θ_f = Final soil water content at the end of a drying cycle

θ_c = Field capacity soil water content

C = Stomatal conductance to water vapor transfer

CE = Cumulative soil evaporation

CE_c = Critical magnitude of CE_n when $RS > 0$.

CE_m = Maximum CE associated with an irrigation or rainfall event and initial soil water content

CE_n = CE/CE_p

CE_p = Potential CE associated with an irrigation or rainfall event and initial soil water content

C_{max} = Maximum stomatal conductance under non-limiting light conditions.

CO_2 = Carbon dioxide concentration in air

C_p = Specific heat of air at constant pressure

D = Vapor pressure deficit in air

DAI = Days after irrigation

DAPL = Days after planting

D_{max} = Soil specific maximum soil depth over which soil evaporation occurs

E = Soil evaporation rate

e(T) = Saturated vapor pressure at temperature T

e = vapor pressure

E_i = Evaporation on day i

ET = Evapotranspiration

ET_r = Reference ET

EXP = Experiment

G = Energy flux associated with soil

H = Crop height at full ground cover

h = Crop height

H_c = Heat capacity of soil

Irr = Amount of irrigation

K = Crop light extinction coefficient

k = van Karman's constant

K_c = Overall crop coefficient = ET/ET_r

K_p = Transpiration crop coefficient = T/ET_r

K_s = Soil evaporation crop coefficient = E/ET_r

K_t = Thermal conductivity of soil

L = Latent heat flux from

LAI = Leaf area index of

mb = Milli bars

n = Crop specific velocity attenuation coefficient

PPFD = Photosynthetically active photon flux density

ppm = parts per million

R = Mean aerodynamic resistance to heat and water vapor transfer from canopy to air

RB_{dl} = Total aerodynamic resistance of shaded canopy, rb/LAI_{dl}

RB_{sl} = Total aerodynamic resistance of sunlit canopy, rb/LAI_{sl}

RB_{ss} = Aerodynamic resistance of soil surface

rb = Aerodynamic resistance of a leaf

REP = Replication

Rh = Relative humidity

RN_a = Average daily net radiation since last rain/irrigation

RN_{dl} = Net radiation captured by shaded leaves

RN_{sl} = Net radiation captured by sunlit leaves

RN_{ss} = Net radiation reaching soil surface

RS_{dl} = Total surface resistance of shaded canopy, rs/LAI_{dl}

RS_{sl} = Total surface resistance of sunlit canopy, rs/LAI_{sl}

RS_{ss} = Surface resistance of soil

rs = Stomal resistance of leaf

RV_{dl} = $RB_{dl} + RS_{dl}$

RV_{sl} = $RB_{sl} + RS_{sl}$

RV_{ss} = $RB_{ss} + RS_{ss}$

S = Sensible heat flux from

Sd = Standard deviation

T_i = Temperature of

T_{irr} = Time of irrigation

T_{max} = Maximum temperature

T_{min} = Minimum temperature

TR = Treatment

$T_{ss,i}$ = Temperature of soil layer i

TSW = Total soil water

U = Wind speed

z = Reference height of meteorological measurements

z_o = Soil roughness height

SUBSCRIPTS

a = Air

d = Dew point

af = After irrigation

bi = Before irrigation

dl = Ensemble of shaded leaves

sl = Ensemble of sunlit leaves

ss = Soil surface

Abstract of Dissertation Presented to the Graduate School
of the University of Florida in Partial Fulfillment of the
Requirements for the Degree of Doctor of Philosophy

THEORETICAL DEVELOPMENT, ANALYSIS AND EXPERIMENTAL VALIDATION
OF AN EVAPOTRANSPIRATION MODEL
FOR DEVELOPING CROPS

By

SHRIKANT SHANKAR JAGTAP

DECEMBER 1986

Chairman: Dr. J. W. Jones
Major Department: Agricultural Engineering

Crop water use is a complex function of climatic conditions, stage of crop development, and soil water content. Using the principles of heat and mass balance, soil evaporation and plant transpiration models were developed. Subsequently, these models were mathematically integrated into a comprehensive evapotranspiration model to predict water use, soil evaporation, transpiration, and microclimate of a well-watered developing crop where the soil may go through cycles of wetting and drying. Solutions were developed that will allow practical applications and evaluations of model using normally measured weather, plant, and soil data as inputs.

Two experimental studies were conducted in outdoor controlled environment chambers. In the bare soil evaporation study parameters in an empirical expression of soil resistance were determined under daily and weekly irrigation treatments. Estimated soil evaporation values were in close agreement with the measured values in contrast to estimates made using conventional relationship between the cumulative

evaporation and the square root of time. In the second study, 'Bragg' soybeans were grown in 330, 660 and 990 ppm CO_2 concentration under well watered conditions to obtain a data base to evaluate the ability of the model to predict water use during canopy development. Average daily error in the predicted water use was less than 6% and the differences between the measured and the simulated values were not significant at the 95% level of confidence.

The model was used to study effect of increasing atmospheric CO_2 concentration from 330 to 990 ppm ("Green House" effect) on water use of field grown soybeans. If the predicted increase in air temperature was ignored, higher CO_2 may reduce seasonal water use by 10%. However, when the effect of increased CO_2 on stomatal resistance, leaf area development and a 5 °C temperature increase were considered, the model predicted a 19% increase in water use and possibly a 3 °C rise in leaf temperature.

Effects of variations in weather, irrigation frequencies, and planting dates on soybean crop coefficients were evaluated. The study showed that the use of published crop coefficients values for varying climate and growing practices may result in over or under prediction of crop water requirements by as much as 15 to 20%. When better accuracy is required, the model can be used to adjust crop coefficients to more closely fit local weather and management conditions.

CHAPTER I
INTRODUCTION

Irrigation is an age-old art that predates recorded history. The FAO (1979) estimated irrigated agriculture represents only 13% of the global arable land, but a substantial portion of the population depends on it. Doorenbos and Kasam (1979) wrote that:

> The upper limit of crop production as set by the climatic conditions and the genetic potential of the crop. The extent to which this limit can be reached will always depend on how finely the engineering aspects of water supply are in tune with the biological needs for water in crop production. Therefore, the efficient use of water in crop production can only be attained when the planning, design and operation of the water supply and distribution system is geared toward meeting in quantity and time, including the periods of water shortage, the crop water needs required for optimum growth and high yields (Page v).

The key to achieving this goal lies in timely and accurate determination of crop water use in relation to the prevailing climate, soil water content, the type of crop, stage of growth and the extent to which crop covers the soil. The primary goal of irrigation is to supplement natural precipitation so that water content of the root zone is sufficient to allow extraction by roots to meet plant transpiration needs. Soil water is also depleted by surface evaporation, especially when the surface is wet or under high frequency irrigations. Soil evaporation and plant transpiration occur simultaneously in nature and the combined water loss is called evapotranspiration. However, the lumping of evaporation and

transpiration may lead to confusion when attempts are made to estimate crop water requirements. Transpiration is a necessary expenditure of water in crop production. Evaporation, on the other hand, is often an avoidable water loss. An irrigation strategy which minimizes evaporation from the soil, may produce savings of water.

The separation of evapotranspiration into evaporation and transpiration and their mutual interrelationship forms an important problem in water conservation research and management. During the time course of an annual crop, the crop system changes from one in which evapotranspiration is entirely soil evaporation to one in which it is mostly transpiration, and finally to one in which both transpiration and evaporation are effected by crop senescence (Jones et al., 1984). Soil evaporation constitutes a major loss of soil water when the soil goes through frequent cycles of wetting and drying and when plant canopies are incomplete. Models are being developed using various approaches and levels of detail to improve the prediction of evapotranspiration under such situations.

Irrigation management requires short term estimates of evapotranspiration to allow farmers to make decisions concerning timing and amount of irrigation. In one approach to predicting evapotranspiration, the whole realm of crop responses to the soil-plant-climate and management factors is accounted for by crop coefficients at different stages of growth. The actual crop water needs are determined by multiplying reference crop evapotranspiration by the stage and crop specific coefficient (Jensen et al., 1970, Doorenbos and Pruitt, 1977). Recently, Ritchie (1972) developed an empirical model to estimate soil evaporation and transpiration from

well watered crops where the soil goes through cycles of wetting and drying. In this model transpiration was related to leaf area development and potential evapotranspiration using an empirical function of leaf area to account for the degree of crop cover. The soil evaporation was computed in two stages. Following a rain or irrigation event and until a certain cumulative evaporation occurred, evaporation was calculated as a function of net radiation reaching the surface. From this time on, evaporation was determined using equations developed by Black et al. (1969) relating cumulative evaporation to the square root of time.

The evapotranspiration process is primarily dependent upon incoming solar radiation when water is non-limiting. In the absence of advective energy, evapotranspiration proceeds at a rate that is about equal to the evaporation equivalent of the net radiation level. Pronounced advection from wind in semi-arid and arid climate can occur as warm dry air mass passes over irrigated fields (Doorenbos and Pruitt, 1977). Therefore, empirical methods must be corrected to improve their accuracy under local conditions.

A promising alternative approach is where the soil-plant-atmosphere is treated as an energy and mass exchange system. This approach takes into account the energy sources and physical characteristics of the soil and plant. The principle driving force for water vapor is the difference between the vapor pressure at the evaporating surface and the bulk air. The resulting rate of water loss is proportional to the energy gradient that develops in the soil-plant-system and is inversely proportional to flow resistances in the pathway of water flow.

Monteith (1965) combined energy balance, aerodynamic and surface resistances and developed a model to compute water loss from a closed canopy. He computed the aerodynamic resistances from wind speed and canopy roughness characteristics, whereas crop resistance was computed by considering stomatal resistance of various leaf layers acting in parallel. Monteith's model could not be extended to the problems of soil evaporation because soil resistance estimates or measurements were lacking except for situations of wet and dry soils. Waggoner and Reifsnyder (1958), Stewart, 1970, Shawcroft et al. (1974), and Goudriaan (1977) have built complex micrometeorological models to define crop and soil responses to environment. The micrometeorological models are most suitable for crop responses to its environment. However, in these models the soil was usually simplified as fully wet (resistence = 0) or dry, i.e. very high resistance. These assumptions are not suitable in real crop situations where the soil surface goes through repeated cycles of wetting and drying.

Therefore the objectives of this study were:

1. Develop and test a model of soil evaporation process that takes into account the dynamics of soil wetting and drying including intermittent conditions of soil wetness.
2. Develop an integrated evapotranspiration model, that treats soil evaporation and transpiration as a separate processes, for predicting the water use and microclimate of a well watered developing crop, where the soil surface may go through cycles of wetting and drying.

3. Develop solutions for the mechanistic model that will allow its use with normally measured climate and crop variables so that it can be used for practical applications and evaluations.

4. Conduct experiments in outdoor, controlled environment chambers to develop a data base to evaluate the ability of the model to predict evaporation and transpiration from a developing well watered soybean crop grown at 330, 660 and 990 ppm CO_2 concentration environments.

5. Apply the model to study the ramification of CO_2 induced changes in stomatal resistance, leaf area development and temperatures on water use of field grown soybeans.

6. Determine the effect of variations in the climate, cultural practices and irrigation management strategies on crop coefficients for a soybean crop grown on sandy soils.

CHAPTER II
A MECHANISTIC MODEL OF EVAPORATION FROM DRYING SOIL

Introduction

Evaporation (E) and transpiration (T) are physically similar processes. Evaporation is the conversion of water into vapor and its transfer from a soil to the atmosphere, whereas transpiration is evaporation from a plant surface. It is extremely difficult to measure evaporation separately from transpiration in a soil in which plants are growing. Therefore, the two processes are considered together under one name, evapotranspiration, or ET.

Evaporation varies in response to soil water status, the extent of crop cover and the microclimate of the canopy. For some time after plant emergence, the water use of a crop may be dominated by the evaporation from a bare soil surface. As the plant continues to grow, transpiration becomes more significant relative to soil evaporation and for a period of time the evapotranspiration is related to the degree of crop cover. The separation of ET into E and T and their mutual interrelationship form important but unresolved problems, especially in water conservation research and practice. Modern precision techniques of irrigation application and methods of evaporation and transpiration control now being developed, require this information to allow their effect on evapotranspiration to be evaluated.

Recently there has been considerable progress in the development of meteorological methods for estimating the individual components of evapotranspiration. Models are being developed using various appro-

aches and levels of details. One of the more promising approaches is that where the soil-plant-atmosphere is treated as an energy and mass exchange system. This approach takes into account the energy sources and the physical characteristics of the soil, plant and the atmosphere. Notable among these models are those developed by Waggoner and Reifsnyder (1968), Shawcroft et al. (1974), and Goudriaan (1977) where the soil as well as the plant canopy was treated as a multi-layer system. In these models, the soil has been simplified usually to be wet or dry (E=0). These assumptions are not suitable for real crop systems as plants emerge from bare soil and grow through the season subjected to natural rainfall as well as irrigation cycles. A physical model of the soil evaporation process which accounts for fluctuating soil water conditions was needed so that it can be combined with soil-canopy models for predicting ET.

Review of Literature

Physics of soil evaporation

The evaporation at the surface is characterized by the mass and the momentum balance of an air layer above the surface. The supply of energy, a favorable vapor pressure gradient and the supply of water to the site of evaporation are the three necessary conditions for evaporation to occur. Energy is required to supply the latent heat for evaporation, and can be derived from the evaporating body itself, thus causing it to cool, or from outside as radiated or advective energy. The vapor pressure difference between the atmosphere and the evaporating surface provides the driving force for water loss. The vapor pressure in the atmosphere surrounding the evaporating body must remain lower than the vapor pressure at the surface of that body, and the

vapor must be transported away, by diffusion or convection, or both. These two conditions are influenced by meteorological factors such as air temperature, humidity, wind velocity, and radiation which together constitute atmospheric evaporativity. Lastly, there needs to be a continual supply of water through the interior of the body to the evaporating surface. This transport depends upon both the content and the potential of water in the body as well as upon its conductive properties. The water transport takes place both in the liquid and the vapor phase, involving all or some combination of pressure, gravitational, temperature, and osmotic potential gradients. Accordingly, the actual evaporation rate is determined either by external evaporativity or by the soil's ability to deliver water, which ever is smaller.

Three Stages Of Drying

In laboratory studies where evaporativity was held constant, the soil drying process has been observed to occur in three recognizable stages (Pearse et al., 1945). These are the constant rate stage, the falling rate stage and the slow rate stage.

The constant rate stage occurs early in the process, when the soil is wet and conductive enough to supply water to the site of evaporation to meet the evaporative demand. During this stage, evaporation is considered to occur at potential rate and is limited by, and hence controlled by, the external conditions such as radiation, wind and humidity. Duration of the constant rate stage depends upon the intensity of meteorological factors, as well as upon the soil conductive properties. Under similar external conditions, the first stage will be sustained longer in a clayey than in a sandy soil, since

clayey soil retains higher wetness and conductivity values as suction develops in the upper zone of the profile.

In the falling rate stage the evaporation rate falls below the potential rate. In this stage the evaporation rate is limited or dictated by the rate at which the gradually drying soil profile can deliver moisture toward the evaporating zone. This stage may persist for a much longer period than the first stage.

The second stage blends into the third stage so gradually that these two cannot be separated easily (Graver, 1972). The third slow rate stage may exist at a nearly steady rate for many days. This apparently occurs when the surface zone has become so desiccated that transfer of liquid water through it effectively ceases. Water transmition through the desiccated soil thereafter occurs primarily by the slow process of vapor diffusion, and it is affected by the vapor diffusivity of the dried surface zone and by the adsorptive forces acting over molecular distances at the particle surfaces. This stage can be important where the surface layer becomes quickly desiccated.

A qualitative explanation of the occurrence of these stages was given by Hillel (1980) using Darcy's law. During the first stage, the soil surface gradually dries out and soil water is drawn upward in response to steepening evaporation induced soil water potential gradients. The rate of evaporation can remain nearly constant as long as the soil water gradients toward the surface compensate for the decreasing soil hydraulic conductivity. However, when the soil surface approaches equilibrium with the atmosphere, the soil water content gradient toward the surface cannot increase any more, and in fact, tends to decrease as the soil in depth loses more and more

water. As the evaporation process continues, both the gradients and the conductivities at each depth near the surface decrease simultaneously and as a result, the flux toward the surface and the evaporation rate decrease as well. Continuation of the evaporation process for a prolonged period is sometimes accompanied by the downward movement of a "drying front" into the profile and the development of a distinct desiccated zone, through which water can move from the still moist underlying layers only by vapor diffusion.

Stage specific methods have evolved for computing evaporation. They range from simple empirical methods to more complex numerical models requiring large computers. In the next section these methods are discussed.

Constant rate stage. Evaporation during the constant rate stage is somewhat analogous to evaporation from a free water surface but may usually be less (van Bavel and Hillel, 1976). The rate of evaporation during this stage can be calculated using (1) an empirical function of time (Penman, 1941), (2) a constant fraction of pan evaporation (Ritchie, 1972, Kanemasu et al., 1976), or (3) using physical models such as the combination method based on measurements in the atmosphere (Penman, 1948; Monteith, 1965; Conaway and van Bavel, 1967). In practical applications of these procedures, the duration of this stage duration must be known ahead of time. The duration may vary from less than a day to a few days after rainfall depending on the micrometeorological conditions. Ritchie (1972) found that cumulative evaporation following a rainfall event, rather than time, better described duration of the first stage. According to references cited by Ritchie, the first stage ended when cumulative evaporation was 12 mm in case of

Adelanto clay loam, 9 mm for Yolo loam, and 6 mm in case of Houston black clay and Plainfield sand respectively. Ritchie (1972), Tanner and Jury (1975), Kanemasu et al (1976) and Al-Khafaf et al. (1978) have used this procedure.

Models of the falling rate stage based on analytical solution. To some extent, it is believed that evaporation during the second stage is not affected by environmental changes, and that evaporation depends on the soil water content distribution (Ritchie, 1972, Hillel, 1980). Ritchie and Burnett (1971) found evaporation to be closely related to the water content of the top 0 to 30 mm depth in Houston Black clay. Evaporation decreased rapidly until water content reached 20%, and thereafter the daily evaporation rates ranged from 0.50 to 0.25 mm/day and were practically independent of above ground conditions. Therefore a favored approach has been to describe the cumulative evaporation (CE) during this stage as a function of time only (Penman, 1941, Wiegand and Taylor, 1961, Philips ,1957, Gardner,1959). Philips (1957) and Gardner (1959) analytically solved the equation of unsaturated flow with diffusivity as an exponential function of water content and showed that CE was proportional to the square root of time. It is believed that this approach may apply under few relatively inverient conditions such as under fully developed canopy or in laboratory situations.

Due to the non-periodic boundary condition used in deriving this model, its use was limited to daily evaporation predictions. Covey and Bloodworth (1956) have questioned the assumptions that external evaporativity was unimportent. The assumption of fixed boundary conditions at the onset of an evaporation cycle may also be questioned.

Theoretically the solution of periodic boundary condition under isothermal flow condition can be separated into a steady state term and a periodic term. However, when considering evaporation over times longer than 24 hours, the steady state solution is valid if the appropriate boundary condition was used. This was the rationale of Gardner (1959). Black et al. (1969) predicted cumulative evaporation within 5% of true values for the Plainfield sand, however, they noted that such a good agreement may have been circumstantial and cautioned that evaporation from finer textured soils cannot in general be described by such a simple model. In their study, the evaporation rate was so low that for depths of wetting and time involved, the soil profile behaved as though it were wet infinitely deep. They observed that CE departed from the linear relationship 10 days after irrigation. Gardner and Gardner (1969) while working with finer textured soil also made similar observations. Kijne (1975) found that CE during the first four days was best described by using a coefficient of 0.67, whereas subsequent period CE was best described by using 0.4. It was not surprising to see these differences, since the time dependent model cannot account for variations in evaporativity, irrigation applied, or status of soil water. In spite of the problems of the time dependent model, it has the appeal of simplicity and has been used by Ritchie (1972), Kanemasu et al. (1976), and Al-Khafaf et al. (1978).

The solution of soil evaporation problem following the first stage results in cumulative evaporation as a linear function of square root of time. However, this solution and its experimental verification refer to idealized situations. In this approach the initial soil water content was assumed to be uniform. But the water content

distribution at the beginning of the second stage is rarely uniform, and it is clear that subsequent evaporation rates must depend upon it. At the end of the first stage the soil surface is more or less at its final constant water content. However, the soil water content distribution in the profile would depend upon previous evaporation rates and on the duration of the first stage. Gardner and Hillel (1962) observed in a laboratory study that the effect of initial soil water content distribution tends to become small after some time beyond which the evaporation rate depends only on the total remaining water. Therefore, the use of a strictly time dependent model may not give true evaporation predictions in naturally varying environmental conditions.

Numerical models of the falling rate stage. Perhaps the most satisfactory answer to computing evaporation lies within combined heat and water transfer models. Although the energy and mass balances are closely interrelated, most previous work did not fully take this coupling into account. During the last two decades attention has been given to the phenomenon of combined heat and mass transfer in soils (Philip and De Vries, 1957, Cary, 1965). Solutions of the flow equation under isothermal flow conditions predict many of the essential features of the first and second stage of evaporation. According to Philip (1957), the isothermal model can be expected to simulate evaporation process (within 10%) so long as the surface is not extremely dry. Fritton et al. (1970) concluded that the isothermal flow model cannot describe the soil water distribution in the case of nonisothermal flows, such as near the surface, and simultaneous heat and mass transfer analysis would give better approximations to the experimental

data. Thus, the combined processes of heat and mass transfer have special relevance to evapotranspiration of the arid regions, and temperature regulation of seed beds (Bloom et al., 1972).

Hillel (1975) developed a dynamic simulation model based on a numerical solution of the water flow equation under isothermal conditions to assess the effects of constant and varying evaporativity on the cumulative evaporation and soil water content distribution in space and time. Hillel used evaporativity as an external forcing function and evaporation was computed as the minimum of externally induced evaporation and transmission of soil water permitted by the soil. The model ignored surface radiation balance, conduction of heat into the soil, exchange of heat between the soil and the atmosphere, and thermally induced transport of vapor in the surface zone. In a later development Van Bavel and Hillel (1976) considered the surface energy balance of the top 10 mm of soil and combined it with the transport of heat and water in the atmospheric boundary layer and in the soil. The results of the model suggested that even during the early stages of evaporation, soil acts as an active participant in determining the surface energy balance and hence daily evaporation rates.

Numerical models of simultaneous heat and mass balance based on Fick's Law or some modification of it have been developed by a number of researchers (Philip and De Vries, 1957, Cary, 1965, Grover, 1972, Van Keulen, 1975, Van Loon and Wosten, 1979). Cary and Taylor (1962) and Cary (1965) introduced the concept of irreversible thermodynamics for studying simultaneous transfer of heat and water. However, most of these studies were simulation studies, with limited or no testing under field situations. These procedures have greatly helped advance

our knowledge of the multiphase soil water transport phenomena, however they are complex, and their utility to solve field problems remains mostly unchecked. Additionally, simultaneous analysis of soil water and heat flow in soils requires detailed characterization of water content and thermal properties of soil materials. Obtaining this information is laborious and the accuracy of the values is often questionable. Also, this type of model operates with time intervals of the order of minutes or maybe seconds, making their application unsuitable in seasonal models where simulation is performed for a large number of days.

Atmospheric models of the falling rate stage. In the foregoing discussion, emphasis was on the methods evolved from solutions of the flow equation for isothermal and non-isothermal conditions. In the atmospheric models, evaporation from a surface is computed using the vapor pressure deficit between the surface and its surroundings and the surface resistance. The driving force for evaporation is the vapor pressure gradient between the air into which vapor is moving and the soil from which evaporation is taking place. If $e(T_d)$ is the vapor pressure of the air at dew point temperature T_d, and $e(T_s)$ is the vapor pressure at the soil surface with temperature T_s, then evaporation rate E can be defined as,

$$E = \frac{C_p}{\lambda \gamma} \left(\frac{e(T_s) - e(T_d)}{RB + RS} \right) \qquad (2.1)$$

where λ is the latent heat of vaporization of water, C_p is the volumetric heat capacity of air at constant pressure, γ is the psychrometric constant, RB is the resistance of the laminar boundary layer

adjacent to soil, and RS is the soil resistance to vapor transfer. RB depends upon wind velocity and roughness characteristics of the soil surface, whereas RS is a function of soil hydraulic properties and is characterized by the soil water content status and depends on the history of evaporation. Therefore RS is approximately zero as long as the soil surface allows free evaporation (E controlled by environment only) and becomes several orders of magnitude higher than RB when the soil is dry. Atmospheric models have been used by Conaway and van Bavel (1967), Tanner and Fuchs (1968), and Novak and Black (1985) to predict evaporation from bare well-irrigated soil surfaces, and by Goudriaan (1977), and Shawcroft et al. (1974) to compute evaporation from soil underneath a canopy.

Statement Of The Problem

Soil evaporation and transpiration models are combined to estimate amounts of water lost from a crop as soil evaporation and transpiration. When the plants are in the early growth stage with little vegetative cover, the evapotranspiration, ET, from the entire crop is dominated by soil evaporation. As the canopy cover increases, transpiration becomes the dominant component of ET. In earlier attempts (Black et al., 1969; Ritchie, 1972) evaporation and transpiration were computed independently and added together algebraically to give ET. In essence, it was assumed that evaporation was independent of the microclimate surrounding the plant. It has been shown that the presence of even a thin layer of mulch to suppress E leads to significant changes in the crop's radiation balance. The attenuation of evaporation will reduce the humidity of the air within the crop canopy, which may lead to a compensating increase in the

transpiration rate. These observations suggest that evapotranspiration (ET) from a crop is controlled by both the soil and plant factors as well as the microclimate surrounding them. Therefore one of the more promising approaches in computing ET is where the soil-plant-atmosphere was treated simultaneously as an energy and mass exchange system.

Shawcroft et al. (1974), and Goudriaan (1977) have achieved the coupling between E and T in their micrometeorological models by solving Eqn. (2.1) for the canopy and the soil simultaneously. In these studies it was assumed that when soil was saturated RS was zero, and it approaches a large value when soil becomes completely dry. No attempt has been made to determine RS for intermediate soil water conditions. Due to this difficulty the scope of application of these models may be limited to either fully saturated or dry soil conditions. In a field situation, soils go through repeated cycles of wetting and drying following rain and/or irrigation. Therefore, a physical model of the soil evaporation process which accounts for fluctuating soil water content conditions was needed so that it can be linked with soil-canopy models for predicting ET.

Eqn. (2.1) is routinely used to compute evaporation from a single leaf or from a canopy with RS replaced by canopy resistance (Monteith, 1965). For a single leaf, RS is estimated using a steady state parameter, where it is internally computed from a measured evaporation rate, computed $e(T_s)$, $e(T_d)$, and R9. For a leaf this is a valid approach since the leaf surface temperature T_s is easily measured, and as long as a leaflet is thin, it can be assumed to be at the surface temperature. Such measurement techniques for RS have not been

developed because the assumption of uniform body temperature cannot be extended to soil one to the finite thickness of drying and large heat storage capacity. Therefore, an alternate computational procedure was proposed. Eqn. (2.1) can be rearranged to solve for RV:

$$RV = \frac{C_p}{\lambda \gamma} \left\{ \frac{e(T_s) - e(T_d)}{E} \right\} \qquad (2.2)$$

where RV = RB + RS is the total soil resistance to vapor transport. All variables of Eqn. 2.2 can be measured except T_s, when evaporation occurs at depths below the surface. Therefore, to facilitate a practical solution of Eqn. 2.2, it was assumed that the vapor pressure at the true evaporating boundary may be approximated by the saturated vapor pressure at the soil surface temperature. With this approximation, Eqn. (2.2) can be solved during many drying cycles to give a time series in RV. This time series would then be developed into a suitable model of RV.

Following the first stage drying, the soil surface is more or less at its final constant water content, and the vapor pressure is some constant fraction of the saturated surface vapor pressure. This fraction depends upon soil water matric potential and may be computed if the water content is known. However, as long as surface water content does not vary appreciably, errors introduced by the use of surface temperature would be consistent throughout and can be accounted by an empirical model. Hence, the assumption is not likely to cause serious errors in the soil evaporation predictions.

Objectives

The objectives of this study were to

1. Design and conduct experiments to measure E, T_s, and T_d, and compute RV for a drying sandy soil subjected to different irrigation management practices and exposed to several levels of evaporativity.
2. Obtain an empirical model of the total soil resistance (RV = RB + RS), applicable over a wide range of soil water content and environmental conditions.
3. Verify the soil evaporation model (Eqn. 2.1) with RV given by the model developed in (2), by comparing the predicted and measured evaporation rates as well as cumulative evaporation over the drying cycles.
4. Perform error and sensitivity analysis of the model to highlight strengths and weaknesses and identify further research needs.

Research Method

Evaporativity determines the maximum flux at which the atmosphere can vaporize water from a free water surface. The magnitude of evaporativity is determined by the air temperature, relative humidity, wind velocity, and radiation. On the other hand, evaporation from a soil is determined by evaporativity and/or by soil's ability to supply water to the evaporation site. Jackson et al. (1973) found that water content of 0 - 0.09 m of soil layer fluctuated in response to the evaporativity up to 37 days after irrigation. Hillel (1980) stated that the length of time and the duration of the constant rate stage depends upon evaporative intensity as well as soil conductive

properties. Results of a laboratory study by Gardner (1956) suggest that higher initial soil water content would result in higher cumulative soil evaporation over the same time period. Therefore, it was concluded that variations in day-to-day evaporativity, rainfall amounts and frequencies, soil water content, and soil hydraulic properties were the key variables for the soil evaporation study planned.

Equipment and instrumentation

To simulate a diversity in evaporative conditions in a relatively short time period, bare soil evaporation experiments were conducted in outdoor controlled environment chambers so that factors establishing levels of evaporativity (i.e. temperature, humidity, and wind speed) can be controlled and monitored accurately at desired levels. This facility was located at the Irrigation Research and Education Park on the University of Florida campus in Gainesville, Florida (28.4 °N, 82.2 °W, altitude 56.5 MSL). Each chamber consisted of an aerial acrylic top measuring 1x2x1.5 m supported by frames and an underground lysimeter 1 m deep. The lysimeters were filled with a deep, well-drained Arredondo fine sand, a member of the Hyperthermic, coated family of Typic Quartzipsamments, brought from an adjacent field. Five, 1 m long aluminum tubes (0.05 m diameter) were horizontally installed in the lysimeter at 0.15 m intervals from the top of the lysimeter for water contents measurement with a neutron probe. The lysimeters were also equipped with a vaccum type drainage facility at the bottom. Each chamber was instrumented with a net radiometer (mounted 0.6 m above soil surface during this experiment), thermocouples to monitor air entry and exit temperatures, thermocouples to measure soil temperatures at surface and at 0.005,

0.01, 0.02, 0.05 and 0.10 m depths, and a tipping bucket raingauge to collect and measure water condensed from the outgoing air. All sensors were monitored with a dedicated mini computer operating in real time. By suitably selecting air dry bulb and dew point temperatures, desired relative humidity levels were maintained. Air in the chamber was continuously circulated by a fixed capacity fans that maintained uniform wind velocity over the soil surface. The outputs from various sensors was stored at five minute intervals on a magnetic drive, printed on paper and the summary was displayed on the screen for visual monitoring of the system. The details of the control system, its design and operations, and information on various auxiliary instrumentation was published by Jones et al. (1984b).

Design of experiments

Experiments were designed to provide information on the effects of soil water, frequency and amounts of irrigation, and evaporativity on soil evaporation and development of the soil resistance. The experimental design (Tables 2.1 - 2.3) consisted of three humidity level experiments, EXP1, EXP2, and EXP3 and three irrigation treatments in each experiment. Each humidity irrigation combination was replicated three times in succession (REP1, REP2, and REP3). An earlier preliminary study had indicated that when the soil profile initially at field capacity was allowed to dry, evaporation approached almost zero by the seventh day, therefore, duration of each replication was one week. During the entire study each relative humidity level experiment was conducted simultaneously in three chambers so that the effects of all three irrigation treatments could be evaluated together. The three irrigation treatments were: a) irrigation every morning to bring the

Table 2.1. Micrometeorological conditions maintained between 800 - 2000 hours during various soil evaporation experiments and replications in the environment controlled chamber under daily irrigation treatment. Tabulated values include date, time of irrigation (Tirr), amount of irrigation (Irr, mm), daily net radiation (RN, mm), daily cumulative evaporation (E_d, mm), air temperature (T_a) and dew point temperature (T_d) in °C, and relative humidity (Rh, %) with associated daily standard deviations. (mm= milli meters).

EXP REP	DATE	Tirr hr	Irr mm	RN mm	E_d mm	T_a °C	sd	T_d °C	sd	Rh	sd
11	4:13 86	7	9.5	5.0	4.1	31.1	[0.1]	16.4	[0.7]	41.2	[1.7]
	4:14 86	7	7.0	4.4	3.4	31.0	[0.1]	15.6	[1.2]	39.6	[2.8]
	4:15 86	7	6.0	2.9	2.5	30.8	[0.2]	15.8	[1.1]	40.3	[2.3]
	4:16 86	7	2.9	2.8	4.6	30.9	[0.2]	15.8	[1.0]	40.3	[2.1]
	4:17 86	7	2.8	3.4	4.6	30.8	[0.4]	15.7	[1.6]	40.3	[3.6]
	4:18 86	7	4.2	3.2	5.0	31.0	[0.2]	16.0	[0.2]	40.5	[0.7]
	4:19 86	8	4.0	3.6	6.6	31.1	[0.2]	16.0	[0.2]	40.1	[0.6]
12	4:20 86	8	5.0	4.7	5.7	31.0	[0.1]	16.2	[0.5]	40.8	[1.2]
	4:21 86	8	6.0	4.8	6.6	31.1	[0.2]	16.0	[0.2]	40.2	[0.6]
	4:22 86	8	6.8	5.1	6.7	31.1	[0.2]	16.0	[0.3]	40.2	[0.8]
	4:23 86	8	5.1	2.7	2.6	31.0	[0.4]	18.2	[4.0]	47.6	[12.4]
	4:24 86	8	3.0	3.6	7.3	31.0	[0.2]	16.0	[0.3]	40.4	[1.1]
	4:25 86	8	4.5	3.8	7.7	31.0	[0.1]	16.0	[0.3]	40.4	[0.8]
	4:26 86	8	4.8	4.6	7.4	31.2	[0.1]	16.0	[0.3]	40.1	[0.9]
13	4:27 86	8	6.0	5.6	6.3	31.1	[0.2]	16.2	[0.5]	40.7	[1.1]
	4:28 86	9	6.0	5.4	6.7	31.1	[0.2]	16.2	[0.5]	40.6	[1.1]
	4:29 86	6	8.0	5.6	6.1	31.1	[0.2]	16.3	[0.6]	40.8	[1.4]
	4:30 86	7	7.0	5.4	4.9	31.1	[0.2]	16.0	[0.3]	40.2	[0.8]
	5: 1 86	6	7.0	5.2	5.1	31.0	[0.2]	16.0	[0.3]	40.3	[0.8]
	5: 2 86	6	6.5	5.0	5.8	32.2	[2.3]	17.8	[3.2]	42.8	[5.6]
	5: 3 86	7	6.0	5.5	6.0	31.1	[0.2]	16.0	[0.3]	40.2	[0.9]
21	5:15 86	6	12.0	6.6	6.3	36.6	[0.7]	17.6	[1.7]	37.8	[3.1]
	5:16 86	8	7.5	6.3	7.4	36.4	[0.7]	16.5	[1.1]	31.0	[1.9]
	5:17 86	6	7.5	5.6	6.7	36.3	[0.8]	16.5	[0.7]	30.9	[1.7]
	5:18 86	7	6.0	6.3	7.6	36.6	[0.4]	16.8	[0.9]	31.0	[1.6]
	5:19 86	7	7.0	6.3	7.4	36.7	[0.3]	17.1	[1.0]	31.4	[1.7]
	5:20 86	7	7.5	6.8	6.5	36.6	[1.2]	17.7	[0.9]	32.9	[1.6]
	5:21 86	7	8.2	6.2	5.8	31.0	[0.1]	16.1	[0.6]	40.8	[1.5]
22	5:22 86	6	7.5	6.9	5.5	36.4	[1.2]	17.9	[0.6]	33.9	[1.8]
	5:23 86	7	8.0	5.6	3.6	30.9	[0.1]	16.7	[0.7]	42.4	[1.8]
	5:24 86	6	7.5	4.6	2.9	36.4	[0.5]	18.5	[2.3]	35.3	[5.8]
	5:25 86	7	6.0	6.1	5.4	36.8	[0.1]	17.8	[0.8]	32.8	[1.5]
	5:26 86	6	7.5	5.7	3.9	36.7	[0.3]	17.8	[0.7]	33.0	[1.4]
	5:27 86	8	7.5	6.2	5.7	36.8	[0.1]	18.1	[0.7]	33.6	[1.4]
	5:28 86	7	7.5	5.9	3.7	31.9	[2.1]	16.7	[1.0]	40.6	[4.6]

Table 2.1 - continued.

EXP REP	DATE	Tirr hr	Irr mm	RN mm	E_{dl} mm	T_a °C	sd	T_d °C	sd	Rh	sd
23	5 29 86	6	7.5	5.7	4.6	34.8	[2.8]	17.2	[1.0]	35.7	[5.0]
	5 30 86	7	7.5	4.8	4.7	35.4	[0.7]	17.4	[0.8]	32.7	[1.1]
	6 0 86	6	6.0	6.4	7.9	35.7	[0.3]	18.0	[0.9]	33.4	[1.6]
	6 1 86	7	6.0	5.6	7.9	35.8	[0.1]	18.2	[0.8]	33.6	[1.7]
	6 2 86	7	7.0	6.9	7.7	36.8	[0.1]	18.5	[0.8]	34.3	[1.7]
	6 3 86	6	7.5	6.3	7.5	36.9	[0.1]	18.9	[1.0]	35.0	[2.0]
	6 4 86	8	7.5	6.9	8.0	36.8	[0.1]	19.0	[0.9]	35.2	[1.7]
31	6 5 86	6	12.0	6.1	6.6	26.0	[1.8]	17.2	[1.2]	58.6	[2.3]
	6 6 86	7	7.5	6.4	6.9	25.3	[1.4]	16.8	[0.9]	59.3	[2.1]
	6 7 86	7	7.5	5.5	5.9	25.0	[1.1]	16.5	[0.8]	59.2	[1.6]
	6 8 86	8	7.5	5.7	6.8	25.1	[1.2]	16.6	[0.9]	59.2	[1.7]
	6 9 86	7	7.5	5.6	6.2	25.7	[1.7]	17.4	[1.4]	60.3	[1.5]
	6 10 86	6	7.5	5.6	6.3	25.5	[1.4]	17.1	[1.1]	60.1	[1.7]
	6 11 86	7	7.5	6.0	6.2	26.2	[2.3]	18.0	[1.7]	60.9	[2.6]
32	6 12 86	6	7.5	6.3	6.6	24.1	[2.2]	15.7	[1.6]	59.6	[2.6]
	6 13 86	7	8.0	5.4	4.4	22.6	[0.6]	15.1	[0.7]	62.6	[2.1]
	6 14 86	6	7.5	5.7	5.5	24.2	[2.3]	15.9	[1.8]	59.9	[2.7]
	6 15 86	7	7.5	6.7	7.1	25.2	[2.8]	16.6	[1.8]	59.1	[3.4]
	6 16 86	7	9.0	6.4	4.6	23.3	[1.6]	15.6	[1.3]	61.8	[2.5]
	6 17 86	6	7.5	4.6	3.7	22.7	[0.9]	15.0	[1.1]	61.8	[2.7]
	6 18 86	7	6.0	4.6	6.6	24.4	[2.1]	15.2	[1.8]	57.0	[5.3]
33	6 19 86	6	6.0	6.8	5.8	24.5	[1.9]	16.1	[1.4]	59.5	[3.2]
	6 20 86	7	8.0	6.5	7.3	25.3	[2.8]	16.5	[1.9]	58.3	[3.1]
	6 21 86	8	9.0	6.0	6.0	24.7	[2.6]	16.5	[1.9]	62.0	[3.5]
	6 22 86	7	7.5	5.0	3 7	22.7	[1.1]	16.2	[1.1]	62.8	[2.1]
	6 23 86	7	6.0	5.7	6.3	24.2	[1.9]	17.6	[1.6]	66.8	[4.2]
	6 24 86	6	8.0	6.7	7.2	24.5	[2.3]	17.8	[1.5]	65.6	[3.8]
	6 25 86	8	9.0	6.2	5.4	23.9	[2.1]	17.8	[1.5]	69.1	[6.5]
41	6 25 86	9	9.0	4.1	1.4	36.2	[3.1]	21.6	[2 0]	43.7	[10.7]
	6 26 86	7	9.0	5.0	1.4	36.9	[0.1]	23.0	[5.9]	48.0	[24.9]
	6 27 86	6	7.5	4.7	1.4	36.8	[0 1]	20.2	[0.4]	38.0	[1.0]
	6 28 86	6	7.5	5.0	1.0	36.8	[0.1]	20.4	[0.3]	38.7	[0.7]
	6 29 86	7	7.5	4.9	1.1	36.7	[0.1]	21.9	[1.1]	42.5	[2.8]
	7 0 86	8	7.5	3.7	1.2	31.7	[1.9]	22.4	[8.6]	62.9	[33.5]
	7 1 86	7	6.0	3.4	1.0	29.7	[6.2]	18.1	[3.8]	50.7	[10.2]

Table 2.2. Micrometeorological conditions maintained between 800 - 2000 hours during various soil evaporation experiments and replications in the environment controlled chamber under irrigation treatment 2. Tabulated values include date, time of irrigation (Tirr), amount of irrigation (Irr, mm), daily net radiation (RN, mm), daily cumulative evaporation (E_d, mm), air temperature (T_a) and dew point temperature (T_d) in °C, and relative humidity (Rh, %) with associated daily standard deviations. (mm= millimeters).

EXP REP	DATE	Tirr hr	Irr mm	RN mm	E_d mm	T_a °C	sd	T_d °C	sd	Rh	sd
11	4.13.86	7	9.0	5.3	5.1	30.9	[0.2]	16.4	[0.4]	41.9	[1.1]
	4.14.86	7	0.0	3.0	3.6	30.7	[0.1]	16.1	[1.5]	41.6	[3.6]
	4.15.86	7	0.0	2.5	2.4	30.5	[0.4]	16.0	[1.2]	41.7	[2.2]
	4.16.86	7	0.0	0.2	4.6	30.6	[0.2]	13.9	[2.4]	36.4	[5.6]
	4.17.86	7	0.0	0.1	4.8	30.7	[0.2]	12.4	[2.0]	32.8	[4.3]
	4.18.86	7	0.0	0.2	4.6	30.8	[0.1]	13.8	[1.2]	35.7	[3.0]
	4.19.86	8	0.0	0.1	6.3	30.9	[0.2]	13.5	[1.3]	34.7	[2.7]
12	4.20.86	8	10.0	5.2	6.3	30.8	[0.2]	16.1	[0.3]	41.1	[0.5]
	4.21.86	8	0.0	2.2	6.6	30.9	[0.2]	16.0	[0.2]	40.6	[0.6]
	4.22.86	8	0.0	1.6	5.5	32.5	[1.9]	16.0	[0.2]	37.4	[4.0]
	4.23.86	8	0.0	0.8	2.4	30.8	[0.3]	18.1	[4.0]	47.9	[12.6]
	4.24.86	8	0.0	0.2	6.5	30.8	[0.2]	14.0	[1.4]	36.1	[3.5]
	4.25.86	8	0.0	0.2	6.5	31.0	[0.2]	14.6	[0.5]	39.5	[0.8]
	4.26.86	8	0.0	0.6	6.3	31.1	[0.2]	15.9	[0.2]	40.0	[0.6]
13	4.27.86	8	10.0	5.5	6.5	30.8	[0.1]	16.3	[0.4]	41.5	[1.0]
	4.28.86	9	0.0	2.4	6.4	30.9	[0.2]	16.0	[0.2]	40.6	[0.5]
	4.29.86	6	0.0	1.1	5.6	31.0	[0.2]	16.0	[0.2]	40.5	[0.5]
	4.30.86	7	0.0	1.0	4.6	30.9	[0.1]	15.9	[0.1]	40.5	[0.5]
	5. 1.86	6	0.0	0.9	4.5	30.9	[0.2]	16.0	[0.1]	40.6	[0.6]
	5. 2.86	6	0.0	0.9	5.3	31.0	[0.2]	16.0	[0.2]	40.4	[0.5]
	5. 3.86	7	0.0	1.2	5.2	30.9	[0.2]	16.0	[0.2]	40.5	[0.6]
21	5.15.86	6	12.0	6.4	6.8	36.5	[0.4]	17.4	[1.6]	32.6	[3.2]
	5.16.86	8	0.0	2.3	6.9	36.5	[0.2]	16.3	[1.1]	30.2	[1.9]
	5.17.86	6	0.0	0.7	5.7	36.6	[0.2]	16.0	[0.2]	29.6	[0.6]
	5.18.86	7	0.0	0.4	6.4	36.6	[0.1]	16.0	[0.1]	29.4	[0.3]
	5.19.86	7	0.0	0.4	6.3	36.7	[0.1]	16.0	[0.1]	29.4	[0.3]
	5.20.86	7	0.0	0.3	5.5	36.6	[1.2]	16.0	[0.5]	29.6	[1.1]
	5.21.86	7	0.0	0.4	4.6	31.1	[0.3]	15.9	[0.6]	40.1	[1.4]
22	5.22.86	6	13.0	6.8	5.8	36.3	[1.2]	17.1	[1.1]	32.3	[2.6]
	5.23.86	7	0.0	4.7	3.6	30.7	[0.1]	16.2	[0.5]	41.6	[1.2]
	5.24.86	6	0.0	3.6	3.1	36.3	[0.3]	17.1	[2.7]	32.7	[6.4]
	6.25.86	7	0.0	2.0	4.9	36.6	[0.2]	16.0	[0.2]	29.7	[0.4]
	5.26.86	6	0.0	1.8	3.5	36.5	[0.2]	16.8	[2.3]	31.8	[6.0]
	6.27.86	8	0.0	1.4	5.0	36.6	[0.1]	16.0	[0.1]	29.5	[0.3]
	6.28.86	7	0.0	2.3	3.1	31.7	[2.1]	16.3	[1.5]	40.1	[6.2]

Table 2.2 - continued.

EXP REP	DATE	Tirr hr	Irr mm	RN mm	E_d mm	T_a °C	sd	T_d °C	sd	Rh	sd
23	5-29-86	6	7.0	6.3	4.7	34.5	[2.8]	16.4	[0.9]	34.5	[5.3]
	5-30-86	7	0.0	2.0	4.4	33.9	[6.6]	15.7	[0.8]	36.4	[18.0]
	6- 0-86	6	0.0	1.0	7.0	35.3	[1.3]	16.0	[0.2]	30.1	[3.1]
	6- 1-86	7	0.0	0.6	6.9	36.6	[0.1]	16.0	[0.2]	29.6	[0.4]
	6- 2-86	7	0.0	0.5	6.9	36.7	[0.1]	16.0	[0.1]	29.4	[0.3]
	6- 3-86	6	0.0	0.5	6.6	36.7	[0.1]	16.0	[0.2]	29.4	[0.3]
	6- 4-86	8	0.0	0.6	6.1	36.7	[0.1]	16.0	[0.2]	29.3	[0.4]
31	6- 5-86	6	12.0	6.0	6.9	26.5	[2.2]	16.9	[1.0]	55.7	[4.1]
	6- 6-86	7	0.0	3.2	6.9	25.9	[1.9]	16.1	[0.2]	54.8	[5.9]
	6- 7-86	7	0.0	1.1	5.4	26.2	[2.1]	16.0	[0.4]	54.0	[6.4]
	6- 8-86	8	0.0	0.8	6.2	26.7	[2.1]	15.7	[0.6]	51.4	[6.0]
	6- 9-86	7	0.0	0.6	5.2	27.0	[2.4]	15.5	[0.9]	49.5	[4.8]
	6-10-86	6	0.0	0.5	5.6	27.2	[2.3]	15.6	[0.8]	49.4	[4.8]
	6-11-86	7	0.0	1.0	5.4	27.0	[3.0]	15.8	[0.4]	51.2	[7.9]
32	6-12-86	6	12.0	6.2	6.4	24.3	[2.6]	14.8	[1.3]	55.4	[4.0]
	6-13-86	7	0.0	3.4	4.8	22.6	[0.7]	14.0	[0.4]	58.6	[2.1]
	6-14-86	6	0.0	1.4	5.4	24.5	[2.6]	13.9	[0.4]	52.2	[7.1]
	6-15-86	7	0.0	1.0	6.5	25.5	[3.0]	13.9	[0.4]	48.4	[8.1]
	6-16-86	7	0.0	0.7	4.2	23.8	[1.9]	13.9	[0.3]	54.1	[5.6]
	6-17-86	6	0.0	0.8	3.2	24.9	[2.1]	14.0	[0.3]	51.0	[6.1]
	6-18-86	7	0.0	0.9	5.2	26.7	[3.4]	14.0	[0.4]	46.3	[8.6]
33	6-19-86	7	18.0	6.8	6.1	24.5	[2.1]	14.7	[1.5]	54.4	[3.6]
	6-20-86	7	0.0	4.4	7.6	25.4	[2.8]	14.9	[1.3]	52.7	[5.3]
	6-21-86	8	0.0	3.0	5.7	25.0	[2.8]	14.7	[0.8]	53.3	[6.3]
	6-22-86	7	0.0	1.5	3.3	22.9	[1.1]	14.0	[0.6]	57.6	[4.6]
	6-23-86	7	0.0	0.7	5.4	24.4	[2.0]	14.7	[0.9]	54.9	[5.5]
	6-24-86	6	0.0	1.1	6.2	25.2	[2.5]	14.5	[0.6]	52.0	[5.9]
	6-25-86	8	0.0	0.5	4.7	24.1	[2.2]	14.7	[1.0]	56.0	[6.4]
41	6-25-86	9	18.0	5.0	2.4	36.4	[3.1]	19.6	[2.2]	38.7	[11.8]
	6-26-86	7	0.0	4.3	2.4	37.0	[0.1]	20.0	[5.6]	39.3	[17.5]
	6-27-86	6	0.0	2.8	2.1	36.9	[0.1]	16.5	[0.5]	29.9	[1.0]
	6-28-86	6	0.0	2.0	1.1	36.8	[0.1]	16.0	[0.3]	29.3	[0.5]
	6-29-86	7	0.0	1.7	1.0	36.6	[0.3]	18.6	[2.8]	35.4	[8.0]
	7- 0-86	8	0.0	1.1	1.3	31.7	[1.9]	19.6	[7.8]	51.3	[24.6]
	7- 1-86	7	0.0	1.0	1.1	29.8	[6.2]	15.3	[3.2]	42.7	[11.8]

Table 2.3. Micrometeorological conditions maintained between 800 - 2000 hours during various soil evaporation experiments and replications in the environment controlled chamber under irrigation treatment 3. Tabulated values include date, time of irrigation (Tirr), amount of irrigation (Irr, mm), daily net radiation (RN, mm), daily cumulative evaporation (E_d, mm) air temperature (T_a) and dew point temperature (T_d) in °C, and relative humidity (Rh, %) with associated daily standard deviations. (mm= milli meters).

EXP REP	DATE	Tirr hr	Irr mm	RN mm	E_d mm	T_a °C	sd	T_d °C	sd	Rh	sd
11	4-13-86	7	18.0	5.2	5.0	31.1	[0.1]	16.0	[0.7]	40.4	[1.7]
	4-14-86	7	0.0	3.7	4.2	30.9	[0.2]	15.4	[1.5]	39.3	[3.1]
	4-15-86	7	0.0	2.2	2.7	30.8	[0.3]	15.7	[1.2]	40.1	[2.3]
	4-16-86	7	0.0	0.9	4.6	30.8	[0.4]	15.5	[1.3]	39.5	[2.3]
	4-17-86	7	0.0	0.5	4.7	30.9	[0.4]	15.5	[1.3]	39.5	[2.6]
	4-18-86	7	0.0	0.6	4.6	31.0	[0.1]	15.9	[0.2]	40.0	[0.6]
	4-19-86	8	0.0	0.4	6.3	31.2	[0.1]	15 6	[0.4]	39.2	[0.9]
12	4-20-86	8	20.0	5.7	6.0	31.1	[0.1]	16.2	[0.6]	40.7	[1.3]
	4 21 86	8	0.0	4.4	7.1	31.1	[0.2]	16.0	[0.3]	40.2	[0.8]
	4 22 86	8	0.0	2.0	5.6	31.1	[0.1]	16.0	[0.3]	40.1	[0.7]
	4-23-86	8	0.0	1.0	2.4	31.1	[0.5]	18.1	[4.0]	47.0	[12.3]
	4-24-86	8	0.0	0.9	5.8	31.1	[0.2]	16.0	[0.3]	40.2	[0.9]
	4-25-86	8	0.0	0.6	6.9	31.2	[0.1]	16.0	[0.2]	40.0	[0.7]
	4-26-86	8	0.0	0.7	6.8	31.2	[0.1]	15.9	[0.3]	39.8	[0.7]
13	4-27-86	8	20.0	6.0	6.5	31.1	[0.1]	16.0	[0.4]	40.4	[1.0]
	4-28-86	9	0.0	4.2	7.2	31.1	[0.1]	16.0	[0.3]	40.3	[0.7]
	4-29-86	6	0.0	2.1	5.8	31.2	[0.2]	16.0	[0.3]	40.0	[0.7]
	4-30-86	7	0.0	1.5	4.5	31.1	[0.1]	15.9	[0.3]	40.1	[0.7]
	5 1 86	6	0.0	0.7	4.6	31.1	[0.2]	16.0	[0.3]	40.2	[0.6]
	5- 2-86	6	0.0	0.5	5.2	31.1	[0.1]	16.7	[2.1]	42.4	[6.4]
	5- 3-86	7	0.0	0.3	5.2	31.1	[0.2]	16.0	[0.3]	40.0	[0.6]
21	5-15-86	6	24.0	6.6	6.9	36.4	[1.1]	17.0	[1.4]	32.0	[2.7]
	5-16-86	8	0.0	6.8	7.7	36.3	[1.1]	16.2	[1.2]	30.5	[2.6]
	5-17-86	6	0.0	2.3	6.3	36.3	[1.1]	15.9	[0.3]	29.9	[2.0]
	5-18-86	7	0.0	0.9	7.1	36.8	[0.4]	16.0	[0.2]	29.2	[0.7]
	5-19-86	7	0.0	0.6	6.8	36.9	[0.3]	16.0	[0.2]	29.1	[0.4]
	5-20-86	7	0.0	0.6	5.8	36.8	[1.2]	15.9	[0.6]	29 2	[1.0]
	5-21 86	7	0.0	0.6	5.1	31.2	[0.2]	15.9	[0.7]	39.8	[1.6]
22	5-22-86	6	26.0	7.3	5.6	35.9	[1.6]	16.4	[0.7]	31.7	[2.6]
	5-23-86	7	0.0	4.9	3.9	30.9	[0.1]	16.0	[0.4]	40.6	[1.0]
	5-24 86	6	0.0	4.2	3.3	35.7	[1.1]	16.8	[2.8]	33.1	[6.4]
	5 25 86	7	0.0	3.3	6.2	36.8	[0.3]	16.0	[0.3]	29.3	[0.7]
	5-26-86	6	0.0	2.5	3.7	36.5	[0.6]	16.0	[0.3]	29.7	[0.9]
	5-27 86	6	0.0	1.8	6.1	36.8	[0.1]	16.0	[0.2]	29.2	[0.5]
	5-28 86	7	0.0	2.6	3.2	31.9	[2.1]	15.8	[0.9]	38.3	[4.4]

Table 2.3 - continued.

EXP REP	DATE	Tirr hr	Ier mm	RN mm	E_d mm	T_a °C	sd	T_d °C	sd	Rh	sd
23	5 29 86	6	14.0	6.2	4.8	34.7	[2.8]	16.2	[0.6]	33.6	[5.6]
	5 30 86	7	0.0	4.1	5.3	36.1	[1.0]	16.0	[0.3]	30.6	[1.9]
	6 0 86	6	0.0	1.8	7.2	36.6	[0.6]	16.0	[0.2]	29.4	[1.0]
	6 1 86	7	0.0	1.0	7.2	36.9	[0.2]	16.0	[0.2]	29.1	[0.4]
	6 2 86	7	0.0	0.7	7.0	36.9	[0.1]	16.0	[0.2]	29.1	[0.3]
	6 3 86	6	0.0	0.7	6.8	37.0	[0.1]	16.0	[0.2]	29.0	[0.3]
	6 4 86	8	0.0	0.7	7.2	37.0	[0.1]	16.0	[0.4]	29.0	[0.7]
31	6 5 86	6	24.0	6.3	6.9	26.8	[1.7]	16.2	[0.6]	52.4	[5.0]
	6 6 86	7	0.0	5.6	7.1	26.3	[1.8]	16.0	[0.3]	53.6	[5.7]
	6 7 86	7	0.0	2.3	5.7	26.5	[2.1]	15.9	[0.4]	52.7	[6.4]
	6 8 86	8	0.0	1.3	6.2	27.2	[2.1]	15.6	[0.5]	49.5	[5.7]
	6 9 86	7	0.0	1.0	5.4	27.6	[2.6]	15.1	[1.3]	46.2	[3.9]
	6 10 86	6	0.0	0.8	5.7	27.7	[2.6]	15.1	[1.2]	46.2	[4.0]
	6 11 86	7	0.0	0.8	5.3	27.5	[3.1]	15.4	[0.9]	48.2	[6.4]
32	6 12 86	6	24.0	6.5	6.4	24.8	[2.4]	13.5	[1.3]	49.9	[4.7]
	6 13 86	7	0.0	4.7	5.1	23.2	[1.2]	13.9	[0.5]	56.0	[2.6]
	6 14 86	6	0.0	2.9	5.5	25.0	[2.7]	13.6	[0.8]	49.8	[6.3]
	6 15 86	7	0.0	1.8	6.4	26.6	[3.1]	13.8	[0.6]	45.9	[7.3]
	6 16 86	7	0.0	1.1	4.1	24.7	[2.3]	13.5	[0.7]	50.2	[5.2]
	6 17 86	6	0.0	1.0	3.2	23.7	[1.8]	13.3	[0.8]	52.3	[3.4]
	6 18 86	7	0.0	1.1	5.0	25.9	[2.8]	13.7	[0.7]	47.5	[6.6]
33	6 19 86	7	30.0	6.8	6.1	25.1	[1.9]	13.7	[1.2]	49.6	[3.3]
	6 20 86	7	0.0	4.9	7.3	25.9	[2.6]	13.9	[0.9]	47.9	[5.1]
	6 21 86	8	0.0	4.0	5.7	25.4	[2.7]	13.8	[0.8]	49.2	[6.6]
	6 22 86	7	0.0	2.0	3.5	23.3	[1.8]	13.5	[0.6]	54.3	[4.4]
	6 23 86	7	0.0	1.2	5.4	25.3	[2.4]	14.3	[0.9]	51.0	[5.6]
	6 24 86	6	0.0	1.5	6.1	25.9	[2.6]	14.0	[0.6]	48.4	[6.5]
	6 25 86	8	0.0	1.4	4.6	24.7	[2.5]	14.2	[0.9]	52.5	[6.7]
41	6 25 86	9	24.0	5.2	2.2	36.1	[2.9]	17.8	[2.1]	34.8	[5.6]
	6 26 86	7	12.0	5.0	2.3	36.9	[0.1]	18.6	[4.7]	35.8	[13.4]
	6 27 86	6	0.0	4.6	2.2	36.8	[0.1]	16.0	[0.3]	29.2	[0.6]
	6 28 86	6	0.0	3.1	1.4	36.5	[0.4]	16.0	[0.2]	29.7	[0.6]
	6 29 86	7	0.0	2.3	1.0	35.1	[1.4]	16.7	[1.1]	33.5	[2.2]
	7 0 86	8	0.0	1.2	1.2	31.7	[1.5]	18.3	[7.0]	49.3	[20.5]
	7 1 86	7	0.0	1.1	1.1	29.7	[6.2]	15.3	[3.2]	42.7	[11.8]

entire soil profile to the field capacity (11.5% by volume); b) First day irrigation to bring entire soil profile to field capacity followed by one week of drying; and c) Similar to (b) but irrigation amount was doubled. Following the first three experiments another one week experiment (EXP4) was conducted to study evaporation under low and relatively constant radiation load simulating situations of a fully developed canopy. To simulate this situation all chambers were covered with a shade cloth.

The daily mean and standard deviation of the day time (7 a.m. to 6 p.m.) micrometeorological conditions such as dry bulb temperature, the dew point temperature, and the relative humidity, as well as the daily measured cumulative evaporation and net radiation amounts are listed in Tables 2.1 - 2.3 for each of the three irrigation treatments respectively. As a part of on-going previous projects, the software controlling the chambers was designed to flush each chamber at nights with ambient air and did not control dew point or dry bulb temperatures. Therefore the night time micrometeorological inputs were ignored, but the evaporation rates were recorded at all times to determine cumulative moisture loss. This loss of data during night hours did not cause any problems since vapor pressure deficits and night time moisture loss was very low.

Prior to each irrigating, the water content of the profile, by depth, was determined using a neutron probe , and the calibration curve reported by Jones et al. (1985b). Due to the small floor area of the chambers (2 m^2) it was not feasible to take gravimetric soil samples. The difference between measured water content and field capacity water content determined the amount of irrigation needed to

replenish the whole profile at least to the field capacity. Once the amount was determined, sprinkler cans were used to apply the irrigation. Additional water content measurements were made every other day. The soil temperatures below the surface were recorded every hour using a Campbell Scientific data logger CR-5. In addition, daily evaporation was measured by weighing the condensed vapor that was collected from each chamber.

At the end of the experimental period the data were transferred to the Agricultural Engineering's PRIME 550-II computer. The data were then averaged (evaporation and net radiation summed) for every 30 minute period for further analysis.

Data Analysis

Overview of experiments

The experimental period was characterized by a wide array of evaporativity conditions. The daily irrigation treatment, TR1, received largest share of net radiation, while the magnitudes of RN from other two treatments were lower due to lower surface water content and higher albedo. As the initially saturated soil surface lost water by evaporation, surface albedo increased, reflecting increasingly more and more shortwave radiation. Decrease in the surface soil moisture also caused higher soil temperature and emitted more long wave radiation thereby reducing net radiation. It was observed that the amplitudes of surface temperatures from TR2 and TR3 were twice that of TR 1 on the last day of evaporation, for intermediate periods the amplitudes were steadily increasing. The daily evaporation rates for TR1 varied in accordance with the daily net radiation, while for TR2 and TR3 the evaporation rates decreased exponentially initially, with more

gradual rate of fall later. However, periodic behavior was visible even on the seventh day, although it was very small in amplitude. The data also showed the effect of large heat storage capacity of the soil on the phase difference between the evaporation flux and surface temperatures. When the surface was saturated the phase lag was almost zero, and became progressively larger as soil drying continued.

Daily and cumulative evaporation

The daily evaporation rates and cumulative evaporation losses for all three irrigation treatments were plotted as a function of time. Some of the observations made here showed disagreement with the commonly held notion regarding stages of soil drying and the effect of atmospheric conditions on the course of soil evaporation. It was found that initiation of a drying stage, transition from one stage into next, and stage duration was a function of evaporativity, available soil water, and the history of evaporation, and not simply a time function as is often assumed.

The results of EXP1 are plotted in Fig. 2.1. During EXP1-REP1, data for only first three days was usable due to problems with the control and measurement system. The first day evaporation from each treatment varied in accordance with the irrigation amount applied ; TR3 had received highest irrigation amount and evaporated 10% more than TR2 and 26% more than TR1 during EXP1-REP2. This probably occurred due to longer duration of the first stage for TR3 than in the other two treatments. In relation with TR2 and TR3, evaporation rates for TR1 following day one represented day-to-day fluctuations in the evaporativity, where as the evaporation rates from TR2 and TR3 varied in relation to the irrigation amount. E for TR3 were consistently

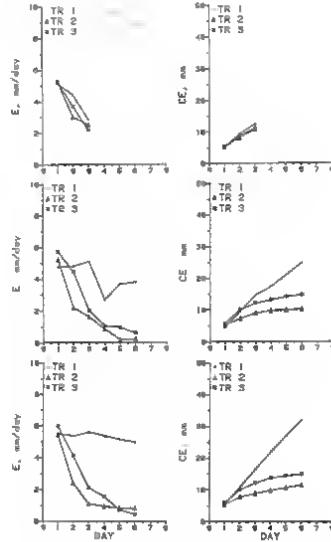

Fig. 2.1 Daily and cumulative evaporation under the three irrigation treatments during EXP1

higher than TR2 and they decreased linearly for the first three days, while E for TR2 dropped exponentially following the first day. Evaporation rates remained practically unchanged 4 days after irrigation, but their magnitudes were different during REP2 and REP3.

The linearity of cumulative evaporation, CE, for TR1 depended on day to day variability in E. Uniformly high evaporativity during REP3 resulted in highest CE among all replication of EXP1. The CE for TR2 lagged CE from TR1 following the first day, whereas CE for TR3 were about same up to two days. This criteria was used by Ritchie (1972) to determine transition time from stage 1 of drying into stage 2. Although the TR1 was not a truly well watered treatment, the results showed that the transition point was delayed with more irrigation. For Houston Black clay, Ritchie (1972) found that stage 1 ended when CE was 4 mm following an irrigation or rainfall event if soil was at field capacity initially. With this criteria, the sandy soil in this experiment required two limits, one for each irrigation treatment.

During EXP2, Fig. 2.2, relative humidity was lowered to increase evaporative potential above that of naturally occurring evaporativity. The natural evaporativity during REP1 and REP3 was fairly uniform and the CE as well as E behaved similarly. On the first day E from TR3 was slightly higher than TR2, on the second day the difference was highest, and it decreased rapidly over the next two days, and finally became almost constant after fourth day. During EXP1, the drying was more gradual and changes in day to day evaporation were less severe. There were large variations in the day to day evaporativity during REP2 that resulted in some interesting observations. The E for TR2 decreased linearly up to four days unlike all previous cases,

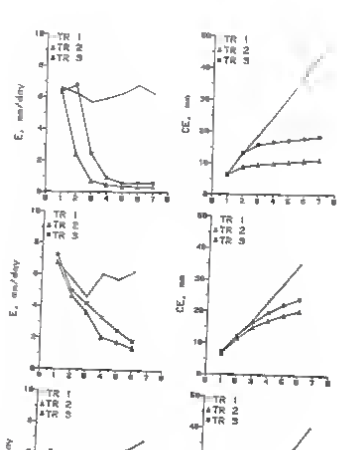

Fig. 2.2 Daily and cumulative evaporation under the three irrigation treatments during EXP2

where as E for TR3, the decrease was linear for six days. A leak due to rain increased E for both the treatments on the last day. The two cloudy days during EXP2 - REP2 following the first day of intense radiation, probably allowed soil rehydration and maintained soil near the surface relatively moist. The fourth day increase in evaporation load caused a sudden depression in E for TR2, illustrating the influence of above ground conditions. Additionally it can be also seen that CE for both the treatments had not levelled off even on the last day which again illustrates the point that under a right combination of conditions, the above ground conditions could affect the evaporation process well after the stage I was over.

Results of EXP3 (Fig. 2.3) and EXP4 (Fig. 2.4a) showed many of the behaviors seen earlier. Very stable environmental conditions during EXP3-REP1 produced results as if experiments were conducted in laboratory. Low evaporativity load during EXP4-REP1, resulted in slow drying and the drop in E was very gradual. Stage 1 duration was about two days longer than all previous experiments.

The cumulative evaporation data for TR2 and TR3 from all experiments were combined together (Fig. 2.4b) to see if it could be described by a time function as suggested by Gardner (1959). There was wide scatter in the daily evaporations amounts. The seventh day CE for TR2 ranged from 10.5 mm to 22.5 mm whereas for TR3 the range was 13.5 mm to 26.5 mm which amounts to more than 100% variation in both the cases. If one looks at the individual CE curve it may seem possible to represent them by a time function, but it would be very difficult to specify one general relationship that would be satisfactory across all experiments and treatments. The scatter in the

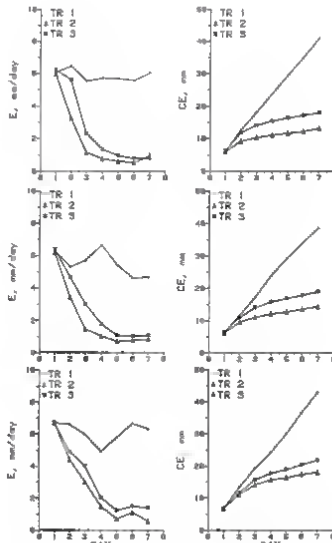

Fig. 2.3 Daily and cumulative evaporation under the three irrigation treatments during EXP3

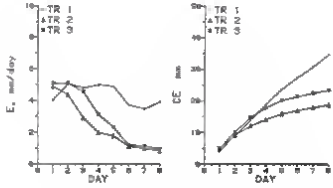

Fig. 2.4a Daily and cumulative evaporation under the three irrigation treatments during EXP4 - REP1

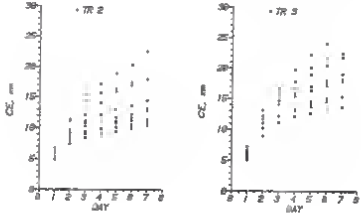

Fig. 2.4b Cumulative evaporation data for the entire study period for irrigation treatments 2 and 3

data was the result of different irrigation amounts, the initial soil water content at the time of irrigation, and variations in the evaporativity. Describing these data using a time function would clearly be a gross approximation. In summary, following conclusions were drawn from the experiments:

1. The duration of stage I was related to both the cumulative evaporation following irrigation and the initially available water for evaporation.
2. Evaporation rates as well as cumulative evaporation amounts were a strong function of amount of water applied and cannot be simply described as a time function.
3. The rate of decrease in evaporation rates depended upon irrigation amount and the history of evaporation.
4. Evaporation rates were influenced by radiation when soil was subjected to cycles of high and low radiation loads.
5. The physical model (Equ. 2.1) may eliminate some or all of these problems if soil resistance RV is appropriately calibrated to account for conditions in the soil as well as in the atmosphere.

Analysis of soil resistance

The time series of RV obtained by solving Eqn (2.2) was plotted as a function of time and cumulative evaporation to determine the appropriate model for describing the data. From the time series analysis it was concluded that RV could not be described by time since it did not account for the intensity of evaporativity as well as soil water status. Some of the problems of the time dependent model were

partially solved by using cumulative evaporation as independent variable instead of time. However this approach was inadequate, because it did not account for variations in irrigation amounts (note differences between TR2 and TR3) as well as residual soil water from previous irrigations.

Gardner (1974) employed a ratio of cumulative evaporation to amount of water applied as the independent variable in modeling evaporation. This approach would work if there is always the same amount of water present in the soil prior to each irrigation and/or that all water from previous application had evaporated or percolated deep into the soil making it unavailable for subsequent evaporation. These requirements may not be always satisfied in a field situation with rainfall occurring at random. Additionally, Gardner and Gardner (1969) had noted that at low application rates almost all applied water as well as some additional water was lost, but as the amount per application was increased , the fraction evaporated decreased with water moving deeper into the soil, suggesting that all the applied water was not lost during subsequent evaporation periods.

Therefore even for a initially saturated soil there must be an approximate upper limit, CE_m, on cumulative evaporation. CE_m would depend upon physical soil properties and the maximum depth, D_m, over which soil evaporation may occur. CE_m could be determined for a soil either by actual measurements or by simulation. Some procedures have been reported for determining location of the drying front but in general, measurement of evaporation front has been a difficult task. Wiegand and Taylor (1962) monitored temperature profiles of a soil column in a laboratory and inferred that the location of the evapo-

ration front was associated with the largest temperature depression; Gardner and Hanks (1966) used a "heat sink" method to locate the evaporation front. Grover (1972) experimentally found that the location of the evaporation front corresponded to a region of fixed moisture content (0.6% over 0.01 m depth). McGowan (1973) identified the evaporation front with a plane of zero moisture flux using time-moisture content relationships; Welling and Bell (1980) followed a similar procedure with soil moisture data. During this study water content profiles were measured every alternate day at 0.15 m intervals and temperatures were measured up to 0.10 m depth. This type of resolution seemed inadequate to implement any of the above procedures.

Therefore a numericel model was developed. Earlier, similar models have been published by Hanks and Gardner (1965), Hillel (1975), and van Keulen (1975). This model was similar to Hillel's model but was written in FORTRAN 77 and used experimentally measured evaporation rates as the surface flux boundary conditions. The model soil profile was divided into eleven layers with thickness varying from 0.02 m at the top to 0.175 m at bottom of profile. Water flux from each layer was found from Darcy's law. The results of water content with depth for each seven day period were used to visually identify the location of the evaporation front using the criteria of McGowan (1973). The results of twenty, seven day periods showed that the plane of zero flux was located approximately 0.30 m from the soil surface. It was also found that the top 0.02 to 0.03 m soil was near 0 % moisture content but lower soil was relatively moist with average moisture content of 5%. Using this basic information CE_m was computed (Table 2.4 - 2.8) for all irrigation events.

Table 2.4 Procedure for computing CE_m, maximum possible cumulative soil evaporation associated with an irrigation or rainfall event.

The implementation of the model required information on CE_m, the maximum possible evaporation associated with an irrigation or rainfall event. The CE_m was less than or equal CE_p, the potential evaporation associated with a soil initially irrigated to field capacity and then subjected to drying. When soil drying occurs, evaporation usually stops well before the soil is completely desiccated. If the average final water content of D_m cm of soil is denoted as θ_f, then CE_p,soil can be defined as

$$CE_p = \int_0^{D_{max}} (\theta_{fc} - \theta_f) \, dz + E_1 \qquad (2.3)$$

where z was the soil depth, θ_{fc} field capacity volumetric water content, θ_f final water content at the end of a drying period, and E_1 was maximum observed first day evaporation amount. Results of numerical simulation suggested that the maximum depth of drying, D_m was 0.3 m, θ_{fc} was equal to 11.5% (Zur and Jones, 1982), and θ_f and E_1 were measured to be 5% and 7.23 mm respectively. Substituting these values in Eqn 2.3 gave CE_p a value of 26.73 mm. The first day evaporation was added to account for evaporation loss while water was distributed to field capacity. Therefore, E_1=0 if soil is at the field capacity at the beginning of the drying. This computed value compared well with maximum 7 day cumulative evaporation of 26.59 mm during EXP2-REP2. To compute CE_m associated with each irrigation event, the following procedure was used:

1. Measure total soil water prior to irrigation (TSW_{bi})

2. Irrigate, and compute total soil water after irrigation, $TSW_{ai} = TSW_{bi} + Irr$

3. From TSW_{ai} subtract water that would be held by the soil at the end of the drying period (7 days in this study),

$$W_h = \int_0^{D_{max}} \theta_f \, dz$$

$$TSW = TSW_{ai} - W_h$$

This allows for drainage below the evaporation zone as well as evaporation water loss.

4. Determine CE_m using following criteria:

$CE_m = TSW$ if $TSW <= CE_p$

$CE_m = CE_p$ if $TSW > CE_p$

The values of CE_m computed using above four criterias are listed in Table 2.5 for TR2 and Table 2.6 for TR3, note that for TR3, CE_m values were usually at the maximum value because enough water was added to bring the evaporation zone to field capacity and allow some drainage below that depth.

Table 2.5 CE_m computed for irrigation treatment 2 following each irrigation event. Tabulation shows total soil water before irrigation (mm), irrigation applied (mm), total soil water after irrigation (mm), estimated amount of water held by soil at the end of a drying cycle (mm), total soil water available for evaporation (mm), potential evaporation for the soil (mm), and maximum possible evaporation from the irrigation event (mm).

EXP	REP	TSW_{bi} mm	Irr mm	TSW_{ai} mm	W_h mm	TSW mm	CE_p mm	CE_m mm
1	1	25.3	9	34.3	18	16.3	26.73	16.3
1	2	24.8	10	34.8	18	16.8	26.73	16.8
1	3	24.5	10	34.5	18	16.5	26.73	16.5
2	1	22.8	12	34.8	18	16.8	26.73	16.8
2	2	22.8	13	35.8	18	17.8	26.73	17.8
2	3	28.0	7	35.0	18	17.0	26.73	17.0
3	1	25.6	12	37.6	18	19.6	26.73	19.6
3	2	25.5	12	37.5	18	19.5	26.73	19.5
3	3	25.0	15	40.0	18	22.0	26.73	22.0
4	1	24.9	18	42.9	18	24.9	26.73	24.9

Table 2.6 CE_m computed for irrigation treatment 3 following each irrigation event. Tabulation shows total soil water before irrigation (mm), irrigation applied (mm), total soil water after irrigation (mm), estimated amount of water held by soil at the end of a drying cycle (mm), total soil water available for evaporation (mm), potential evaporation for the soil (mm), and maximum possible evaporation from the irrigation event (mm).

EXP	REP	TSW_{bi} mm	Irr mm	TSW_{ai} mm	W_h mm	TSW mm	CE_p mm	CE_m mm
1	1	26.8	18	44.8	18	26.8	26.73	26.73
1	2	25.1	20	45.1	18	27.1	26.73	26.73
1	3	23.6	20	43.6	18	25.6	26.73	25.60
2	1	21.8	24	45.8	18	27.8	26.73	26.73
2	2	21.8	26	47.8	18	29.8	26.73	26.73
2	3	27.6	14	41.6	18	23.6	26.73	23.60
3	1	23.4	24	47.4	18	29.4	26.73	26.73
3	2	24.3	24	48.3	18	30.3	26.73	26.73
3	3	25.8	30	55.8	18	37.8	26.73	26.73
4	1	25.3	36	61.3	18	43.3	26.73	26.73

RV computed for TR2 and TR3 was plotted as a function of normalized cumulative evaporation CE_n, ($CE_n = CE/CE_{ss}$) in Figs. 2.5-2.8. The trend in progression of RV during different experiments was similar, indicating that one functional form may be adequate to describe RV under various experimental conditions experienced during this study. Initially RV remained constant for about 7 to 8 hours following an irrigation and then increased exponentially as CE_n increased beyond a threshold, CE_c. The constant phase of RV corresponded to the stage 1 of evaporation, i.e. when RS remained zero. The resistance during this phase was only from the laminar air layer adjacent to the surface. Since the experiments in this study were conducted in uniform wind velocity, the boundary layer resistance RB remained relatively constant. As the drying continued, the soil was no longer able to meet the atmospheric demand, and to maintain the balance between the demand and supply, soil resistance RS increased.

RS oscillated showing maxima at noon and minima during mornings and evenings. These oscillations may have partly been an artifact of computational procedure caused by Eqn. 2.2, diurnal oscillations in surface temperature, evaporation E, and the phase difference in the two. The moisture front migrates in response to diurnal variations in the atmospheric demand, the front being farthest from the surface in the afternoon and closer to the surface during other times. An analogy seems apparent between the oscillation in RS and location of the evaporation front. In case of EXP2-REP2, RV remained low compared to all other cases. This situation arose because of alternating cycles of cloudy and clear days that caused moisture migration and perhaps rehydration of dry upper soil layers. These drying and

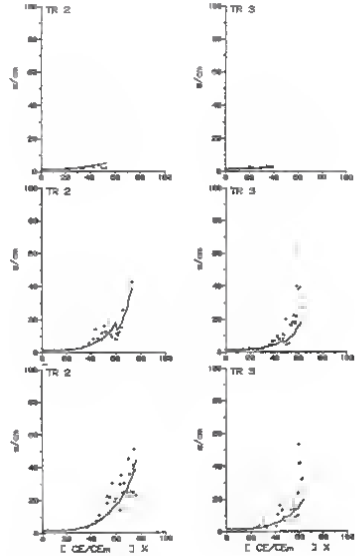

Fig. 2.5 Computed total soil resistance, and its simulation with the non-linear least square model for EXP1

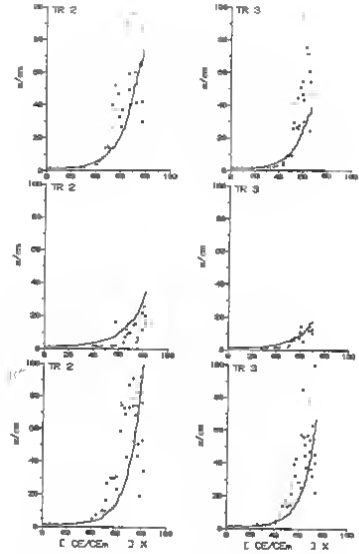

Fig. 2.6 Computed total soil resistance, and its simulation with the non-linear least square model for EXP2

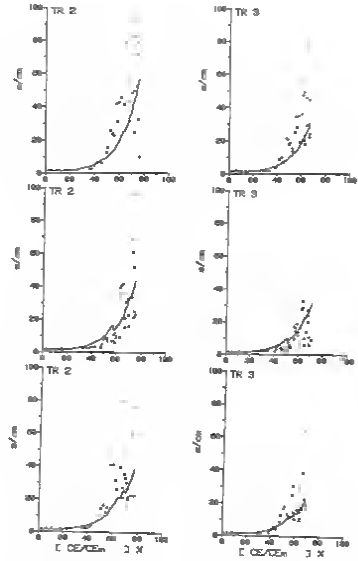

Fig. 2.7 Computed total soil resistance, and its simulation with the non-linear least square model for EXP3

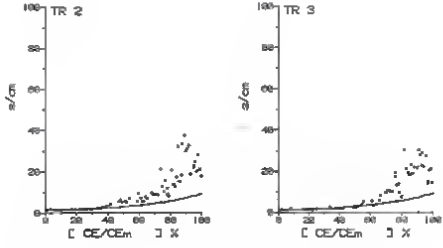

Fig. 2.8 Computed total soil resistance, and its simulation with the non-linear least square model for EXP4

wetting cycles maintained high prolonged evaporation rates, kept surface temperatures low, and resulted in lower RV estimates. Therefore it was also concluded that to completely describe the soil evaporation process some provision for simulating varying sky conditions was needed. Employing a running average of net radiation was found to be a feasible solution.

In summary four factors were needed to completely describe soil resistance and subsequently the evaporation process between any two water application events.

1. Cumulative evaporation, CE.
2. Amount of water applied.
3. Available soil water for evaporation, CE_m.
4. Daily running average of net radiation following an irrigation or rainfall event.

Model Development

From the following model for RV was proposed:

$$RV = RB \qquad \text{if } CE_n \leq CE_c \quad (2.4a)$$

$$RV = RB \; a^{(\alpha + \beta RN_a)(CE_n - CE_c)^{\eta}} \qquad \text{if } CE_n > CE_c \quad (2.4b)$$

where α, β and η were constants to be found from non-linear least square fitting procedure and RN_a was the running average of daily net radiation. Net radiation was included to account for day to day variations in the sky conditions and allow simulation of rehydration. Additionally RB and CE_c were also unknowns in the RV equation. In the

literature, methods to compute RB based on wind speed and surface roughness are recommended (Monteith, 1965, Goudriaan, 1977). On the other hand CE_c is a soil specific constant. Since the soil independent stage of evaporation lasted for a day in most cases, the values of RV during the first day were analyzed to discern value of CE_c and RB using following procedure:

1. RV was plotted as a function of CE_n during first two days following irrigation.
2. RV values oscillated during the day, but the point in time when RV increased and continued to do so thereafter was taken as indication of the end of the soil independent stage of evaporation. The value of CE_n at this time corresponded to CE_c.
3. RB was computed as the arithmetic average of RV values up to that point.

From the analysis, RB had a mean of 153.8 s/m with standard deviation of 33.1 s/m and 80% of the values were within one standard deviation of the mean. The value of RB compared well with some published values (Table 2.7). From this analysis CE_c was 15% and it required 7.5 hours (sd = 0.5 hours) for CE_n to equal this value. With RB and CE_c determined, optimal values of α, β and η were predicted using a non-linear least square procedure

$$\alpha = 1.0942 * 10^{-3} \qquad (2.5a)$$

$$\beta = 2.0197 * 10^{-3} \qquad (2.5b)$$

$$\eta = 1.36757 \qquad (2.5c)$$

TABLE 2.7. Comparison of boundary layer resistence (s/cm) obtained in this study and from some selected literature under similar situations.

Source	Surface type	RB, s/m
This study	Bare soil wind speed 0.085 m/s	153
Goudriaan, 1977 Eqn. 3.28	soil, clod size 0.05 m wind speed=0.085 m/s	138.0
Conway and van Bavel, 1969 Eqn. 3	Z_o= 0.0256 cm, Z=1 m wind speed=1m/s	428.0
Rijtema, 1973	crop less than 0.9 m most wind velocities	30-60

With these choices of parameters the soil evaporation model became:

$$E = \frac{C_p}{\lambda \gamma} \frac{e(T_s) - e(T_d)}{153.8} \qquad CE < 15\ \% \quad (2.6a)$$

and when CE > 15 % E is given by:

$$E = \frac{C_p}{\lambda \gamma} \frac{e(T_s) - e(T_d)}{153.8\, e^{(a + g\, RN_n)\,(CE_n - 15)^{1.36757}}} \qquad (2.6b)$$

The model predicted values of RV were superimposed on Figs. 2.5-2.8 for direct comparison with the data. The model seems to simulate RV well early during the drying cycle, however later it simulates some average path rather than the oscillations of RV. However at higher RV values , E would be very small and was not expected to give any noticeable errors. During EXP 4 the model predicted low resistance perhaps due to the running averaging of net radiation and was likely to introduce some errors.

Model Verification

To determine the accuracy of the model and establish confidence in its predictions, it was used to compute evaporation in response to irrigation amounts, soil and air temperatures, and evaporativity. The hourly evaporation rates as well as cumulative evaporation was compared with the experimental measurements in Figs. 2.9-2.10.

During the design of the experiment it was expected that the soil independent evaporation stage (stage I) could be maintained for at least 24 hours, which was the irrigation frequency. To verify this, simulations were carried out by assuming that RV = R0 between two irrigations. The model simulated evaporation rates fairly accurately up to 6-7 hours after irrigation and then resulted in overestimation

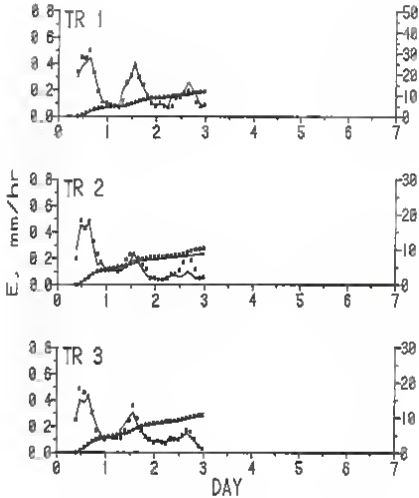

Fig. 2.9 Comparison of measured and simulated evaporation, EXP1 - REP1

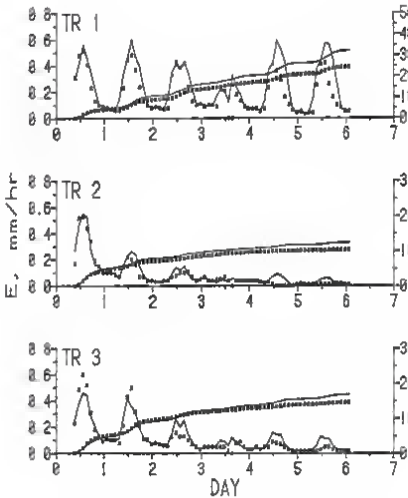

Fig. 2.10 Comparison of measured and simulated evaporation, EXP1 - REP2

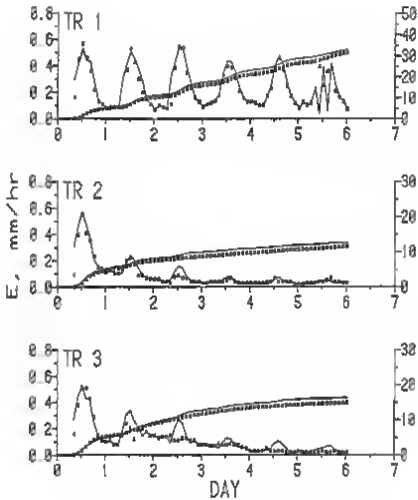

Fig. 2.11 Comparison of measured and simulated evaporation, EXP1 - REP3

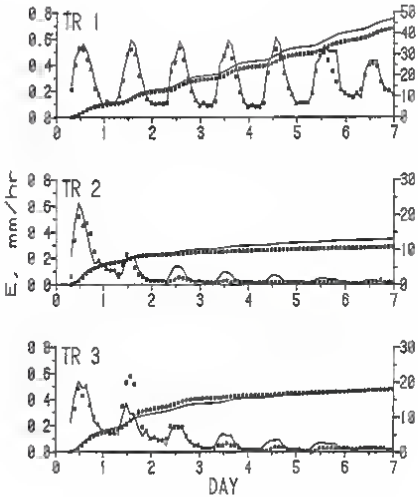

Fig. 2.12 Comparison of measured and simulated evaporation, EXP2 - REP1

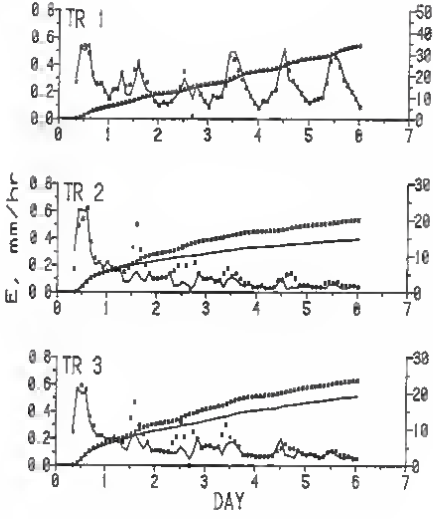

Fig. 2.13 Compartson of measured and simulated evaporation, EXP2 - REP2

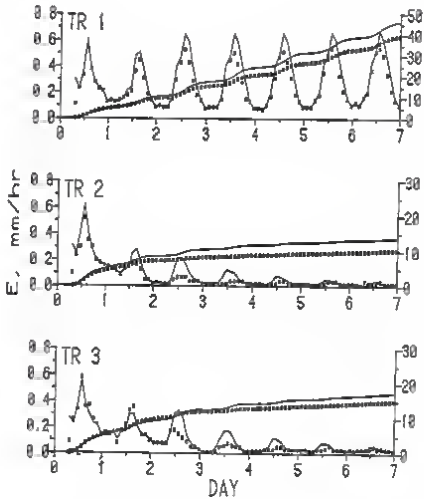

Fig. 2.14 Comparison of measured and simulated evaporation, EXP2 - REP3

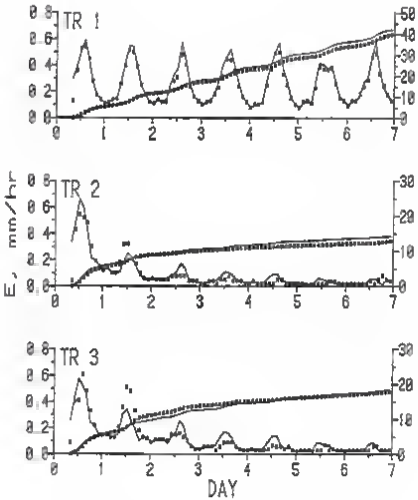

Fig. 2.15 Comparison of measured and simulated evaporation, EXP3 - REP1

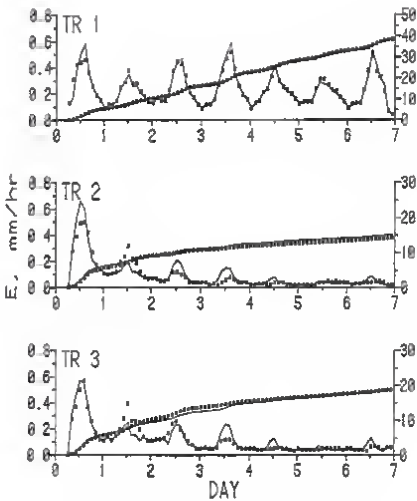

Fig. 2.16 Comparison of measured and simulated evaporation, EXP3 - REP2

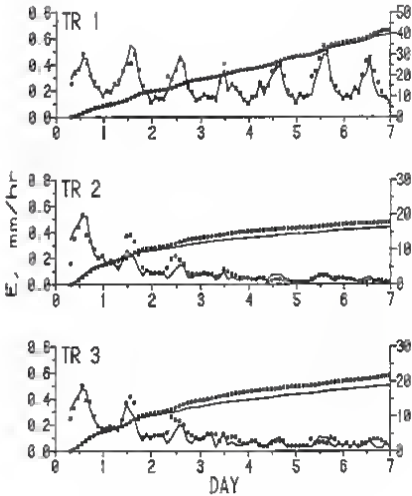

Fig. 2.17 Comparison of measured and simulated evaporation, EXP3 - REP3

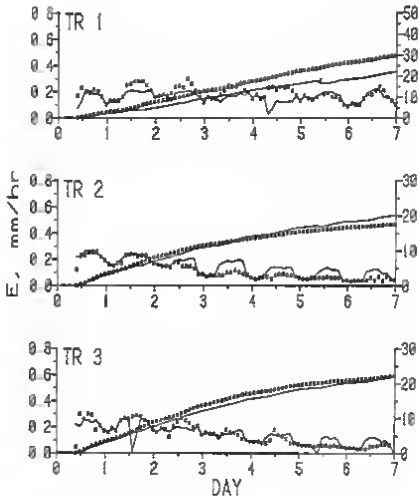

Fig. 2.18 Comparison of measured and simulated evaporation, EXP4 - REP1

suggesting that the stage 1 duration was smaller than expected initially. It was found that stage I lasted an average of 7.5 hours.

Perhaps the true test of the model was provided by TR2 and TR3 which were subjected to a week of drying. The model accuracy was good early in the drying cycle when evaporation rates were high. The model predictions were on average within 3% of the measured value on the first day, 10% on the second day, and 15% on the third day. However the model was less sensitive at low evaporation rates. An equation relating cumulative evaporation to time, Eqn. 2.7, was developed to determine if the soil evaporation model developed in this study provided improvement over currently used approache. The equation was fit tp combined data of TR2 and TR3 using non-linear least square procedure. The data for TR1 were not included since that treatment had received daily irrigation. The resultant model had a R^2 of 0.92 and the exponent of time was 0.825 which was different than 0.5 as derived by Gardner (1959) and Phillips (1957) from their solutions of the flow equation

$$CE = 4.16\, t^{0.825} \qquad (2.7)$$

Kijne (1975) had recommended two different exponents, 0.67 for the first four days of drying and 0.4 for 15 to 20 days there after. Relative errors (Eqn. 2.8) between measured daily evaporation rates and predicted evaporation rates using Eqn. 2.6 and 2.7 were compared in Table 2.8 for TR2 and Table 2.9 for TR3.

$$\text{Relative Error} = \frac{(E_{simulated} - E_{measured})}{E_{measured}} * 100 \qquad (2.8)$$

It can be seen from these tables that the individual as well as

Table 2.8 Relative errors in predicting cumulative evaporation on various days by the new and the CE vs Time 'old' models during various experiments, and average and standard deviation in relative errors for each day across all experiments and replications for irrigated treatment 2.

EXP	day 1		day 2		day 3		day 4		day 5		day 6		day 7	
REP	new	old	new	old	new	old	new	old	new	old	new	old	new	old
11.	-2	-20	-16	6	-38	16	---	---	---	---	---	---	---	---
12.	5	-20	22	46	17	80	0	224	295	1220	166	962	---	---
13.	10	-23	9	32	40	161	7	187	-9	210	-12	193	---	---
21.	3	-34	0	33	100	324	124	513	105	633	82	649	18	551
22.	1	-38	-42	-31	-50	-19	-27	33	-36	49	-28	80	---	---
23.	12	-21	23	62	104	199	105	367	66	450	29	442	-5	319
31.	9	-29	-17	0	43	159	57	263	55	333	40	390	-7	157
32.	10	-32	-26	-6	36	100	49	165	18	277	-6	222	5	191
33.	6	-37	-25	-27	-26	-2	-26	85	43	272	-3	131	19	342
41.	-3	-14	-19	-26	18	1	57	40	33	49	37	127	82	152
Av.	6	-26	-8	7	24	101	38	208	63	388	33	355	18	285
St.	5	8	22	31	52	110	54	157	96	361	59	292	32	153

Table 2.9. Relative errors in predicting cumulative evaporation on various days by the new and the CE vs Time 'old' models during various experiments, and average and standard deviation in relative errors for each day across all experiments and replications for irrigated treatment 3.

EXP	day 1		day 2		day 3		day 4		day 5		day 6		day 7	
REP	new	old	new	old	new	old	new	old	new	old	new	old	new	old
11.	-3	-20	-1	-13	-9	33	---	---	---	---	---	---	---	---
12.	-6	-26	0	-27	44	45	44	165	68	174	101	319	---	---
13.	-3	-30	14	-22	32	34	4	76	58	241	-25	442	215	852
21.	9	-34	-27	-52	-7	21	71	203	90	363	79	339	16	326
22.	-5	-42	-28	-35	-33	-29	-21	-15	-13	5	-12	37	---	---
23.	-3	-31	-7	-23	58	56	90	197	73	272	33	259	15	253
31.	2	-32	-26	-42	8	27	44	109	55	175	47	226	30	213
32.	4	-34	-23	-31	-10	-2	38	55	24	142	1	147	15	127
33.	0	-38	-14	-34	-27	-27	-28	36	13	113	-5	71	-25	78
41.	-7	-17	-13	-36	-11	-35	0	-10	13	14	36	112	53	119
Av.	-1	-30	-12	-31	4	12	26	89	43	169	28	216	46	281
Sd.	4	7	14	11	30	33	40	81	35	118	43	135	78	266

average relative errors on each day were much smaller with the new model when compared with the time dependent model. The smaller standard deviations among all experiments suggest that the daily evaporation rates simulated with the new model were more close to the measured values on any day than the time-model.

Late in the drying cycle the relative errors and standard deviations were high with the new model, but still much smaller than the time dependent model. In this study this phenomena was observed approximately three days after drying, when approximately 80% of evaporation had been completed and the daily evaporation rates were much less than 1 mm/day and therefore the errors were insignificant in terms of total water lost. The RV computed from the data showed diurnal oscillations, whereas the model predicts an average RV for each day. Since the evaporation rates were small during these periods, this approximation was not expected to give serious errors.

The maximum errors in cumulative evaporation were recorded during EXP2-REP2 which was characterized by variable cloudy conditions. The errors were heavily biased by wrong calculations on the second and the third day in both the cases. Extreme variations in the above ground conditions may have produced oscillations in the evaporation front, resulting in cycles of drying and rehydration of dried zones that resulted in sustained evaporation rates. This model can adjust the rate of upward trend of RV under low radiation conditions but does not have any mechanism to reduce the resistance as it may occur due to rehydration of soil. To incorporate such a mechanism in the model, a combined heat and moisture balance model would be required.

The errors (differences between measured and simulated daily

evaporation) were normally distributed suggesting that the errors were independent. The data base developed had covered a wide variety of situations and performed well in all cases except under extreme situations. The periodicity in evaporation, though small in amplitude, prevailed well after the end of stage I. This was contrary to the classical assumption that evaporation following stage I was environment independent. It appeared that there was a transition stage between stage I and the environment independent stages II and III, and the duration of this stage depended not only on the atmospheric demand but also on the strength of the evaporation source, mainly the water content of the evaporation zone.

Sensitivity Analysis

In the preceding discussion it was shown that the new model was superior compared to the strictly time dependent model. This model allows diurnal simulation of evaporation and will be simple to integrate with the canopy models to develop an integrated soil-plant-atmospheric model to predict E, T and ET in response to soil, plant and atmospheric factors. The new model required more information and the additional effort in obtaining them seemed justified. The success of the soil evaporation model depends upon the accuracy with which the soil resistance model parameters P_B, CE_C, α, β and η are specified. To illustrate model sensitivity to these variables, seventh day CE was computed by varying one variable at a time. For this computation three one week periods were selected based on the accuracy with which they were simulated. The selections were the best simulated week (EXP3-PEP2, TP3), the worst simulated week (EXP2-PEP2, TR2) and an average week (EXP1-PEP1, TK3). Computations were done at

the model assigned values for these parameters, as well as 80%, and 120% of that value. The relative errors in seventh day CE were compared in Table 2.10 The negative errors in the table indicate that simulated values were less than measured values and positive values indicate over estimation. The model was most sensitive to n, and least sensitive to α. The importance of RS and CE_c was only for a short period in drying cycle, and since the predictions were satisfactory (see Figs. 2.9 - 2.13) during this time, the errors associated with them were small. The effect of 20 % variation in β resulted in only 7% variation in CE, which also suggest that its accuracy was not that critical. The most errors were due to variations in n, therefore care must be taken in determining its value. In applying this model to other soil types these parameters may be obtained either by direct measurements and curve fitting as done in this study, or a combined heat and moisture model may be used to derive values of CE_c, α, β and n using model fitting procedures similar to the ones outlined in this chapter.

Direct measurements of RS has been difficult and the disagreement between various measurements is evident from Table 2.7, where RS computed in this study was compared with some published values. Therefore perhaps the best way of obtaining it is by calibration of the observed data. The model is sensitive to RS only during stage I of evaporation (RS=0), following this stage, RS becomes several orders of magnitude higher than RS and RS will not have any noticeable impact on the predictions. In sandy soils stage I duration is small, therefore small errors in RS will not have much impact on the long time predictions. But this may cause appreciable errors in heavy soils where the stage I

Table 2.10 Results of sensitivity analysis. Percent change in CE on day 7 caused by ± 20% change in the best picked parameters of the soil evaporation model Eqn. 2.5.

CASE	RB 0.8	RB 1.2	CE_c 0.8	CE_c 1.2	α 0.8	α 1.2	δ 0.8	δ 1.2	η 0.8	η 1.2
BEST	5	-4	-4	4	0	0	7	-6	48	-26
WORST	4	-4	-3	3	0	0	7	-5	55	-24
AVERAGE	5	-4	-4	4	0	0	7	-6	49	-25

duration is likely to be longer. Therefore the procedure used to compute RB must be decided accordingly.

CE_c measures the duration of stage 1 following an irrigation or rainfall event. It can also be used to calibrate a model as was done in this study so that the simulated and measured values were similar. The calibration procedure predicted CE_c=15% in this study. However this choice of CE_c results in underprediction of evaporation from EXP2-REP2, probably because of moisture migration that sustained evaporation rates.

Summary And Conclusions

The need to predict evaporation and transpiration components of a developing crop canopy was identified as an important issue in determining appropriate water saving strategies. Various techniques differing in details and complexity have been developed to tackle this problem. Evaporation and transpiration can be computed as independent components and added together to give ET from the crop (Ritchie, 1972) or they can be treated simultaneously as interdependent processes (Shawcroft et al., 1974, Goudriaan, 1977). The later approach seemed more promising because it treats soil-plant-atmosphere as an energy exchange system and has potential of simulating even the microclimate of the canopy. To implement this later approach, a soil evaporation model based on vapor pressure difference and soil resistance was desired. The principles applied in measuring plant resistance cannot be applied to a soil due to the lack of information of the precise location of the drying front and also due to the finite thickness over which evaporation occurs. Therefore soil resistance, RV, was computed from measured evaporation rates, soil temperature and air

humidity, by assuming that evaporation was proportional to the vapor pressure difference between the soil surface and atmosphere. A ten week evaporation study was completed in a controlled environment where soil was subjected to natural radiation but temperature and surrounding humidity were controlled to give three evaporativity levels. During the study the soil was irrigated daily, and once every week. There were two once a week irrigated treatments, with the second receiving twice the amount of the first. The resulting time series in RV was used to develop a semi-empirical model of RV, the soil resistance. The model performed well and the errors were estimated to be much smaller than a strictly time dependent model suggested by Gardner (1959).

In this model many of the possible factors controlling evaporation were accounted for. This model has the characteristics that, following an irrigation or rainfall event, the soil will start out in stage I and will remain in stage I a variable length of time depending on the amount of water added. To further improve the accuracy of this model, one may need a combined heat and mass transfer model.

CHAPTER III

MODEL FOR PREDICTING WATER USE AND MICROCLIMATE OF A DEVELOPING CROP

Introduction

Crop yield is set by the genetic potential of the crop, ecological conditions, and by proper and timely supply of water, fertilizer and pest control. Water is perhaps the most important of all management variables and must be supplied in quantity and time in accordance with the crop water needs for optimum growth and yields. The timing and amount of water applied is governed by prevailing climatic conditions, stage of crop growth, soil water holding capacity and the extent of root development. Estimating ET for a specific crop can be a very complex issue depending upon the degree of accuracy desired. To obtain most accurate estimates, all of the above crop and environmental conditions need to be taken into account.

Since Dalton first introduced the mass transport equation, there have been numerous models and methods to evaluate crop water needs. These methods include various types of lysimeters, portable chambers, sap flow techniques, atmometers, and pan evaporimeters (Bled, 1982). Precision weighing lysimeters provide the only direct way of accurately measuring ET. However due to the expense and time involved in using field measurement methods, predictive means of estimating ET with varying level of accuracy and complexity have evolved.

The choice of a ET estimation method depends upon the intended use and the time scale of application. For example crop irrigation

management requires only daily or maybe hourly estimates of ET to allow timely irrigation decisions to avoid water stress and yield reduction. On the otherhand, monthly estimates may be adequate for a regional water management problem. In this paper short term methods are considered.

Thornthwaite (1944) and Penman (1948) introduced the concept of potential ET, to characterize the effect of climate on crop water requirements. Potential ET was defined as the rate of evapotranspiration from an extensive surface 8 to 15 cm tall, green grass cover of uniform height, actively growing, completely shading the ground and not short of water (Jones et al., 1984a). Several ET methods requiring meteorological data have been proposed and are used to estimate potential (or now more commonly referred to as the reference) crop evapotranspiration (Doorenbos and Pruitt, 1977). The simplest among these models require only the average air temperature, day length, and crop coefficients. The generally better performing methods need daily radiation, temperature, vapor pressure and wind speed data (Jones et al., 1984). The actual crop water requirement is computed from reference evapotranspiration using a crop coefficient, which is characteristic of the crop, and its stage of growth. These methods have been reviewed along with their potential applications by Jensen et al. (1970), Doorenbos and Pruitt (1977), Burman et al. (1981), and by Sled (1982).

The concept of potential ET is useful for many purposes and the crop coefficient method has gained widespread acceptance. Potential ET requires that plants behave passively as wicks and that plants exercise no control over transpiration (T). In reality ET is influ-

enced by soil and plant factors and consequently it is lower than potential ET. Monteith (1965) combined energy balance, aerodynamic parameters, and surface parameters in an equation valid for vegetation of any type in any state of water stress. The development of the Monteith model was a historic event and the model has become the building block of many ET models for closed canopies (Zur and Jones, 1982, Jagtap et al., 1984, Sinclair et al., 1976) and has been widely quoted in the literature. However, their approach is vague about soil evaporation and as a result the Monteith model has not been applied to the problem of soil evaporation and incomplete canopy cover.

Ground cover affects ET. When plants cover only a small portion of the soil surface, ET is dominated by E. As the plant cover increases, evaporation from the soil surface is decreased and the relative importance of transpiration increases. Klocke et al. (1982) in a field study showed that soil evaperation was reduced with canopy development but it did not cease even at full crop cover. Phene et al. (1985) reported that with dry soil surface and constant soil water content, the bare soil evaporation rate was 14% of potential ET for alfalfa. The importance of soil evaporation at small LAI cannot be ignored and even at full ground cover, soil evaporation, though small, influences canopy microclimate (humidity and temperature).

Recently Black et al. (1969), Ritchie (1972), and Tanner and Jury (1975) developed empirical models to estimate soil evaporation and transpiration from well watered crops where soil goes through cycles of drying and wetting. In these models transpiration was related to leaf area development and was computed by multiplying potential ET with an empirical function of leaf area to account for the degree of

crop cover. The soil evaporation was computed in two stages. Following a rain or irrigation event and until a certain cumulative evaporation occured, E was calculated based on the net radiation reaching the soil surface. From this time on, E was determined using the equation developed by Black et al. (1969) relating cumulative evaporation (CE) to the square root of time. The transpiration and soil evaporation components were then added together to give ET.

The separation of ET into E and T and their mutual interrelationship forms an important problem in water management. Modern precision techniques of irrigation application and methods of evaporation and transpiration control now being developed, require this information to allow their effect on evapotranspiration to be evaluated. One of the promising approach to achieving this separation is to treat the soil-plant-atmosphere continuum as an energy and mass exchange system. Therefore the objectives of this paper were to:

1. Develop a mechanistic model, that treats soil evaporation and transpiration as separate processes, for predicting the water use and microclimate of a well watered developing crop, where the soil surface may go through cycles of wetting and drying.
2. Develop solution for the mechanistic model that will allow its use with normally measured climate variables so that it can be used for practical applications and evaluations.
3. Illustrate with an example the various prediction capabilities of the model
4. Conduct a sensitivity analysis of the model parameters.

Modal Development

In this section the fundamental equations governing the energy exchange between an evaporating body and its surroundings are presented. The discussion will explain how the energy exchanges in the canopy and soils are integrated, and assumptions involved. The proposed model includes a number of rarely measured canopy and soil attributes, so algorithms and theory required to obtain them from some commonly measured inputs will be presented.

Fundamental Equations

The evaporation and temperature of a single leaf can be predicted from its energy balance if the resistances to heat and vapor transfer from the leaf are known. Since the photosynthetic heat flux and time rate of canopy heat storage are usually small compared to other energy balance terms, the principal of energy balance states that the net radiation (RN) absorbed goes into latent (L) heat (evaporation or dew), and the balnce goes into sensible (S) heat (heating or cooling of air). The latent heat flux density from a leaf is proportional to the water vapor concentration gradient between the inside of the leaf and turbulent air just outside the boundary layer and is inversely proportional to the sum of the stomatal and boundary layer resistance. Similarly, sensible heat flux density is given by temperature gradient across the boundary layer resistance. Mathematically,

$$RN = L + S \tag{3.1}$$

$$L = \frac{C_p}{\gamma} \frac{a\,(T_s) - e_a}{r_s + r_b} \tag{3.2}$$

$$S = C_p \frac{T_s - T_a}{r_b} \tag{3.3}$$

Where C_p is the volumetric heat capacity of the air, γ is the psychrometric constant, $a(T_s)$ is saturated vapor pressure at leaf surface temperature T_s, a_a and T_a are vapor pressure and temperature of the air, and r_s and r_b the stomatal and boundary layer resistances respectivaly. To compute the evaporation loss from the leaf, the sensible heat flux density S, is replaced by mathematical substitution using the saturation vapor pressure vs. temperature relationship,

$$\begin{aligned} a(T_s) - a_a &= \Delta (T_s - T_a) + (a(T_a) - a_a) \\ &= \Delta (T_s - T_a) + D \end{aligned} \tag{3.4}$$

that gives

$$L = \frac{\Delta (RN \ \ ) + C_p D/r_b}{\Delta + \gamma (1 + r_s/r_b)} \tag{3.5}$$

where D is vapor pressure deficit or dryness of the air. Monteith (1965) for the benefit of simplicity ignored the vertical dimension of the canopy and used the single leaf model to estimate latent heat loss from a canopy at full cover by replacing single leaf resistances with corresponding canopy resistances. Also the net radiation absorbed by the canopy was computed by subtracting soil heat flux, G, from the net radiation above the canopy. Accordingly, the latent heat loss from a canopy was given by

$$L = \frac{\Delta (RN - G) + C_p D / RB}{\Delta + \gamma (1 + RS/RB)} \tag{3.6}$$

where RA and RS are the canopy aerodynamic and surface resistances to heat and vapor flow respectively. Monteith computed the canopy surface resistance to vapor transport, RS as the mean resistances of various layers of leaves acting in parallel. Thus if r_s is the mean stomatal resistance (considering top and bottom surfaces acting in parallel), and the canopy with leaf area index of LAI, RS becomes,

$$RS = r_s/LAI \tag{3.7}$$

Eqn. (3.7) relates changes in the canopy resistance with the crop development and consequently the water loss through Eqn. (3.6). Therefore Eqn. (3.5) could be applied over the entire growing season, provided that (RN-G) is replaced by energy absorbed by the canopy only. However, a similar model for soil evaporation and soil resistance was lacking which made it difficult to apply the energy balance equations to soils except when the soil was saturated or dry. A model of soil evaporation using expressions to characterize soil resistance was developed and tested in Chapter II. Therefore it is now possible to combine Monteith's canopy model with the soil evaporation model along with an appropriate energy distribution model to develop an integrated soil-canopy model applicable over the entire range of growing season.

Implicit in Eqn (3.5) is the assumption that the entire canopy acts as a single isothermal sink for total absorbed energy, Rn-G. On the contrary this assumption is rarely true except may be for canopies with low LAI. In reality the canopy behaves as multiple sources and sinks distributed throughout the canopy depending upon distribution of radiation absorption and stomatal resistances. Roughly, the state of leaves in the canopy can be described as either sunlit or shaded that

change dynamically as a function of sun elevation, row geometry, canopy extinction characteristics and LAI. As a result, only a fraction of LAI is exposed to direct radiation, while remaining LAI experiences only the diffuse radiation. Since the amount of light incident on a leaf affects its stomatal resistance, the sunlit and shaded leaves should be distinguished to obtain more accurate estimates of transpiration. Sinclair et al. (1976) developed a "big leaf" model where the canopy was mathematically condensed into a single plane, with all leaves exposed to same microenvironment. They calculated the stomatal resistance of the sunlit and shaded leaves separately and summed it with the boundary layer resistance in series. RS was obtained by summing in parallel the total resistances of sunlit and shaded leaves weighted by their respective leaf areas. More recently Shuttleworth and Wallace (1985) have theoretically shown how to integrate one zone canopy model of transpiration with soil evaporation to develop an integrated ET model applicable over entire growing period.

The Combined ET Model

In the approach presented here, the canopy was divided into sunlit and shaded leaves with leaves in each zone at different leaf temperatures. The two zone canopy structure integrated with the soil substrate is presented as an electrical analog in Fig. 3.1. The model is valid for a non-stressed crop where the soil may go through cycles of drying and wetting due to irrigation or precipitation events. This representation, consisting of potential and current sources and resistors greatly helps setting the system of equations and solving it for various energy fluxes. There are three zones to be considered

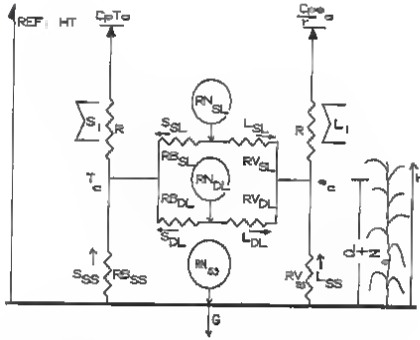

Fig. 3.1 Schematic of the evapotranspiration model for incomplete and complete canopies presented as an electrical analog.

the soil zone, the sunlit canopy zone and the shaded canopy zone. In each zone there is a current source of net radiation which is balanced by the sensible (S) and latent heat (L) fluxes The driving forces (potential sources) for the sensible heat flux and the latent heat flux away from the canopy are shown as $C_p T_a$, and $C_p e_a / \gamma$ where T_a and e_a are the temperature and vapor pressure at the reference height above the canopy (usually 2m for agronomic crops).

The microclimate in the canopy was assumed to differ from the ambient conditions above the canopy. Lack of this consideration leads to underestimation of fluxes as found by Sinclair et al. (1976). It was assumed that the aerodynamic mixing within the canopy can be sufficiently good so that the microclimate of the canopy was described by one value of temperature and humidity and its location corresponded to the mean canopy airstream height (Lemon, 1966, Thom, 1972). Models based on this assumption have been previously tested (Black et al., 1970; Sinclair et al., 1976). Within each zone the exchange of sensible and latent heat occurs in response to the temperature and vapor pressure gradients between the mean canopy air flow height and the mean surface properties of the three zones respectively.

To develop the energy balance equation it is generally assumed that the canopy is homogeneous in the horizontal direction and horizontal fluxes are much smaller relative to the vertical fluxes of energy exchange so that they can be ignored. The vertical transfer of vapor and heat between the canopy air stream and the air was proportional to the vertical differences in humidity and temperature and it was controlled by a bulk aerodynamic resistance, R. Based on the electrical analog, and the principle of energy balance, the model shown in Fig.

3.1 can be mathematically described by the fundamental equations as follows.

Zone of sunlit leaves.

$$RN_{sl} = L_{sl} + S_{sl} \tag{3.8a}$$

$$L_{sl} = \frac{C_p}{\gamma} \frac{e\,(T_{sl}) - e_c}{(RS_{sl} + RB_{sl})} \tag{3.8b}$$

$$S_{sl} = C_p \frac{T_{sl} - T_c}{RB_{sl}} \tag{3.8c}$$

Zone of shaded leaves.

$$RN_{dl} = L_{dl} + S_{dl} \tag{3.9a}$$

$$L_{dl} = \frac{C_p}{\gamma} \frac{e(T_{dl}) - e_c}{(RS_{dl} + RB_{dl})} \tag{3.9b}$$

$$S_{dl} = C_p \frac{T_{dl} - T_c}{RB_{dl}} \tag{3.9c}$$

Soil surface.

$$RN_{ss} - G = L_{ss} + S_{ss} \tag{3.10a}$$

$$L_{ss} = \frac{C_p}{\gamma} \frac{e(T_{ss}) - e_c}{(RS_{ss} + RB_{ss})} \tag{3.10b}$$

$$S_{ss} = C_p \frac{T_{ss} - T_c}{RB_{ss}} \tag{3.10c}$$

Similarly exchange between the mean canopy airstream height and the

reference height is given by

$$L_{sl} + L_{dl} + L_{ss} = \frac{C_p}{\gamma} \frac{e_c - e_a}{R} \qquad (3.11a)$$

$$S_{sl} + S_{dl} + S_{ss} = C_p \frac{T_c - T_a}{R} \qquad (3.11b)$$

Where T_i are the temperature (subscript a=air, c=canopy, sl=sunlit leaves, dl=dark leaves, ss=soil surface), RB_i and RS_i the sunlit and shaded leaf ensemble boundary layer and surface resistances to heat and vapor transfer (the sum of RB + RS will be denoted by RV, total resistance to vapor transfer), R the turbulent eddy diffusive resistance to vertical transfer, $e(T_i)$ are the saturated vapor pressure at temperature T_i and RN_i are the net radiation absorbed at each zone.

The soil resistance RS_{ss} in s/m was defined in Chapter II as

$$RS_{ss} = 154 \left\{ e^{(\alpha + \beta RN_a)\left\{ CE_n - CE_c \right\}^{\eta}} - 1 \right\} \qquad (3.12)$$

$\alpha = 1.0942 * 10^{-3}$, $\beta = 2.0197 * 10^{-3}$ and $\eta = 1.36757$ were empirically determined constants for the sandy soil in this study. RN_a was the average daily net radiation (mm of water) since beginning of the drying period but RN_a should not go below 2 mm. CE_n was normalized cumulative evaporation (in %) obtained by dividing cumulative evaporation in mm by potential cumulative evaporation (CE_p=18.5 mm for fine sand initially at the field capacity water content) associated with last water application event, and CE_c was the critical value of CE_n when stage one of soil evaporation ends(CE_c=15% of CE_p for Arredando fine sand). Procedures on how to obtain these parameters for specific soils were discussed in Chapter II.

Distinguishing Between Sunlit and Shaded Leaves

The relative contribution of sunlit and shaded leaves to canopy transpiration depends upon the LAI, at small LAI most water loss would be expected from the sunlit leaves while at full canopy the shaded leaves may make substantial contribution. In practice only the net radiation above the canopy (measured or computed) and leaf area index could be easily supplied, while the radiation regime within the canopy, the resistances, as well as sunlit and shaded LAI's are rarely measured. The following sections describe procedures to determine these unknowns.

The total LAI, LAI_t, can be apportioned into sunlit LAI (LAI_{sl}) and shaded LAI (LAI_{sh}) using Beer's law. Accordingly, the net radiation RN_{LAI} falling on a horizontal surface below leaf area index of LAI is related to the net radiation above the canopy (RN), and the canopy extinction coefficient K

$$RN_{LAI} = RN * \exp(- K*LAI) \qquad (3.13)$$

The ratio (RN_{LAI}/RN) is also equal to the fractional area of sunlit leaves on a horizontal surface below the LAI. Therefore the total area of sunlit leaves in the canopy is obtained by integrating Eqn. (3.14) from top (LAI=0) to bottom (LAI=LAI_t).

$$RN_{LAI}/RN = \exp (-K*LAI) \qquad (3.14)$$

$$LAI_{sl} = \int_0^{LAI_t} \exp (- K * LAI) \, d (LAI) \qquad (3.15)$$

$$LAI_{sl} = (1/K)*(1. - \exp(-K*LAI)) \quad (3.16a)$$

and $$LAI_{dl} = LAI_t - LAI_{sl} \quad (3.16b)$$

Similarly, the net radiation captured by the sunlit canopy (RN_{sl}) and that reaching the soil surface (RN_{ss}) is radially obtained from Eqn. (3.13)

$$RN_{sl} = RN * (1 - \exp(-K*LAI_t)) \quad (3.17)$$

$$RN_{ss} = RN * \exp(-K*LAI) - RN_{dl} \quad (3.18)$$

where RN_{dl} is the net radiation received by the shaded leaves. An empirical expression relating RN and RN_{dl} was developed using measurements in a fully developed well-watered soybean canopy. Accordingly, RN_{dl} was computed as

$$RN_{dl} = 0.05 * RR * K * LAI_{dl} \quad (3.19)$$

Leaf Resistance

To apply the fundamental Eqns. (3.1-3.7) to the sunlit and shaded regions of the canopy, individual leaf stomatal and boundary layer resistances are required. The stomatal diffusive conductance was expressed as a function of photosynthetic photon flux density (PPFD)

$$C = C_{max}(1 - \exp(-s * PPFD / C_{max})) \quad (3.20)$$

and $$r_s = 1/C \quad (3.20b)$$

Where C_{max} was the maximum conductence, and s the initial slope of C vs PPFD. All the parameters in Eqn. (3.20) are inputs to the model. However, the PPFD on the shaded leaves is usually not available. Due to lack of better information, similar to RN_{dl}, a locally developed empirical function to compute the PPFD on shaded leaves was used. Consequently, PPFD on shaded leaves was computed as 5% of the above

canopy PPFD. The mean stomatal resistance of the sunlit and shaded leaves was obtained by substituting their respective PPFD in Eqn. (3.20).

The individual leaf boundary layer resistance was assumed constant at 10 s/m in this model. Under field conditions it may vary with leaf geometry, but for a plant community as a whole, it will be always under 100 s/m and will probably range from 6 to 50 s/m (Jackson, 1982, Monteith, 1973). It will be shown later that the model is not very sensitive to the leaf boundary layer resistance and the value selected is an appropriate approximation.

The leaf ensemble resistances of sunlit and shaded leaves were obtained using LAI_{sl} and LAI_{dl} in Eqn. (3.7)

Diffusion Resistance

In the model two additional diffusive resistances, Rbss from the soil to the mean canopy airstream and R from there on up to the reference height were introduced. The diffusion resistances depend upon the wind speed distribution within and above the canopy. According to Thom (1972) turbulent eddy diffusive resistance between two heights z_1 and z_2 is obtained by following equation:

$$R = \int_{z_1}^{z_2} (1/\phi)\, dh \qquad (3.21)$$

where ϕ is the eddy diffusivity coefficient. ϕ above a fully developed crop of height H is given by,

$$\phi(H) = k^2 U (H - d)/ \ln [(z - d)/z_0] \qquad (3.22)$$

where k is the von Karman's constant (0.4), d is the zero plane displacement height, z is the reference height (2 m), and z_0 is the roughness characteristic of the vegetation. The size of z_0 specifies the bulk effectiveness of vegetation as a momentum absorber, while d can be considered to indicate the mean level at which momentum is absorbed by the plant community. Thus in crops of uniform height, $(d + z_0)$ defines the height where mean canopy flow conditions apply. In practice d is found by plotting U(z) against ln (z-d), for various d values until the value of d for which a straight line plot results is the accepted value of d. The z_0 can be then found from the intercept of this straight line on the ln(z-d) scale. Stanhill (1969) found a relationship between d and H and Szelcz et al. (1969) found a relation between z_0 and H valid for a number of crops,

$$d = 0.7\ H \tag{3.23a}$$

$$z_0 = 0.13\ H \tag{3.23b}$$

The wind speed and the diffusivity coefficient are assumed to extinguish exponentially with height (h) in the canopy (Lemon, 1965, Thom, 1972) and it is given in terms of the velocity attenuation coefficient n

$$\delta(h) = \delta\ (H)\ \exp\ (\ -n\ (H - h)\ /H\ ) \tag{3.24}$$

For most agricultural crops n varies between 2 to 4 (Lemon, 1965). R can be computed by integrating Eqn. (3.21) first from $d+z_0$ to H and then from H to z (see Fig. 3.1 for details) with diffusivity coefficient given by Eqn. (3.22) and (3.24) and d and z_0 by Eqn. (3.23).

$$R = \int_{d+z_0}^{H} \frac{dh}{\delta(h)} + \int_{H}^{z} \frac{dh}{\delta(H)} \tag{3.25a}$$

$$R = \frac{\ln [\ (z-d)/z_o\ ]}{k^2\ U}\ [\ \ln [(z-d)/(H-d)\ ] + \frac{H}{n(H-d)}(C_6 - 1)] \qquad (3.25b)$$

Similarly, RR_{ss} can be obtained as

$$RR_{ss} = \int_{z_o}^{d+z_o} \frac{dh}{k\ (h)} \qquad (3.26a)$$

$$RR_{ss} = \frac{\ln [\ (z-d)/z_{o'})]}{k^2\ U}\ \frac{H}{n\ (H-d)}\ [\ C_7 - C_6\ ] \qquad (3.26b)$$

where $C_6 = \exp [\ n(H - d - z_o)/H]$ and $C7 = \exp [\ n(H - z_{o'})]$.

For bare soil R and RR_{ss} are given by Eqns. (3.27) and (3.28).

$$R = \ln (z/z_o^{\prime})\ \ln (z/(d+z_o))/\ k^2U \qquad (3.27)$$

$$RR_{ss} = \ln(z/z_{o'})\ \ln[(d+z_o)/z_{o'})]/\ k^2U \qquad (3.28)$$

where $z_{o'}$ was the roughness height of the soil, normally taken as the clod height or in flat fine sand we assumed it 0.01 m. In deriving Eqns. 3.27 and 3.28 it was assumed that the height of mean canopy airstream remains at $(d+z_o=0.83H)$ for both the bare soil and fully developed canopy.

The effect of crop height at full canopy on water balance will be farther discussed in the sensitivity analysis section. For the time being it can be stated that for short crops this assumption will not have much quantitative effect on the water balance components. The validity of this assumption especially for bare soil and tall crops may be questionable. Sinclair et al. (1976) used different estimates of mean source/sink heights for sensible $(d+z_o=0.75H)$ and latent

$(d+z_o=0.5H)$ heat respectively. There is no doubt that the crop height and planting density will have some effect on RB_{ss} and R, however at this time there is no quantitative information available to characterize this effect. However if the information on the variation of mean source/sink height with canopy height is available one can use Eqns. (3.25) and (3.26) to compute R and RB_{ss}. In the model presented, R and RB_{ss} were computed at full canopy height and bare soil using user-specified mean wind speed and their values at intermediate stages were computed using linear interpolation between the two limits. Following the stage of full canopy, the source sink height remained constant at 0.83H, and Eqns. (3.25) and (3.26) were used to compute R and RB_{ss} in response to varying wind speed.

Model Solution

The model was described by eleven simultaneous equations (Eqns. 3.8-3.11). The model has a total of twelve unknowns- four temperatures (T_{s1}, T_{d1}, T_{ss}, and T_c), vapor pressure e_c, three latent and 3 sensible heat fluxes, and soil heat flux G. This system of equations can be solved only if one of the twelve unknowns is known or using an iterative solution. Here both the solution scenarios are presented.

First we will show how to eliminate T_c and e_c by mathematical substitution using the saturation vapor pressure vs. temperature relationship (Eqn. 3.4) to obtain three simultaneous equations dependent on surface temperatures. Substituting for e_c using Eqn. (3.11e) in Eqns. 3.8b, 3.9b, and 3.10b and then using the definition of Δ from Eqn. 3.4, these three equations can be written in matrix form.

$$\begin{bmatrix} R+RV_{s1} & R & R \\ R & R+RV_{d1} & R \\ R & R & R+RV_{ss} \end{bmatrix} \begin{bmatrix} L_{s1} \\ L_{d1} \\ L_{ss} \end{bmatrix} = C_2 \begin{bmatrix} T_{s1}-T_a \\ T_{d1}-T_a \\ T_{ss}-T_a \end{bmatrix} + C_3 \begin{bmatrix} D \\ D \\ D \end{bmatrix}$$

or simply

$$[\ RL\ ][L_f] = C_2\ [T_1-T_a] + C_3{}^*D$$

Since all the elements of [RL] are known, both sides can be multiplied by the inverse [iRL] of [RL] to obtain an equation in L's. Therefore.

$$[L_f] = C_2\ [iRL]\ [T_1-T_a] + C_3{}^*D\ [iRL] \qquad (3.29a)$$

Similarly T_c can be replaced from Eqns. 3.8c, 3.9c, and 3.10c using Eqn. (3.11b), to obtain a matrix for sensible heat.

$$\begin{bmatrix} R+RB_{s1} & R & R \\ R & R+RB_{d1} & R \\ R & R & R+RB_{ss} \end{bmatrix} \begin{bmatrix} S_{s1} \\ S_{d1} \\ S_{ss} \end{bmatrix} = C_1 \begin{bmatrix} T_s-T_a \\ T_{d1}-T_a \\ T_{ss}-T_a \end{bmatrix}$$

or $[\ RS\ ][S_f] = C_1\ [T_1-T_a]$

and $[S_f] = C_1\ [iRS]\ [T_1-T_a] \qquad (3.29b)$

Where $C_1=C_p$, $C_2=C_1/Y$ and $C_3=AC_2$. [RL] and [RS] are the matrices of latent heat and sensible heat associated resistances, with inverse [iRL] and [iRS], $[T_1-T_a]$ is a matrix of temperature differences between each of the three surfaces and air at the reference height. Finally substituting Eqn. (3.29a) and (3.29b) in the energy balance Eqns. (3.8a, 3.9a, and 3.10a, gives

$$[RN_f] = [L_f] + [S_f] \qquad (3.29c)$$

Rearranging the terms after substitution gives the desired set of three simultaneous equations.

$$\begin{bmatrix} T_{s1}-T_a \\ T_{d1}-T_a \\ T_{ss}-T_a \end{bmatrix} = [iC_4] \begin{bmatrix} RN_{s1} \\ RN_{d1} \\ RN_{ss}-G \end{bmatrix} - [C_5] \qquad (3.30)$$

where $[IC_4] = C_1\ [IRS] + C_2\ [IRL]$ and $[C_5] = C_3 * 0\ [IRL]$. Eqn. (3.30) is a set of three simultaneous equations with four unknowns G, T_{ss}, T_{sl} and T_{dl}.

Case I: Known Soil Surface Temperature

Among the four unknowns, soil surface temperature T_{ss} is perhaps the easiest to measure. With the soil temperature known, first G can be obtained from Eqn. (3.30) after rearranging.

$$G = \{IC_{4,31} * RN_{sl} + IC_{4,32} * RN_{dl} - C_{5,31} + T_e - T_{ss}\}/IC_{4,33}$$

where $IC_{4,jk}$ stands for element in the j'th row and k'th column of inverted matrix $[C_4]$. A similar explanation follows for $C_{5,31}$. Knowing G, first the sunlit canopy temperature (T_{sl}) and the shaded canopy temperature (T_{dl}) are obtained from Eqn. (3.30). These temperatures when substituted in Eqns. (3.29a) and (3.29b) give the latent and sensible heat fluxes. Finally to complete the solution, Eqns. (3.28a) and (3.29b) are used with known fluxes of L_l's and S_l's to obtain temperature T_c and vapor pressure e_c describing the mean canopy microclimate. Thus E, T and ET at any time is obtained by dividing the respective latent heat flux density with latent heat of vaporization.

$$ET = (L_{ss} + L_{sl} + L_{dl})/\lambda \qquad (3.31a)$$

$$E = Lss/\lambda \qquad (3.31b)$$

$$T = (Lsl + Ldl)/\lambda \qquad (3.32c)$$

Case II Unknown Soil Surface Temperature

In many situations soil temperature is not known and an iterative scheme is needed to solve Eqn. (3.30). In the iterative scheme first G would be guessed to obtain surface temperature from above ground

Eqn. (3.30), say $T_{ss,a}$. Since the above ground and below ground processes are coupled, soil surface temperature can also be obtained from a heat balance of soil surface using a numerical model of layered soil, say $T_{ss,b}$. When these two temperatures agree with each other within a certain error bound the convergence criteria is met.

To develop the general purpose numerical sub-model of heat flow, the soil was represented by e nine layers varying in thickness from 0.1 to 0.4 m (Fig. 3.2). The heat flow rate in and out af a layer is calculated from the temperature difference between adjacent layars and the the thermal conductivity. The instantaneous heat flow rates are realized over a small time interval, and based on tha principle af conservation af energy, the net change (input-output) in heat is used to obtain the valumetric heat content af each layer e finite instant af time later. The calculations are then repeated for the next time step (De Wit and van Keulen, 1972). It was assumed that the soil surface temperature varies in response to the energy balence af the top soil layer, and there is no heat flow across the bottom at 2.1 m depth.

Therefora, if the soil surfece temperature is T_{ss}, the heat flow G into the top soil layer af thickness T_1, temperature $T_{ss,1}$ and thermal conductivity K_t is given by:

$$G = K_t (T_{ss} - T_{ss,1})/T_1 \qquad \text{,a}$$

ar $$T_{ss} = T_{ss,1} + (T_1/K_t)G \qquad \text{,b} \qquad (3.33a)$$

Initially (at time=0) $T_{ss,1}$ is known from the initial condition and at times greater that zero, it is again known from the previous step calculatians. Therefare from known G and $T_{ss,1}$, soil surfece tempera-

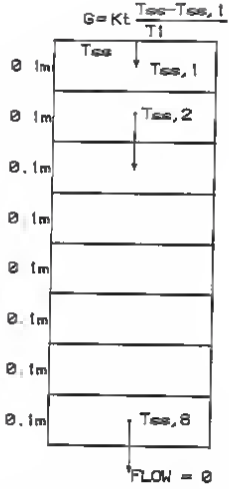

Fig. 3.2 Schematic of the numerical heat flow model of the soil. The soil was divided into a number of layers, and the heat flow was proportional to the temperature gradient between the centers of adjacent layers.

ture can be obtained from below ground calculation using Eqn. (3.33a). If $T_{ss,a}$ and $T_{ss,b}$ are equal within some tolerance limit we have the right magnitude of G and all remaining unknowns can be obtained as outlined in the earlier section above. Usually, they will be different and few iterations would be necessary. The aim of the iteration scheme is to find an increment of G that will make above ground computed soil temperature $T_{ss,a}$ and $T_{ss,b}$ equal. This can be done with the idea suggested by Chen (1984). Let the required increment of G be denoted as G' and the corresponding surface temperature T_{ss}'. then we can write

$$T_{ss}' = T_{ss,a} + (dT_{ss,a}/dG)\ G' \qquad (3.33b)$$

and

$$T_{ss}' = T_{ss,b} + (dT_{ss,b}/dG)\ G' \qquad (3.33c)$$

where $dT_{ss,a}/dG$ and $dT_{ss,b}/dG$ denotes the derivative of $T_{ss,a}$ and $T_{ss,b}$ with respect to G respectively. Eliminating T_{ss}' from Eqns. (3.33b) and (3.33c) the increment for G can be found as

$$G' = (T_{ss,a} - T_{ss,b}) \,/\, (dT_{ss,b}/dG - dT_{ss,a}/dG) \qquad (3.33d)$$

Expression for $dT_{ss,b}/dG$ can be readily obtained from Eqns. (3.33a) and $dT_{ss,a}/dG$ can be obtained by first combining Eqns. (3.10a-c) and then differentiating with respect to G:

$$(T_{ss,a} - T_c)\, C_p \left(\frac{\Delta}{RV_{ss} * \gamma} + \frac{1}{RH_{ss}}\right) = RN_{ss} - G - C_p \frac{e\,(T_c) - e_c}{RV_{ss}}$$

$$\text{or } dT_{ss,e}/dG = (-\gamma/C_p)\, RB_{ss} * RV_{ss} / (\Delta RB_{ss} + \gamma RV_{ss}) \qquad (3\ 33e)$$

thus G' can be computed at each step to obtain the next value of G and continue this iteration procedure until the error between $T_{ss,e}$ and $T_{ss,b}$ is within certain limit. When the convergence criterion is met, the soil temperatures of all layers are computed using the numerical model.

The iteration scheme outlined above converges quickly. Calculations have shown that with the top layer of 0.01 m thickness and 30 minute time step, two iterations were needed to get convergence within 2%. The solution method presented above requires repeated matrix inversion operations which may also be feared to slow the computations. However since we are dealing with only a 3x3 matrix this is not expected to be a problem if a proper matrix inversion method is used. The Ganss-Jordan elimination procedure with pivoting strategy was used in the present model.

Model Inputs/Outputs

The model inputs were grouped into three groups- the weather conditions, plant specific variables, and soil specific variables. The parameters which remain constant are indicated by a star in the front.

Weather Variables

Weather parameters needed are

1. Net radiation (RN) in w/m^2
2. Photosynthetic photon flux density (PPFD) in $\mu E/m^2$-sec
3. Air temperature (T_a) in °C
4. Dew point temperature in °C

5. Wind speed (U) in m/sec

Plant Variables

Plant characteristics required are

1. Leaf area index (LAI)
2. * Canopy light extinction coefficient (K)
3. * LAI, at full canopy
4. * Height at full canopy (H) in m
5. * Wind attenuation factor (n)
6. * Maximum stomatal conductance (C_{max}) in m/s
7. * Initial slope of conductance vs. PPFD (s) in m^3/ μ E

Soil Variables

Soil characteristics:

1. * Constants α, β and n in the RS_{ss} model
2. * Critical value of normalized cumulative evaporation (CE_c) in %
3. * Potential soil evaporation (CE_p) in mm
4. * Thickness of evaporation zone in m
5. * Soil roughness height (z_0') in m
6. Thermal conductivity of soil as a function of water content in J/m-sec-°C
7. Heat capacity of the soil as a function of water content in J/m^3- °C.
8. * Number of soil layers and their thicknesses in m
9. * Error bound if iterative solution is desired
10. Initial soil temperatures in °C
11. Initial soil water content by layer on volumetric basis
12. * Field capacity water content by layer on volumetric basis

13. * Lower limit of soil water extraction by layer on volumetric basis

Outputs

The main output variables are listed here. Other variables may be outputed as per objectives.

1. E, T and ET
2. Temperatures of sunlit, shaded canopy zones
3. Soil surface temperature
4. Mean canopy temperature and vapor pressure

Organization of The Model

The model was written in FORTRAN 77 and was organized in modular form so that it would be easier to integrate it with other models or into other models. Program MAIN is the driver and calls other subroutines. Common blocks were used to share information between various subroutines. Two output routines, one daily and one seasonal are included to obtain a variety of output variables. The flow chart of the model is presented in Fig. 3.3.

The model begins with initializing certain key variables such as seasonal evapotranspiration, evaporation and transpiration. The time invariant variables are read next in the subroutine FIXED1 (FIXED input) from the input file. One of the constants read in this routine is a key for selection of the solution method outlined earlier (KEY=1 solution for known soil surface temperature, KEY=2 for unknown soil surface temperature).

At the beginning of each day, half hourly weather data beginning at 0.5 hours for air temperature, dew point temperature, net radiation, PPFD, wind speed, soil surface temperature (if KEY=1) is

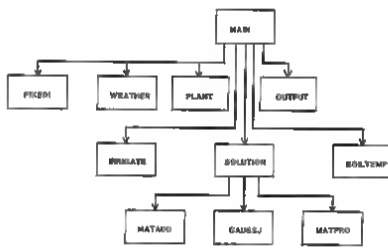

Fig. 3.3 Overall flow chart of the evapotranspiration model showing information flow and organization of the subroutines.

read in the subroutine WEATHER. Next subroutine PLANT reads LAI once every day. At the present time subroutine IRRIGATF is called at user specified irrigation frequency. It is assumed that irrigation amount is adequate to refill the soil profile to its field capacity. Soil temperature in each layer (if KEY=2) is updated using weighted soil and irrigation water temperature by assuming that irrigation water was at air temperature. Cumulative soil evaporation (CE) and cumulative running average radiation on soil (RNa) are initialized to zero.

During the day at each time step, RN_{sl}, RN_{dl}, RN_{ss}, LAI_{sl}, LAI_{dl}, RV_{sl}, RV_{dl}, RV_{ss} are computed in the MAIN program. Subroutine SOLUTION includes all equations and steps described in the solution section. It calls three other subroutines to perform intermediate calculations. Subroutine GAUSSJ is a matrix inversion algorithm based upon the Gauss-Jordan elimination method using pivoting strategy. Subroutines MATPRO, and MATADD perform matrix multiplications and additions respectively. Subroutine SOLUTION returns L_{sl}, L_{dl}, L_{ss}, S_{sl}, S_{dl}, S_{ss}, G, T_{sl}, T_{dl}, T_{ss} (if KEY=2), T_c and e_c values to the MAIN program. If KEY=2 soil temperatures are computed in the subroutine SOILTEMP.

The diurnal energy balance components are integrated in the subroutine OUTPUT (OUTPUT). Additional calculations performed by the routine include

- Difference between canopy mean temperature and air at 1000 h
- Maximum and minimum mean canopy temperature
- Maximum and minimum soil surface temperature

The user may need to modify this routine to obtain specific outputs.

Water lost to evapotranspiration is used to update the soil water

in the evaporation zone. Since the crop is assumed well watered, water content below the evaporation zone remains at the field capacity. Soil evaporation occurs entirely from the evaporation zone. Transpiration loss may also occur from the evaporation zone. If so, the user defines a table look-up-function which includes fraction of transpiration coming from the evaporation zone as a function of LAI. It is possible to change this functional form, say, to days after planting instead of LAI. This feature is included so that rooting patterns specific to a crop, soil and management practice could be incorporated in the model.

At the end of the day, the output routine OUTPUT is called to generate daily summary. Then the next day's weather and LAI is read and all the calculations are repeated. This process continues until the end of the growing season.

Model Applications

This model has a variety of potential applications to water management. In this section a brief highlight about short and long term model predictions is presented for an example of soybean crop The soybean crop was assumed to be grown in the constant weather conditions shown in Fig. 3.4 The model SOYGRO (Wilkerson et al. 1983) was used to generate the leaf area index for the variety 'Bragg', irrigated throughout the season. The crop reached full cover (LAI=3.5) after 49 days and attained maximum LAI of 5.56 after 66 days in the growing season. At full canopy the height of the crop was assumed 0.5 m, had light extinction characteristics of a spherical leaf angle distribution (K=0.5), with velocity attenuation coefficient n=3. The stomatal conductance data reported in Chapter IV was used to

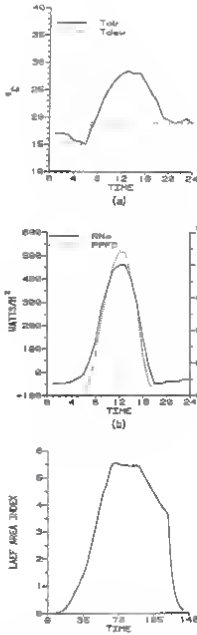

Fig. 3.4 Diurnal variation in air temperature, dew point temperature, net radiation, PPFD, and leaf area index as a function of days after planting used in the simulation.

estimate the canopy leaf ensemble resistance RS_{sl} and RS_{dl}. Using the wind velocity of 1.5 m/s, R and RS_{ss} were calculated to be 34.5 and 82.5 s/m for bare soil and 42 s/m and 296 s/m at full canopy. r_b the leaf boundary layer resistance was assumed 10 s/m and held constant throughout the simulation.

Diurnal Model Predictions

Two diurnal simulations were performed. The canopy LAI was 2.0 and in the first case the soil surface was saturated (daily irrigation) whereas in the second case it was dry (no irrigation). It was expected that with dry soil surface and no soil evaporation, the humidity in the canopy would be lower and transpiration should increase. The changes in the overall energy balance above the canopy, in the canopy and at the soil surface, and canopy temperature and vapor pressure were compared (Fig. 3.5) to show model predicted interactions between the canopy microclimate and the canopy and soil.

Energy balance components when the soil was wet indicate that, the T from the canopy was negligible because of high leaf resistance, but soil evaporation occurred due positive vapor pressure gradient. The pre-dawn soil evaporation cooled the soil surface, lowered vapor pressure gradient, and soil evaporation got progressively smaller. With a rise in the net radiation, and air temperature, both soil evaporation and transpiration increased simultaneously. For most of the day, the net radiation intercepted by the canopy exceeded energy dissipated by transpiring water. Due to the wet surface, soil surface temperature remained cooler than the mean canopy temperature (negative sensible heat transfer during the day time), and soil evaporation was low. The evaporation occurred mainly in response to the

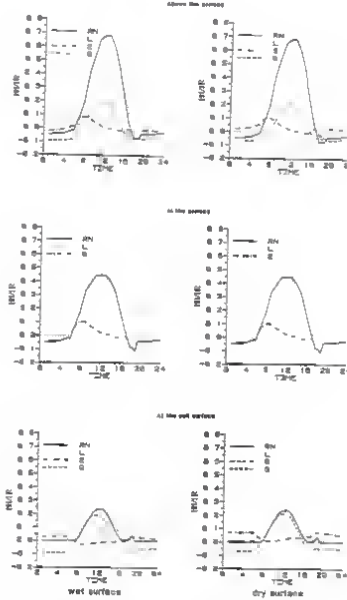

Fig. 3.5 Comparison of simulated diurnal energy balance above the soybean canopy, within the canopy and at the soil surface for a wet and dry soil surface conditions.

vapor pressure gradient. Due to low soil temperature early in the day, the excess net radiation was stored as soil heat. As the net radiation and air temperature decreased, there was a inversion in the soil heat flux. The transpiration dropped rapidly with net radiation. However due to slow cooling of the soil, soil evaporation decreased very gradually. For the 24 hours of simulation, in terms of amount of evaporated water, the canopy intercepted an equivalent of 2.74 mm of net radiation, had transpiration of 2.84 mm and sensible heat of -0.1mm. Similarly, at the soil surface 1.31 mm of net radiation was distributed among evaporation 1.20 mm, sensible heat 0.16 mm, and soil heat flux -0.05 mm.

The energy balance above the canopy summarizes energy distribution within the canopy and at the soil surface. In summary, most of the energy available (4.05 mm) was expended for ET (4.04 mm) and a negligible fraction went into the sensible heat. Therefore over a day, the heat flux into the soil was practically zero.

The energy balance with dry soil surface was similar. Due to zero soil evaporation, soil surface was warmer than the canopy air (positive sensible heat flux). Also the heat flux into the soil was higher, 0.27 mm compared to -0.05 mm with the wet surface. The ET was low and concurrently the humidity was low (Fig 3.6b) while canopy temperature was higher (Fig 3.6a). The ET was reduced from 4.04 mm to 3.11 (23% lower), however the transpiration was higher by about 10 % (3.11 mm vs. 2.84 mm) due to lower humidity. The combination of high canopy temperatures and low humidity caused slight increase in the sunlit leaf temperatures (Fig 3.7a). The main effect of wet versus dry surface was visible on the daily course of soil surface

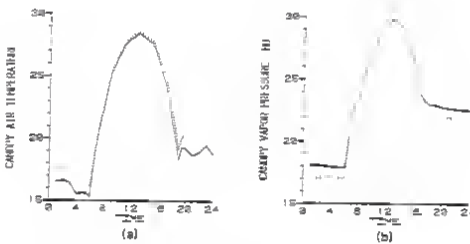

Fig. 3.6 Comparison of simulated canopy air temperature and canopy vapor pressure for wet (solid line) and dry (datted line) soil surface conditions.

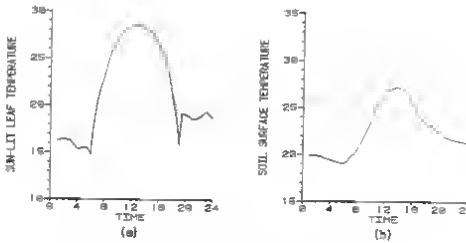

Fig. 3.7 Comparison of sun-lit leaf temperature and soil surface temperature for wet (solid line) and dry (dotted line) soil surface conditions

temperature. In general with dry soil, temperatures were 5 to 6 degrees higher than with wet soil surface.

Long Term ET Predictions

Using the leaf area development data presented in Fig. 3.4c, the model was used to simulate one growing season of soybean. In the first case soybeans were irrigated daily and in the second case weekly. During this simulation it was assumed that there were no roots in the evaporation zone so that it was depleted by soil evaporation alone. The consequence of root water extraction from the evaporation zone is discussed later.

In the daily irrigated experiment, the daily ET rates were almost constant until 119 days after planting (DAPL), which was the day of crop maturity (Fig. 3.8e). Irrigation was terminated at crop maturity. Soil evaporation decreased gradually as the canopy developed and less energy was available at the soil surface. ET during the first 32 days was dominated by soil evaporation. Thereafter, ET continued to decrease and finally became constant when LAI exceeded 5. Following crop maturity soil evaporation increased as LAI dropped and more radiation reached the soil surface, but soon this trend was reversed as the soil became dry.

In the weekly irrigation cycle, the soil surface went through cycles of wetting and drying, as illustrated by the varying amplitudes of E and ET in Fig. 3.8b. It was interesting to see that initially, ET on the irrigated days was higher compared to the daily irrigation cases. This can be explained by examining the variations in the soil surface temperature shown in Fig. 3.9. With progression in drying, the soil surface temperature increased much more than the daily irrig-

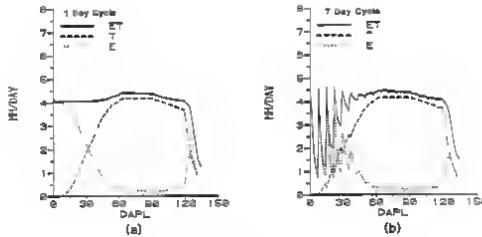

Fig. 3.8 Simulated daily ET, T and E from planting to harvest for the daily and weekly irrigation cycles

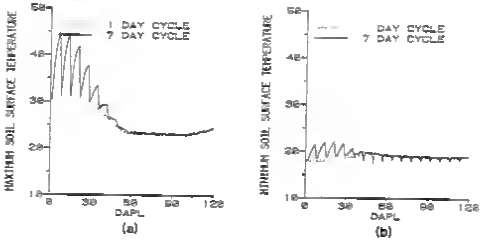

Fig. 3.9 Daily simulated maximum and minimum soil surface temperature under the soybean canopy with daily and weekly irrigation cycles

ated case. Following irrigation, the soil surface was cooled, but remained higher than the daily irrigation case. The higher soil temperature coupled with saturated soil resulted in higher vapor pressure gradient that caused more evaporation. It was also interesting to note the lowering of transpiration rate following an irrigation ("dips" in T curve), due to higher soil evaporation and humidity. The interaction between E and T had mutually compensating effect on ET. The feedback of E on T became less significant at lower E magnitudes.

The seasonal water use with the weekly irrigation cycle was 7% lower than the daily irrigation practice. For example, seasonal E with weekly irrigation was 120.4 mm compared to 163.5 mm with the daily cycle, while the seasonal transpiration less 382.8 mm was slightly higher than 377.6 mm in case of the daily irrigation. For the daily irrigation practice it took 65 days for the cumulative T to equal the cumulative soil evaporation in contrast to 51 days with weekly irrigation.

Soil Temperature

Simulated maximum and minimum soil surface temperatures under the two irrigation frequencies are compared in Fig. 3.9. For the bare soil the maximum temperature varied from 30 to 45 degrees. Similar temperature variation was observed in the bare soil evaporation studies. With canopy development, the amplitude reduced progressively and at LAI exceeding 2.8 it remained practically constant. On the other hand the minimum surface soil temperature varied by less than 5 degrees during the incomplete canopy stage. At high LAI following an irrigation, the soil was cooled temporarily ("dips" in the minimum temperature). The cooler soil produced low soil evaporation as seen

in the Fig 3.8b.

Canopy - Air Temperature

The temperature at the mean canopy source/sink height was assumed to be representative of the mean canopy temperature. The difference between canopy and air temperatures computed at 1000 and 1200 h for the two irrigation are shown in Fig. 3.10. Since the crop was well-watered the differences in the temperature at two times was mainly due to the change in the air temperature relative to the canopy temperature. This temperature is sometimes used to determine water stress on the crops (Ehrler, 1973). These figures reveal that diurnal patterns may occur even in well watered crops.

Root Water Extraction From The Evaporation Zone

In the earlier discussion it was assumed that there were no roots in the evaporation zone. This may not be true in reality. Simulations were performed by assuming that 0 , 25, 50 and 100 % of transpiration was derived from the evaporation zone. The results of seasonal water demand under these situations are summarized below in Table 3.1. As the water was applied every day, the extraction fraction had little effect on the water demand of the daily irrigated treatment. With weekly irrigation cycle, increasing extraction reduced soil evaporation due to quicker drying. On the whole, as long as the crop is able to extract adequate amount of water from deeper depths (except the 100% case above), these results suggest that computed water use of the crop would be little affected by this assumption.

Sensitivity Analysis

In this section model sensitivity to various input parameters listed in the Table 3.2 is examined. For the sensitivity analysis

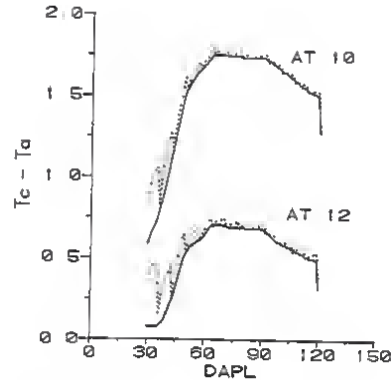

Fig. 3-10 Comparison of canopy to air temperature difference recorded at 1000 and 1200 h

TABLE 3.1 Influence of amount of transpiration occurring from the evaporation zone on the seasonal water use under daily and weekly irrigation cycle.

Extraction %	1 DAY CYCLE Seasonal water use			7 DAY CYCLE Seasonal water use		
	E	T	ET	E	T	ET
	<----- mm -------->			<----- mm -------->		
0	163.5	377.6	541.1	120.4	382.8	503.3
25	160.9	378.5	539.4	111.6	385.1	496.7
50	160.3	379.1	539.4	104.9	386.4	491.3
100	161.6	379.6	541.2	95.5	388.1	483.6

TABLE 3.2 Parameters selected for the sensitivity analysis, and their standard values. Soil thermal conductivity Kt and heat capacity are listed as function of water content.

K	C_{max} m/s	rb s/m	n	H m	Water content %	K_t J/sec-m-°C	H_c J/m³°C
0.5	180	10	3	0.5m	0	0.57400	1.126E6
					13	4.52200	2.663E6

TABLE 3.3 Results of sensitivity analysis for the daily irrigated treatment. For sensitivity analysis one variable at a time was varied and change in ET compared with the standard ET value was computed as a percentage. The ET estimates at standard values are in mm/day. The variables are listed along with their values.

		LAI				
		1	2	3	4	5
STANDARD, mm/day		4.04	4.07	4.12	4.21	4.33
		%				
K	0.25	5.3	5 7	5.3	5.0	3.7
	0.75	-4.6	-5.0	-3.9	0.0	3.2
C_{max}	0.90	-6.4	-7.6	-7 5	-7.1	-6.7
	2.70	2.4	2.7	2.7	2.5	2.4
rb	5	0.6	0.5	0.4	0.3	0.3
	15	-0.5	-0.5	-0.4	-0.3	-0.3
n	1.5	4.0	3.4	2.2	1.0	0.7
	4.5	-5.9	-3.0	-0.9	0.7	1.2
H	0.25	-5.2	-5.9	-5.9	-5.8	-5.9
	0.75	4.3	5.3	5.8	5.9	6.1
K_t	0.27170 2.25720	0.3	-0.1	-0.4	-0.5	-0.3
	0.84436 6.77160	0.1	0 1	0 2	0.3	0.1
H_c	0.562E6 1.333E6	0.6	0.0	-0.4	-0.7	-0.8
	1.688E6 4.000E6	-0.5	-0.1	0.2	0.4	0.4

daily ET rates were first simulated at LAI from 1 to 5 with the standard values listed in Table 3.2 and then one parameter at a time was varied by ± 50 % of its original value to compute new ET. The sensitivity was calculated as fraction change in ET with respect to the standard ET estimate and the values in percentage are summarized in the Table 3.3 for the daily irrigated treatment and in Table 3.4 for the weekly irrigated treatment. From the tables it can be seen that the effect of rb and n, the two most uncertain variables, was less than 10%. The model is more sensitive to C_{max}, H and K which can be measured or obtained to reduce the model uncertainty.

Summary And Conclusions

The development and analysis of a mechanistic three zone soil-canopy-atmosphere interaction model was presented. This model provides a useful tool to study the water use of a crop under the influence of climatic, agronomic and management practices. Evaporation from the soil may constitute a significant fraction of total ET over a season. The amount of soil evaporation varies with crop growth stage, available soil water as well as net radiation input. It was observed that high soil evaporation would reduce transpiration. The model predicts canopy and soil temperatures and the simulation showed that they could differ significantly from the air temperature depending upon the soil surface water content, weather and stage of crop growth. Knowledge of these temperatures could be useful in irrigation scheduling and predicting possible pest attacks.

The model presented here differed from the works of Waggoner and Reifsnyder (1968), Stewart (1970), Shawcraft et al. (1974), and Goudriaan (1977) where the soil and the canopy was stratified into a

TABLE 3.4 Results of sensitivity analysis for the weekly irrigated treatment. For sensitivity analysis one variable at a time was varied and the change in ET compared with the standard ET value was computed as a percentage. The ET estimates at standard values are in mm/day. The variables are listed along with their values.

		\A1				
		1	2	3	4	5
STANDARD, mm/day		4.38	4.11	4.27	4.31	4.40
		%				
K	0.25	2.6	-2.6	4.4	7.0	4.9
	0.75	-4.4	-3.2	-4.5	-0.5	3.0
C_{max}	0.90	-5.9	-7.8	-7.1	-6.8	-6.4
	2.70	2.2	2.8	2.5	2.4	2.3
rb	6	0.6	0.6	0.4	0.3	0.2
	15	-0.5	-0.5	-0.4	-0.3	-0.2
n	1.5	1.7	-1.0	1.5	1.7	1.1
	4.5	-4.4	-0.6	-1.5	0.1	0.9
H	0.25	-4.3	-4.4	-5.8	-5.9	-5.8
	0.75	3.4	3.9	5.5	5.9	6.0
K_t	0.27170	-2.4	-0.6	-1.4	-1.2	-0.6
	2.25720					
	0.84436	1.8	0.3	0.7	0.5	0.0
	6.77160					
H_c	0.562E6	-1.3	-0.9	-1.9	-2.0	-1.9
	1.333E6					
	1.686E6	0.5	0.4	0.8	0.9	1.1
	4.000E6					

number of horizontal layers. In the present model the canopy was conceived to consist of two canopy zones, the sunlit leaves and the shaded leaves, regardless of their position in the canopy. The soil evaporation was treated using the model developed in Chapter II. Two types of solution algorithms were presented based on whether soil temperature was a known input or a desired output. With soil temperature known, an analytical solution was developed to predict less commonly measured canopy temperatures, humidity and energy fluxes. However, a rapidly converging iterative solution scheme was developed for situations when soil temperature was a unknown.

The model has a practical utility in irrigation scheduling, predicting ET, E and T under various types of environments as well as estimating crop microclimate. With advances in computer technology a farmer can install an automatic weather reporting system for less than the cost of a garden tractor. Such self-sustained systems are already providing weather and soil information necessary for the model. Crop growth models such as SOYGRO are becoming widely available to provide crop specific information. Therefore this model could help provide up to date information relative to crop water use and its management.

The model can be easily integrated into crop growth models like SOYGRO or can be used as stand alone version. Further work is required to validate the model under field conditions. For general application of this model, additional work is required to integrate a companion soil water and a crop growth yield prediction model to assess water use and efficiencies under conditions of limited water supply.

CHAPTER IV
EFFECT OF ATMOSPHERIC CO_2 CONCENTRATIONS ON SOYBEAN WATER USE SIMULATION AND EXPERIMENTAL VERIFICATION

Introduction

The mean atmospheric CO_2 concentration is steadily increasing due to the release of CO_2 by combustion of fossil fuel. Forecasts suggest that atmospheric CO_2 levels will have doubled by the end of next century from the pre-industrial concentration (Clark 1982b). It is a classic observation that aerial CO_2 is necessary for plant growth and that CO_2 enrichment usually has a simulating effect on growth rate. Increased CO_2 will increase net CO_2 fixation, leading to increased plant dry weight and probably increased leaf area in plants with C_3 photosynthesis (Kramer, 1981). On the other hand high CO_2 will increase stomatal resistance, reducing transpiration and therefore increasing water use efficiency. These two effects of high CO_2 on leaf area per plant and on transpiration per unit leaf area may have compensating effects on water use per plant.

Another anticipated effect of atmospheric CO_2 enrichment is a 1 to 5 °C increase in the global temperature with each doubling of the atmospheric CO_2 concentration, a consequent decrease in precipitation and an increase in aridity in many important areas of the world (Morison and Gifford, 1984). Such climatic alterations will also affect crop water use.

There have been many investigations of plant responses to CO_2 and atmospheric conditions. McNaughton and Jarvis (1983) emphasized that in short vegetation such as arable crops, vapor pressure deficit in

and above the plant canopies is influenced by, and partly depends on the evaporation loss from the canopy. Thus a reduction in plant evaporation due to increased CO_2 may increase vapor pressure deficit that will drive more evaporation. This feed back mechanism, if it exists in most crops, could undermine the effect of increased CO_2 on lowering crop water use. Jones et al. (1985) experimentally showed that for soybeans grown in CO_2 concentration of 880 ppm, increasing the ambient temperature from 28 to 35 °C resulted in 25 % increase in daily transpiration while daily photosynthesis was reduced by 4 %. This apparent increase in water use reduced the water use efficiency by 22%. Gifford (1979) found that relative yield of water stressed wheat grown in twice the normal environmental CO_2 concentrations was as large as well watered wheat grown in normal CO_2 concentrations. However the total water loss was similar.

The actual long term water use of CO_2 enriched crops under field conditions needs to be investigated. Plants grown in high CO_2 environments will have high leaf area which tends to increase transpiration. They will also have a larger, more vigorous root system and be able to extract more water, resulting in less water stress, higher yields, but possible higher total water use (Kimball and Idso, 1983). Any decrease in transpiration will make more energy available for soil evaporation. Mechanistic models of soil-plant-atmosphere can be used to study the individual and combined effect of environmental conditions. Therefore, the objectives of this paper were to

1. Evaluate the ability of a mechanistic evapotranspiration model to predict water use by soybeans grown under different CO_2 environments in outdoor, controlled growth chambers, and

2. Apply the model to estimate the individual and combined effects of CO_2 induced changes in stomatal resistance, leaf area development, and temperature on water use by soybeans in the field.

Description Of The Model

The schematic of the soil-canopy model developed in Chapter II is shown in Fig. 4.1. The canopy was divided into zones of sunlit and shaded leaves with soil forming the lower boundary. The division of canopy into sunlit and shaded zones was based on the light extinction characteristics of the canopy and leaf area index. The resistances considered were the boundary layer resistances (RB), the surface resistances (RS), and the vertical aerodynamic diffusion resistance R. The subscripts sl, dl, and ss were used to denote the canopy sunlit zone, the shaded zone, and the soil surface. The canopy microclimate differed from ambient conditions above the canopy and was described with an average temperature and vapor pressure. Similarly properties of bulk air above the canopy were represented by air temperature T_a, and vapor pressure e_a. The $d+z_o$ denoted the height of momentum transfer from the air to the canopy. The model was described using a steady state approach and principles of energy balance by a series of simultaneous equations. Two types of solution algorithms were presented based on whether soil surface temperature was known or unknown. The climatic input to the model included above canopy temperatures, humidity or dew point temperatures, net radiation, and wind speed. Besides these, leaf area index, stomatal resistance and canopy light extinction characteristics were also needed. The model predicts diurnal fluxes of latent and sensible heat from the soil, the shaded

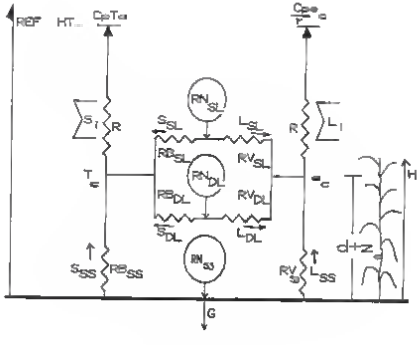

Fig. 4.1 Schematic of the evapotranspiration model for incomplete and complete canopies presented as an electrical analog

canopy and the sunlit canopy, along with their surface temperatures and mean canopy humidity and temperature.

Studies were conducted between September and November of 1984 at the Irrigation Research and Education Park of the University of Florida in Gainesville, Florida to obtain model inputs and a data set to validate the model.

Materials And Methods

Soybeans [Glycine max(L.) Merr. cv. Bragg] were grown in CO_2 concentrations of 330, 660 and 990 ppm (Parts Per Million, mole fraction basis, or moles of CO_2 per mole of atmospheric air) in naturally sunlit controlled environment chambers (Jones et al. 1984b) located in the field. In this study three levels of CO_2 were considered 330, 660, and 990 ppm, respectively. The daytime dry bulb and dew point temperature controls were set at 31 and 18 °C and were maintained within 1 - 1.5 °C. These experimental conditions were continuously monitored by a dedicated computer operating in real time. The environmental data were collected every 5 minutes throughout the growing season and consisted of dry bulb temperature, dew point temperature, soil surface temperature, net radiation, photosynthetically active photon flux density (PPFD), and CO_2 concentrations. Canopy transpiration rates were measured every 5 minutes by collecting water that condensed on cooling coils which were used to control air humidity.

Bragg soybeans were planted in North-South oriented rows with 0.5 m row spacing on 14 September 1984. Because of late planting, four incandescent lights were placed above each chamber to extend photoperiod and prevent premature flowering. As the canopy developed shade cloths were maintained at the canopy height to simulate natural canopy

exposure to incident radiation. The soybeans were kept well watered during the entire study period. Irrigation was frequent and on demand during first two weeks after planting, however thereafter a fixed irrigation schedule (irrigation on Monday and Thursday at 1600) was followed with occasional supplemental irrigation on Sunday evenings. The soybeans were hand watered until Oct 11 (27 DAPL) and thereafter a trickle irrigation system was used. This change was necessary as the wind was causing lodging when the acrylic tops were removed during irrigation. Starting on Oct 3, during each subsequent week, the soil was covered with polythene sheets beginning Wednesday morning (800 EST) until just before irrigation on Thursday (1600 EST) to eliminate soil evaporation. This sequence was repeated over four consecutive weeks (last sequence ended on Oct 24) and thereafter the soil surface was completely sealed off for CO_2 exchange measurements. By this time most treatments had reached full cover with LAI of 5.45, 4.53, and 6.54 for CO_2 treatments 330, 660, and 990 ppm, respectively. Data collection for this study continued thereafter until Nov 7.

During the season the plant height and width were measured on 13, 22, 26, 31, 34, 39 and 46 DAPL and LAI was measured on 13, 24, 34, 46, and 66 DAPL. Stomatal resistances of individual sunlit and shaded leaves were measured on 21, 28, 31 and 33 DAPL using a LI-COR 1600 steady state porometer. Measurements were made on both the abaxial and adaxial leaf surfaces of three randomly selected sunlit and shaded leaves. Ambient canopy air temperature, relative humidity, sunlit and shaded leaf temperatures were also recorded to verify the model predicted estimates.

Results Of Experimental Study

The time course of the cumulative LAI for the three CO_2 treatments is shown in Fig. 4.2. The LAI increased rapidly in the 990 treatment whereas the rates of development were almost same in the 330 and 660 treatment for the first 35 DAPL. There was some chewing insect damage early in the 660 ppm chamber which may have delayed LAI development. The maximum LAI reached by the three treatments were 5.61, 6.88 and 6.73, respectively.

Stomatal resistances of individual leaves were calculated as the reciprocal of the sum of the reciprocals of the diffusive resistance for both surfaces. A non-linear relationship was developed between leaf conductance and PPFD for individual CO_2 treatments. There was a lot of scatter in the measured values especially for the 660 CO_2 treatment. The resistances used in simulations are listed in Table 4.1.

Model Calibration

The aerodynamic boundary layer resistance at the soil (RB_{ss}) and the leaf surface (RB_{sl} and RB_{dl}) , and the vertical diffusion resistance (R) shown in Fig. 4.1 were related by the classical theory to the logarithmic wind speed profile above the canopy and its exponential extinction within the canopy. Due to the air circulation patterns and size of the chambers, these theories could not be applied to compute these resistances. Therefore the model was calibrated using selected days (Table 4.2) to characterize the variation of these resistances with the leaf area development. The leaf boundary layer resistance was assumed constant in this study. Under natural field conditions it should be under 100 s/m and will probably range from 6 to 50 s/m (Jackson, 1982; Monteith, 1963). The values reported by Deanmead

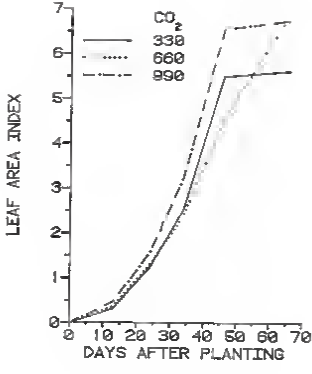

Fig. 4.2 Leaf area development as a function of days after planting for Bragg soybean grown in controlled environment chamber under three levels of CO_2 concentrations

TABLE 4.1 Parameters in the stomatal conductance function.

$$C = C_{max} \left(1 - e^{-\frac{s\ PPFD}{C_{max}}} \right)$$

where C_{max} in m/s , PPFD in E/m^2-sec and s has units of m^3/ E.

CO_2	C_{max}	$s * 10^6$
330	0. 180	38.14
660	0.080	30.17
990	0.060	20.00

TABLE 4.2 The results of calibration for the vertical aerodynamic resistance R and the soil resistance in the control chambers.

Date	DAPL	LAI	R, s/m	Date	DAPL	LAI	Rbss, s/m
				Sep 14	0	0	153.8
Oct 3	19	0.51	1	Oct 6	22	1.06	200.0
Oct 10	26	1.49	10	Oct 12	28	1.75	225.0
Oct 17	33	2.41	15	Oct 20	36	3.03	300.0

(1976) ranged from 5-7 s/m for temperate cereals. In the chamber the air was continuously circulated at a constant rate so a constant value of 10 s/m on a leaf basis was assumed. The bare soil boundary layer resistance value of 154 s/m reported in Chapter II was used as the initial value for RB_{ss} before LAI started developing.

With these initial selections the resistances R and RB_{ss} were calibrated using three days during early development (Table 4.2). To calibrate R we chose days from the 330 ppm treatment when the soil surface was covered and varied R until measured and simulated values agreed reasonably well for most of the day. Due to scatter in the stomatal resistance measurements the C_{max} of 0.0180 m/sec consistently gave better fit than the estimate (0.0208) made using the steady state porometer values. Therefore this value was used in the simulations. RB_{ss} was calibrated using days when both soil evaporation and transpiration occurred simultaneously. Days selected for calibration of both R and RB_{ss} were within one or two days of each other depending on the data availability. The calibrated values of R and RB_{ss} varied until LAI became 3.03. Thereafter the chambers floors were closed permanently and no further calibration for RB_{ss} was needed and the value of R and RB_{ss} was assumed constant there after. No adjustment in the leaf boundary resistances were made. The sensitivity analysis in Chapter III had demonstrated that 50% change in leaf boundary layer resistances would result in less than 1% change in daily ET from a well watered canopy. The results of calibration are summarized in Table 4.2.

Simulation of diurnal ET

Data collected during the first two weeks after planting were not considered for simulation due to irregular irrigation schedules.

Selected days beginning with 14 days after planting (DAPL) until 58 DAPL were simulated. On many occasions during the study, the chambers were opened for plant measurements, irrigation, spraying, and emergency maintenance. These days as well as days when there were control and instrumentation problems were omitted from the analysis. The instantaneous net radiation data were available from 700 to 1900 hours each day and therefore all the results reported here are for this time period only. Hereafter, the three CO_2 treatments will be referred simply as 330, 660, and 990 treatments, respectively.

The individual CO_2 treatments as well as the time course of simulated and measured evapotranspiration (ET) during early (19 DAPL, Oct 3), middle (28 DAPL, Oct 12), and at near full canopy (36 DAPL, Oct 20) are compared in Figs. 4.3-4.5. On Oct 3, the soil was covered with plastic sheets to measure transpiration (T) only, while on Oct 12 and Oct 20 both soil evaporation (E) and T were occurring simultaneously. The results clearly show the differences in total water loss due to the CO_2 treatments and in general the water use was reduced with increased CO_2 concentrations.

It was observed that simulated values consistently exceeded measurements in the mornings but were similar during the rest of the day. There were three probable explanations. First, transpiration was measured by condensing water vapor from outgoing air that passed through each chamber cooling coils. In the mornings, the coils were known to accumulate condensate for a certain amount of time before water was released to be measured. As a result the measurements lagged the true water loss rate from the canopy. This problem was more noticeable especially when the canopy was small. Secondly, it was

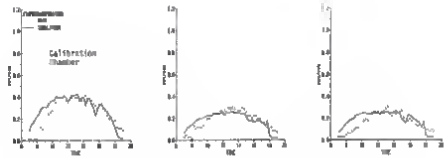

Fig. 4.3 Daily time course of simulated and measured transpiration rates on Oct 3 (19 DAPL) for the 330, 660, and 990 (left to right) CO_2 treatments. The LAI were 0.81, 0.85, and 1.08 respectively and the soil was covered

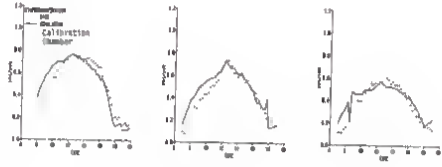

Fig. 4.4 Daily time course of simulated and measured evapotranspiration rates on Oct 12 (28 DAPL) for the 330, 660, and 950 (left to right) CO_2 treatments. The LAI were 1.75, 1.73, and 2.40 respectively

Fig. 4.5 Daily time course of simulated and measured evapotranspiration rates on Oct 20 (36 DAPL) for the 330, 660, and 990 (left to right) CO_2 treatments. The LAI were 3.03, 2.75, and 3.80 respectively

noticed that on cool mornings water was condensing on the side walls which would reduce water vapor passing through the cooling coils. Thirdly, the chambers tended to loose sensible energy to the environment in the mornings and gain sensible energy in the afternoons. This would tend to decrease ET in the morning and increase ET in the afternoon. Finally, at each time step in the simulation, the model assumes steady state and point values of net radiation and PPFD were used to compute energy balance components. The measurement system was responding to average conditions over the whole time step (15 minutes). This was particularly important during mornings when radiation was increasing rapidly. This is an important issue in using steady state models and the errors could be reduced to some extent by using inputs averaged over the whole time step.

Simulated and measured values agreed well during noon hours when none of the system related problems as well as the assumption of steady state was approximately correct. On days when there was variable cloud cover, the model, again due to the assumption of steady state, tended to underestimate ET (see Fig. 4.5) late in the afternoon. However, on the clear days, even the late afternoon errors were small. On Oct 20, which was the third day after irrigation, the model predicted condensation on soil surface in the the 950 treatment.

Simulation of Canopy Temperatures

The model also predicted temperatures of the sunlit, and shaded canopy as well as mean canopy humidity and temperature. A representative daily sample output comparing leaf temperatures with air temperature is shown in Fig. 4.6 for Oct 12 which was a relatively clear day except for some clouds at the beginning and end of the day. Leaf

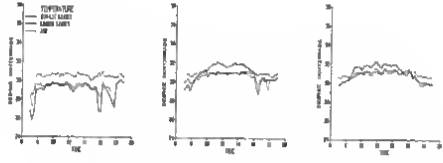

Fig. 4.6 Comparison of daily course of simulated sun-lit and shaded leaf ensemble temperatures with the air temperature on Oct 12. The leaf temperature in high CO_2 chambers were warmer

temperetures increased ebove eir temperature with en increese in CO_2 levels. This response was the direct result of CO_2 effect on stometel behevior ceusing lower transpiretion and simulteneous rise in the leef temperetures. The measured leaf tenperatures with the LI-1600 steady stete porometer were usuelly lower than the simuleted temperatures. This error wes attributed to the physicel operetion of the porometer. First, during leaf temperetore measurements e leaf is enclosed between the metel rings which dempens the temperetore end additionel-ly the fen in the cuvette blows air directly on te the leef causing evaporative ceeling that lowers leaf temperatures. J. M. Bennett. (Persone! Communication) compered infrared thermometer measured leef temperetures with the steady stete porometer measured values and found thet the values were lower by as much es 5-7 °C. The simuleted tempe-ratures response to CO_2 were simller to the single leef temperatures reported by Velle et al. (1985).

Long Term Water Use

Simulation of delly cycles end their egreements with meesurements geve confidence in the model structure and the essumptions mede in its development. The model was next used to simulete ET on the remaining days to eveluete the ability of the medel to simulete delly water use. The summary results comparing simuleted end measured ET ere presented in Tebles 4.3-4.5. In summery the low CO_2 treatment had higher weter loss compered to its counterperts. The climetic condi-tions were se verieble during the study perled thet clear trends in the water use dete ere not visible. However the water use seems te heve stebilized when the cenoples reached an LAI eround 3-3.5. The correletionel diegrams (Fig. 4.7) compering simulation and meesure-

TABLE 4.3 Measured ET, simulated Et, T and E and errors between the measurement and simulation for the 330 CO_2 treatment on various days after planting (DAPL) and days after irrigation (DAI). The extension -C following the DAI column indicates that the soil surface was covered, whereas as the extension -S indicates supplemental irrigation. A '*' after DAPL indicate days usad in the calibration.

DAPL	LAI	MEASURED ET,mm	SIMULATED ET,mm	ERROR mm	SIMULATED T,mm	SIMULATED E,mm	DAI
14	0.39	2.68	2.67	0.01	0 78	1.90	1
15	0.48	3.90	4.21	-0.31	2.15	2.06	2
16	0.56	2.80	2.79	0.01	I.93	0.86	3
19*	0.81	3.25	3.38	-0.13	3.38	0.00	2-C
22*	1.06	4.93	5.10	-0.17	3 88	1.12	2
23	1.15	3.96	4.30	-0.34	3.24	1.06	3
24	1.23	4.64	4.54	0.10	3.80	0.74	1-S
25	1.36	5.55	6.32	-0.77	4.55	1.77	1
26*	1.49	4.41	4.38	0.03	4.38	0.00	2-C
27	1.62	4.61	4.65	-0.04	4.65	0.00	3-C
28*	1.75	5.71	5.99	-0.28	4.64	1.35	1
29	1.88	5.40	5.67	-0.27	5.08	0.58	2
30	2.02	5 52	5.82	-0.30	5.21	0.61	3
31	2.15	5.65	6.03	-0.38	4.58	1.45	1-S
33*	2.41	5.49	5.02	0.47	5.02	0.00	2-C
34	2.54	5.89	5.42	0.47	5.42	0.00	3-C
36*	3.03	7.10	7.58	-0.49	5.91	1.68	2
37	3.28	5.93	6.05	-0.12	4.74	1.31	3
38	3.52	6.26	6.17	0.08	4.82	1.35	4
39	3.77	6.84	6.00	0.84	4.75	1.25	1
40	4.01	5.31	5.63	-0.32	5.63	0.00	2-C
41	4.26	7.90	7.11	0.79	7.11	0.00	C
43	4.75	7.51	6.61	0.90	6.61	0.00	C
48	5.50	7.39	6.67	0.72	6.67	0.00	C
53	5.53	7.75	7.17	0.58	7.17	0.00	C
54	5.54	7.46	7.04	0.42	7.04	0.00	C

TABLE 4.4 Measured ET, simulated ET, T and E and errors between the measurement and simulation for the 660 CO_2 treatment on various days after planting (DAPL) and days after irrigation (DAI). The extension -C following the DAI column indicates that the soil surface was covered, whereas as the extension -S indicates supplemental irrigation.

DAPL	LAI	MEASURED ET,mm	SIMULATED ET,mm	ERROR mm	SIMULATED T,mm	SIMULATED E,mm	DAI
14	0.45	2.26	2.29	-0.03	0.73	1.55	1
15	0.54	3.79	4.03	-0.24	2.20	1.83	2
16	0.62	2.78	2.78	0.00	1.87	0.91	3
18	0.79	3.66	4.50	-0.85	2.68	1.82	1
19	0.85	2.45	2.37	0.08	2.37	0.00	2-C
22	1.12	4.33	4.33	0.00	3.10	1.23	2
23	1.21	3.70	3.84	-0.14	2.75	1.09	3
24	1.29	2.71	3.12	-0.41	2.42	0.70	1-S
25	1.40	5.12	5.02	0.10	3.37	1.65	1
26	1.51	3.61	3.65	-0.04	3.65	0.00	2-C
27	1.62	3.81	3.76	0.05	3.76	0.00	3-C
28	1.73	5.25	5.27	-0.02	3.95	1.32	1
29	1.84	4.53	4.95	-0.42	4.10	0.85	2
30	1.96	4.72	4.79	-0.07	4.01	0.71	3
31	2.07	4.81	4.73	0.08	3.67	1.06	1-S
34	2.40	3.31	3.39	-0.08	3.39	0.00	2-C
35	2.58	4.48	4.43	0.05	3.57	0.86	I
36	2.75	5.45	5.31	0.14	4.01	1.30	2
37	2.93	4.92	5.11	-0.19	4.01	1.10	3
39	3.29	4.27	4.20	0.07	3.04	1.16	1
40	3.46	5.27	5.02	0.25	5.02	0.00	2-C
41	3.64	4.16	4.03	0.15	4.03	0.00	3-C
43	4.00	4.92	4.90	0.02	4.90	0.00	C
45	4.35	5.27	5.26	0.01	5.26	0.00	C
54	5.50	5.36	5.22	0.14	5.22	0.00	C

TABLE 4.5 Measured ET, simulated Et, T and E and errors between the measurement and simulation for the 990 CO_2 treatment on various days after planting (DAPL) and days after irrigation (DAI). The extension -C following the DAI column indicates that the soil surface was covered, whereas as the extension -S indicates supplemental irrigation.

DAPL	LAI	MEASURED ET,mm	SIMULATED ET,mm	ERROR mm	SIMULATED T,mm	SIMULATED E,mm	DAI
19	1.06	2.05	2.19	-0.14	2.19	0.00	2-C
26	1.90	3.22	3.27	-0.05	3.27	0.00	2-C
27	2.07	3.64	3.49	0.15	3.49	0.00	3-C
33	3.08	3.28	2.70	0.58	2.70	0.00	2-C
34	3.25	4.01	3.99	0.02	3.99	0.00	3-C
35	3.52	4.30	3.87	0.43	3.87	0.53	1
36	3.80	4.92	4.60	0.32	4.60	-0.08	2
37	4.07	5.07	5.05	0.02	5.05	1.07	3
39	4.62	4.51	4.55	-0.04	4.55	1.36	1
40	4.89	4.64	4.54	0.10	4.54	0.00	2-C
41	5.17	4.06	3.98	0.08	3.98	0.00	3-C
42	5.72	4.94	4.83	0.11	4.83	0.00	C
45	6.54	4.85	4.49	0.36	4.49	0.00	C
46	6.85	5.35	4.98	0.37	4.98	0.00	C
47	6.96	5.80	5.60	0.20	5.60	0.00	C
48	6.57	5.02	4.92	0.10	4.92	0.00	C

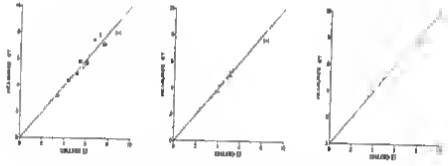

Fig. 4.7 Co-relational diagram os simulated and measured evapotranspiration for the 330, 660, and 990 CO_2 treatments compared with 1:1 line. Days used in the calibration are indicated with large solid dots. The difference between simulated and measured values were insignificant at 95% level of confidence

ments and the t-test revealed that there were no significant differences between the simulation and measurements at 95% confidence level. The maximum errors during the entire simulation were 12%, 23%, and 18% while the average absolute errors were 6%, 3.8% and 4.7% for the 330, 660, and 990 treatments respectively.

Soybean Water Use With Increased CO_2 Levels

The development of the computer simulation has made possible rapid evaluation management alternatives. In this section, the model was used to forecast water use of a field grown soybean under the present CO_2 level (330 ppm) and future anticipated CO_2 level of 990 ppm. In the experimental study it was found that the stomatal resistance was increased and leaf area development was rapid in the high CO_2 treatments compared over the low CO_2 level. It is anticipated that the rise in environmental CO_2 will lead to global increase in average air temperature by 1 to 5 °C. The water use under the influence of each of these three factors was examined.

Assumptions

Soybean crop was assumed to be grown in the constant weather conditions shown in Fig. 4.8. The leaf area index data for the 330 and 990 treatments presented in Fig. 4.2 was assumed. The soybeans in this study were harvested 115 DAPL, therefore between 66 and 115 DAPL, LAI was decreased linearly with time. The assumed LAI during 66 to 115 day interval was similar to recorded field measurements (E. Bisbal, personal communication). At full canopy the height of the crop was 0.8 m, light extinction coefficient 0.5, velocity attenuation coefficient 3, and uniform wind speed of 1.5 m/sec. Refer to Chapter III for detail model inputs and soil characteristics.

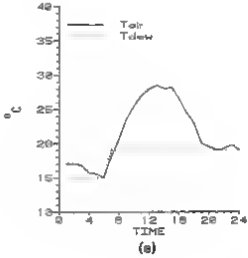

Fig. 4.8 The diurnal variation in air temperature, dew point temperature, net radiation, and PPFD used on all days in the simulation of CO_2 induced effects

Stomatal Resistance

The CO_2 concentrations affects leaf stomatal resistance. If all conditions such as light, water and temperature are at optimum values, the minimum stomatal resistance occurs when the external CO_2 level is about equal to the CO_2 compensation point, the point where the photosynthetic CO_2 uptake just balances CO_2 released by respiration (Ting, 1982). Whereas low CO_2 tends to cause stomatal opening, high CO_2 will tend to close stomata. The stomatal resistance data presented in Table 4.1 were used to simulate the relative contribution of this CO_2 induced change in crop water use. The results of the simulation runs are summarized in Table 4.6. In the following discussion the abbreviation SR was used to indicate stomatal resistance, and the two CO_2 levels and corresponding LAI and SR were referred as low (330 treatment) and high (990 treatment) respectively. The simulation result showed that, with LAI and SR that occurred in 330 ppm CO_2, over the 115 days of simulation, the crop transpired 348.5 mm of water (80% of total water consumption) compared to 289.3 mm (75 % of total water consumption) with the same LAI but with SR for the 990 CO_2 plants. There was a net reduction in water use. More realistically, however, increases in CO_2 will cause higher LAI due to higher photosynthesis.

The true comparison must be made between low LAI and low SR with high LAI and high SR. The total water loss from soybeans grown in high CO_2 environment was reduced from 436.5 mm to 394.1 mm (a 10% reduction) whereas transpiration loss was reduced by 13%. The results of simulation compare well with water saving reported by Jones et al. (1985). They reported that a 10% savings in transpiration when soybeans were grown in 660 CO_2 concentration compared with

TABLE 4.6 Effect of stomatal resistance and leaf area development of weekly irrigated soybeans in 330 and 990 ppm CO_2 concentrations on seasonal water use.

	330 ppm LAI		990 ppm LAI	
	SR-330 (LOW)	SR-990 (HIGH)	SR-330 (LOW)	SR-990 (HIGH)
	mm			
ET	436.5	384.8	446.0	394.1
T	348.5	289.3	362.9	303.3
E	88.0	95.3	83.3	90.8

330 CO_2 grown soybeans and that the total water loss was 346 mm compared to 400 mm over the 105 day growing season. The cumulative transpiration loss due to changes in stomatal resistance are compared in Fig. 4.9. Increased stomatal resistance led to 1.5 to 1.75 °C rise both the sunlit and shaded leaf temperatures (Fig. 4.10 and Fig. 4.11).

Leaf Area Development

The effect of leaf area development by itself on transpiration at low and high SR is compared in Fig. 4.12. In this case it can be seen that the water use by transpiration was not very sensitive to leaf area development, probably because leaf areas were similar under both CO_2 environments.

Air Temperature

To simulate the effect of increased temperature on water use, each hourly temperature was increased by 5 °C and simulations were performed for high LAI under both the low and high SR. The water use components are summarized in Table 4.7. Increase in air temperature caused increased vapor pressure deficit and seasonal transpiration (Fig. 4.13) and caused about 3 °C (Figs. 4.14 -4.15) higher leaf temperature. In the previous simulations with increased stomatal resistance, the effect of increase in temperature on stomatal resistance was ignored. Therefore a true test to see the effect of CO_2 induced environmental changes on water use, would be to compare the effect of stomatal resistance, leaf area and temperature together. This comparison can be derived from the first column of Table 4.6 and the last column of Table 4.7. According to the model, the total water loss will be increased to 520.4 mm compared to 436.5 by increasing

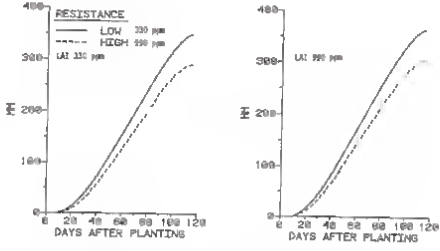

Fig. 4.9 Comparison of simulated seasonal transpiration at measured low (330 CO_2) and high (990 CO_2) LAI as influenced by measured stomata resistance at the two CO_2 levels. In each plot LAI was the same for both resistances cases

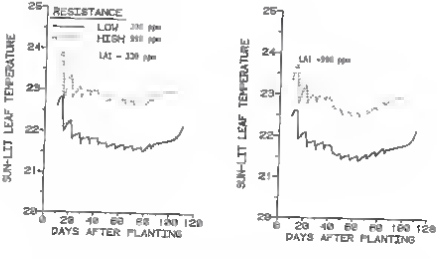

Fig. 4.10 Comparison of simulated average daily sun-lit leaf ensemble temperature at low (330 CO_2) and high (990 CO_2) LAI under the influence of measured stomatal resistance of the low and high Co_2 treatments

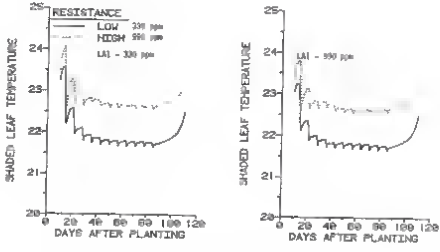

Fig. 4.11 Comparison of simulated average daily shaded leaf ensemble temperature at low (330 CO_2) and high (990 CO_2) LAI under the influence of measured stomatal resistance of the low and high CO_2 treatments

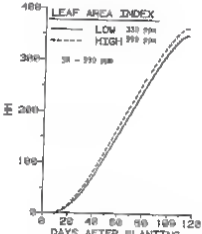

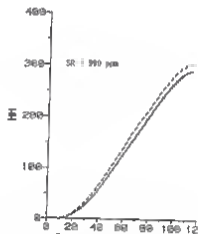

Fig. 4,12 Comparison of simulated transpiration corresponding to low (330 CO_2) and high (990 CO_2) stomatal resistance as influenced by leaf area development

Table 4.7 Comparison seasonal water use of soybeans with stomatal resistance corresponding to 330 and 990 ppm CO_2 concentrations under present and future global air temperature. LAI of 990 CO_2 treatment was used.

	SR -330 CO_2		SR -990 CO_2	
	Tair	Tair + 5	Tair	Tair + 5
	mm			
ET	446.0	583.6	394.1	520.4
T	362.9	474.5	303.3	402.5
E	83.8	109.1	90.8	117.8

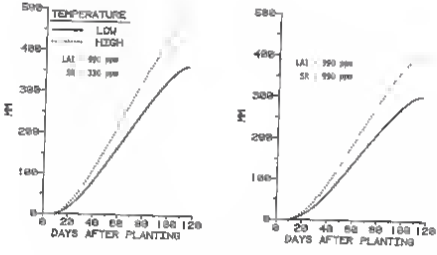

Fig. 4.13 Effect of 5 °C changes in global temperature on seasonal transpiration simulated using measured leaf area and stomatal resistance values corresponding to 990 CO_2 concentration. The 'LOW' temperature refers to standard weather conditions of Fig. 4.8 and 'HIGH' temperature refers to 5 °C rise in hourly values

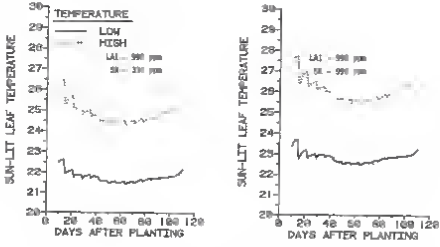

Fig. 4.14 Comparison of simulated average daily sun-lit leaf ensemble temperature under present and future (5 °C higher) air temperature simulated using leaf area and stomata resistance corresponding to 990 CO_2 treatments

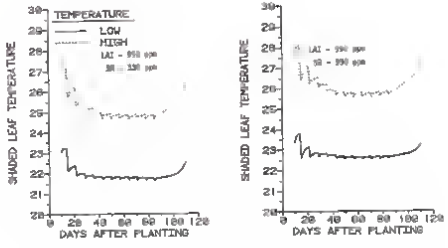

Fig. 4.15 Comparison of simulated average daily shaded leaf ensemble temperature under present and future (5 °C higher) air temperature simulated using leaf area and stomata resistance corresponding to 990 CO_2 treatments

atmospheric CO_2 levels to 990 compared to present 330 ppm. This analysis used the extreme value predicted for a temperature change (5 °C) and no change in atmospheric vapor pressure. However, it is likely that the atmospheric vapor pressure would be increased with an increase in temperature. These results show a wide range in predicted water use, varying from a decrease by 10% if atmospheric temperature does not change, to an increase by 19 % if atmospheric temperature changes by 5 °C and no change takes place in atmospheric vapor pressure.

Summary And Conclusions

The principle goals of this paper were to evaluate the evapotranspiration model of Chapter III with data from soybean crop grown in controlled environment chambers under three CO_2 concentrations of 330, 660 and 990 ppm and constant dry bulb and dew point temperatures, and to apply the model to study the possible effects of changes in atmospheric CO_2 concentration on water use of field grown soybeans.

The model simulated results agreed well with the measurements at all times of the day except in the mornings. The probable reasons for this were attributed to the natural lag in the measurement system, cold outside temperature relative to the controlled chamber temperature causing condensation on the side chamber walls, and the validity of the steady state assumptions during rapidly changing morning environment, heat sinks in chamber walls, and to the use of instantaneous rather than average net radiation values over the time step used in the simulation. The average daily errors over the simulated period were 6%, 3.8% and 4.7% for CO_2 treatments of 330, 660, and 990 ppm respectively.

The sunlit and shaded leaf temperatures increased with CO_2 levels. The simulated values agreed well with the single leaf temperatures responses to CO_2 reported by Valle et al, (1985) but were lower than the steady state porometer values.

The model provided an excellent tool to analyze changes in the microclimate and water use by a developing soybean crop. Although it is difficult to extend the model findings to field situations due to the constant environmental conditions of the chamber, it is certainly a valuable tool to analyze climate and crop interactions. Simulation studies were conducted to study the effect of CO_2 induced changes in stomatal resistance, leaf area development and global air temperature. For a fixed leaf area, increased stomatal resistance reduced water use and increased leaf temperatures. Transpiration water use under low and high CO_2 treatments differed by only 13 % and agreed well with experimental findings of Jones et al, (1985). The individual effect of a 5 °C in air temperature on leaf temperature and water use was dramatic. The leaf temperatures may be higher by as much as 3 °C, and water use was predicted to increase. When the projected effects of CO_2 on stomatal resistance, leaf area develoment, and temperature were combined, model predictions of water use were increased by as much as 19% due to CO_2 enrichment plus 5 °C temperature increase.

The study provided an excellent first test and validated many of the model predictions. The overall assessment of the model was satisfactory and further test of the model under the field conditions is recommended.

CHAPTER V
ESTIMATING CROP COEFFICIENTS FOR SOYBEAN UNDER DIFFERENT IRRIGATION MANAGEMENT PRACTICES

Introduction

In many parts of the world where water holding capacity of the soil is low and precipitation falls short of water requirements or is irregular during the growing season, irrigation is practiced to avoid drought and loss of yields. A critical problem in irrigation is to determine just when, how and how much water to apply to maximize the benefit to cost ratio. There are at least three approaches to determine the optimal timing and quantity of irrigation. One way is to observe crop indicators such as change of color or leaf angle in an attempts to detect early signs of stress. Secondly, the direct measurements of soil water content can be made to assure that soil water available is adequate to permit water extraction by roots at potential rates. Finally the weather can be monitored to determine evapotranspiration (ET) demand of a crop and compare it with the supply of water from rainfall and irrigation events.

Irrigation scheduling using ET computed from weather record is appealing because the approach is relatively simple compared to on-site ET measurements. In one approach to estimating ET, the whole realm of crop responses to the soil- plant-climate and management factors is simply taken care by " crop coefficients " for various crops at different stages of growth. In this approach ET of a disease-free crop grown in large field under optimum soil-water and

fertility conditions and achieving full production potential under a given environment is determined using reference crop evapotranspiration (ET_r) and a coefficient (K_c) to account for stage of growth of the crop. Accordingly,

$$ET = K_c\ ET_r \tag{5.1}$$

where K_c is the crop coefficient. Crop coefficients for many crops have been developed in field experiments and are summarized by Doorenbos and Pruitt (1977). Crop coefficients are sensitive to soil evaporation especially when canopies are small with incomplete ground cover and if irrigation or rainfall occurs. The data presented by Doorenbos and Pruit (1977) showed as much as 70 - 80 % variation in crop coefficient during the early phase of crop development depending on whether the soil surface was dry or wet. As the crop cover develops, crop coefficients become less sensitive to variation in the soil surface conditions. Therefore, attempts have been made to synthesize the overall crop coefficient into plant and soil coefficients (Wright, 1982; Phene et al., 1985). Accordingly, Eqn (5.1) can be rewritten to include soil specific coefficient K_s and plant transpiration coefficient K_p as:

$$K_c = ET/ET_r = E/ET_r + T/ET_r = K_s + K_p \tag{5.2}$$

it is argued that with differences in weather accounted for by ET_r, the transpiration coefficient K_p would be universally valid for a specific well-watered crop. On the other hand, K_s would vary locally depending upon irrigation frequency, method of irrigation, soil characteristics and degree of soil cover (Wright, 1982, Phene et al., 1985; Hanks, 1985).

It is common practice to use mean climatic data for determining ET_p. However due to changes in weather, ET_p will vary from year to year, for each period within a year and also due to changes in surface conditions. Smajstrla et al. (1984) have presented probability distribution of monthly ET_p values for nine Florida locations using 25 years of weather data. According to Doorenbos and Pruitt (1977) the monthly values could vary by 50% or more from one year to the next. The daily values can also vary drastically, with low values on the days that are rainy, cloudy, humid and calm with high values on dry, sunny, and windy days. There are no clear guidelines to adjust crop coefficients due to weather changes. Therefore the accuracy of crop coefficients is questionable unless both the ETr and crop coefficients are obtained under the same climate.

ET Models

Determination of crop coefficients with a direct method is a time consuming and expensive procedure. To determine crop coefficients, generally a minimum of two sensitive weighing lysimeters are required in such a study so that both the ET and ET_p are measured simultaneously. Alternatively crop coefficients could also be determined using a computer simulation model that computes evaporation and transpiration separately in response to soil, climate and crop variables. Models have been developed that compute evaporation and transpiration separately (Ritchie, 1972, Tanner and Jury, 1975, Chapter III). The models of Ritchie (1972) and Tanner and Jury (1975) have related transpiration to the leaf area index (LAI) and potential transpiration using empirical functions. Similarly, soil evaporation was related to the potential evaporation when soil surface was wet followed by an

empirical time function as soil dries. On the other hand the model of Chapter III treated the soil-plant-atmosphere as an energy exchange system. This approach takes into account the distribution of energy sources in the canopy and soil as well as physical characteristics of soil, plant and atmosphere, and their interactions to compute soil evaporation, transpiration, canopy microclimate (temperatures and humidity), soil temperatures, and soil heat flux. The model is diurnal in nature and requires half hourly values of air temperature, dew point temperature, net radiation, and wind speed as inputs. It also needs LAI, crop light extinction characteristics, and LAI and height at full canopy

The objectives of this paper were to use the model of Chapter II and III to:

1. Determine the effect of variation in climatic variables such as temperature, vapor pressure deficit (VPD), radiation and wind speed on crop coefficients K_c, K_p, and K_s under three irrigation frequencies: irrigated daily, once every three days and weekly.
2. Determine the effect of planting dates, crop development rates, and length of the growing season on water use and crop coefficients for a soybean crop grown in sandy soil and using actual weather data in humid Florida climate.
3. Discuss possible applications and linkages of the model with crop growth models.

Materials And Methods

The simulation study was divided into two parts to fulfill the first two objectives. During the first part, a set of input values

for soil, crop and meteorological parameters were selected to represent a soybean crop grown on sandy soil in Florida. The soil was represented by eight layers (of 10,10 10,30,30,40,40,40 cm thickness) with each layer having field capacity water content of 10% and lower extraction limit of 5% on the volumetric basis. The thermal conductivity and heat capacity were 0.674 J/m-sec-°C and 1.126E6 J/m^3-°C (at 0% moisture content) and 4.522 J/m-sec-°C and 2.663E6 J/m^3-°C (at 13.1 % moisture content) based on data reported by Herva (1975) for granitic sand. The thermal properties at intermediate water contents were linearly interpolated. Soil temperatures were simulated using a one dimensional heat transfer model with uniform initial temperature of 26 °C. After each irrigation new initial temperatures were computed as the weighted average temperature of soil and water by assuming that added water had average air temperature.

Soil evaporation occurred from the top 30 cm of soil while transpiration loss occurred throughout the soil profile. When the canopy was small (LAI < 0.5) all of the transpiration loss occurred from the top 30 cm, however afterward this proportion was reduced to 5% for the remaining growth period. The percent extraction values of transpiration were selected arbitrarily to include the effect of root growth. In Chapter III it was found that seasonal water use of a well watered crop was insensitive to this ratio. The leaf area index (LAI) with days after planting (DAPL) was computed using the SOYGRO model (Wilkerson et al., 1984), for the variety Cobb planted on June 26 and August 15, and the variety Williams planted on March 15 in Gainesville Florida with a planting density of 36 plants/m^2, and row and plant spacing of 0.762 and 0.0365 m respectively (Fig. 5.1). The crop light

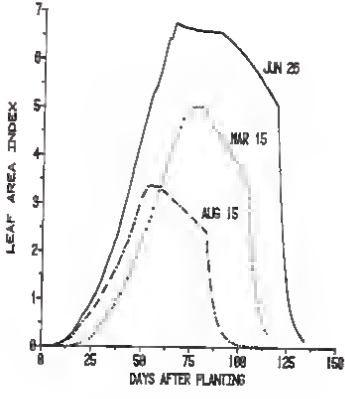

Fig. 5.1 Leaf area developed during three planting dates

extinction coefficient of 0.5 (spherical leaf angle distribution) and stomatal conductance as a function of PPFD, from Chapter III, is given by:

$$C = C_{max} \left(1 - e^{-\frac{s \, PPFD}{C_{max}}} \right)$$

where C_{max} was maximum conductance (0.018 m/sec) and s ($38.14 * 10^{-6}$) was initial slope of C vs PPFD ($E/m^2/sec$).

The climatic data typical for the June planting date was obtained from Jones et al. (1984a) and is listed in Table 5.1. The hourly air temperatures were computed using the diurnal algorithm in the SOYGRO model. The dew point temperature and wind speed were assumed constant. Daily net radiation was computed using the procedures of Jones et al. (1984) and it was distributed diurnally between sunrise and sunset using a sine function. The PPFD between sunrise and sunset was obtained by multiplying net radiation with 0.10, a locally determined empirical constant.

To assess the impact of weather on water use and crop coefficients the sensitivity tests were carried out by varying standard air temperature, relative humidity, radiation and wind speed as per the summary in Table 5.1. The temperatures were varied such that the maximum and minimum daily temperature difference was always 10 °C. In a natural system changes in temperature would bring changes in the VPD. However, during this phase of the simulation simulation experiments, the relative humidity was adjusted to maintain a constant VPD of 7.5 mb (millibar). The range of temperature variation was typical of moderate to warm agro-eco-system. The relative humidity levels

TABLE 5.1 Weather data used for the sensitivity analysis and the range of variations considered.

Parameter	Symbol	Units	Standard value	Simulated values
Maximum temperature	Tmax	°C	32	27 , 37
Minimum temperature	Tmin	°C	22	17 , 27
Radiation	RAD	cal/cm^2	444	222 , 722
Relative humidity	RH	%	79	58 , 37
Wind speed	WS	Km/day	86.4	259.2, 518.4

were characteristics of humid, sub-humid and arid regions. For this region the clear sky daily radiation averages as high as 744 cal/cm^2 (Jones et al., 1984a). Therefore to study the effect of variability in the cloud cover, situations with clear sky with maximum possible radiation and 50% of average seasonal radiation were considered. Wind speed ranged from 86.4 to 518.4 Km/day.

Water holding capacities of the sandy soils are low. Therefore, small frequent applications early in the growing season, and greater, less frequent applications later are suggested to improve irrigation scheduling (Clark, 1982a). Therefore daily, once every three days, and weekly irrigation frequencies were considered. Since the primary goal of this paper was to determine crop coefficients, soybeans were assumed to be well watered at all times. Irrigation was applied at the beginning of each day, and no irrigation was applied following physiological maturity of the crop.

To fulfill the second objective of this study, two additional experimentally feasible planting dates, spring (March 15, variety Williams) and fall (August 15, variety Cobb) were considered in addition to the June planting date. Monthly historical weather data reported by Jones et al. (1984a) was used for the simulation (Table 5.2). Daily values were obtained by linear interpolation of each variable, assuming the tabular values occurred on the middle of the month. Soil and crop characteristics, irrigation frequencies as well as all other procedures were identical. The ETr was computed using the Penman method (Jones et al., 1984a) and crop coefficients were computed using Eqn. (5.2).

TABLE 5.2 Average monthly climatological data used to simulate effect of planting dates on water use and crop coefficients of soybeans grown in Florida. The data is for the Belle Glade, Florida, weather station (Jones et al., 1984).

Month	Solar radiation 1971-79 cal/cm^2-day	Mean air temperature 1924-75 °C	Relative humidity 1958-76 %	Wind speed at 2m 1934-39,78-79 Km/day
Jan	282	17.8	76	121
Feb	340	17.8	74	131
Mar	436	19.4	73	125
Apr	510	21.1	72	119
May	507	23.9	75	100
Jun	472	25.6	78	87
Jul	452	26.7	78	83
Aug	447	27.2	78	75
Sep	405	25.6	79	85
Oct	370	22.8	77	100
Nov	302	19.4	76	106
Dec	281	17.8	75	106

$$\square_r = \frac{\Delta}{\Delta+\gamma} \left[(1-\alpha) R_s - R_b \right] / \lambda +$$

$$\frac{\gamma}{\Delta+\gamma} \left[0.263 \left(e_a - e_d \right) (0.5 + 0.006\, U) \right] \quad (5.3)$$

where $R_b = \sigma T^4 (0.56 - 0.08\ e_d^{\frac{1}{2}}) (1.42\ R_s / R_{so} - 0.42)$

and T = average daily air temperature in °K (°C + 273)

e_a = vapor pressure = $(e_{max} + e_{min})/2$, mb

e_d = vapor pressure at dew point temperature, mb

e_{max} = maximum vapor pressure of air during a day, mb

e_{min} = minimum vapor pressure of air during a day, mb

R_{so} = total daily cloudless sky radiation

Δ = slope of saturated vapor pressure curve of air, mb/°C

γ = psychrometric constant, 0.66 mb/°C

λ = latent heat of vaporization of water 58 cal/cm^2

α = albedo of surface for R_s

σ = Stefan-Boltzmann constant

R_s = total incoming radiation cal/cm^2.day

U = wind speed at height of 2 m, Km/day

RESULTS

Simulations were performed on the PRIME 550 computer in the Agricultural Engineering Department at University of Florida. The length of growing season varied with planting dates, 117 days for the March 15 planting, 134 days for the June 26 planting and 110 days for the August planting. Therefore, to compare the simulated results the duration after planting was normalized to give time elapsed as a

percentage of growing season unless mentioned otherwise.

Irrigation Frequency

Evapotranspiration (ET), soil evaporation (E) and transpiration (T) along with crop coefficients for the standard constant weather condition and the June planting date are shown in Fig. 5.2. With the daily irrigated treatment, the surface was re-wetted each morning and allowed soil evaporation to occur at potential rate. Soil evaporation was less than ETr and caused increase in soil surface temperature. As the soil surface temperature increased, the saturated vapor pressure was higher causing more soil evaporation until soybeans emerged on the ninth day. Similar phenomena was observed during the three and seven days irrigation frequencies. The seven day frequency allowed soil surface to warm even more than the other two treatments and therefore resulted in relatively higher evaporation following an irrigation event. As the canopy developed, the energy available at the soil surface became limited and soil evaporation was reduced. At high LAI during 50-119 DAPL, almost a constant portion of the incoming radiation was captured by the canopy, allowing only a small, constant amount to reach the soil surface as illustrated by the constant evaporation during this period. Following crop maturity (119 DAPL) irrigation was stopped and soil evaporation increased as LAI dropped and more radiation reached the soil surface. Soon this trend reversed as the soil became dry.

As the irrigation interval was increased to 3 and 7 days, the soil surface went through cycles of wetting and drying as illustrated by the varying amplitudes of E and ET. The soil evaporation occurred at the potential rate following irrigation, but decreased rapidly as

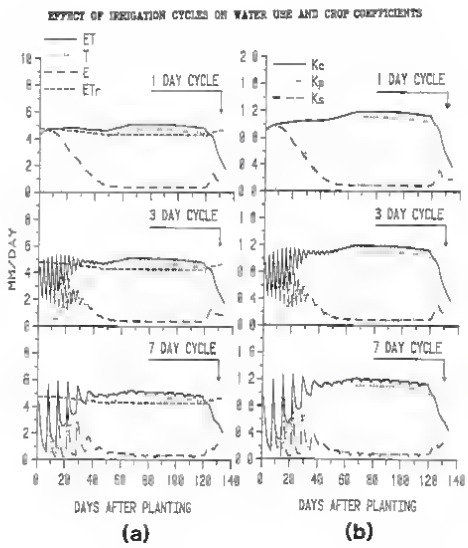

Fig. 5.2 Variation in daily components of water use rates and corresponding crop coefficients under 1 day, 3 day and 7 day irrigation cycles

the surface dried. As with the daily irrigation, the canopy development reduced available energy at the soil surface, the amplitudes were damped out, but were not completely eliminated even at maximum LAI. It was also interesting to see the "dips" in the T rates following an irrigation which increased soil evaporation and humidity surrounding the canopy or reduced the vapor pressure gradient between the leaves and canopy. The interaction of E and T seemed to have mutually compensating effects. This relationship could only be observed and studied using a physical model of this nature which is one of the major advantages of this model over Ritchie's (1972) or Tanner and Jury's (1975) models. The feedback of E on T became less significant at lower magnitudes of E. The daily variation in K_c, K_s, and K_p were similar to ET, E and T as the ET_r was not affected by the irrigation cycles.

Unlike ET, by definition ET_r was not influenced by the irrigation management practice. Therefore the behavior of crop coefficients were similar to the corresponding water loss components. Excluding the first nine days (bare soil) and the period following crop maturity, ET exceeded ET_r ($K_c > 1$). The soil evaporation was lower than ET_r, except during the second and third drying cycles with the three and seven day frequencies, therefore K_s was less than unity. Similarly, transpiration was lower than ET_r until LAI of 4.63 ($K_p < 1$) and then exceeded ETr ($K_p > 1$) up to the beginning of leaf senescence. ET_r decreased gradually with canopy development due to the effect of difference between soil and crop albedos.

The seasonal water use (Table 5.3) was affected by the irrigation method, mainly due to changes in soil evaporation during early development. During the first fifty days cumulative evaporations from the

TABLE 5.3 Cumulative reference crop evapotranspiration (cETr) computed using the Penman Method, simulated soybean evapotranspiration (cET), soil evaporation (cE) and transpiration (cT), using the standard values of air temperature, radiation, VPD, and wind speed (Table 1), under daily, once every three days and weekly irrigation cycles.

Variable	1 Day cycle	3 Day cycle	7 day cycle
cETr, mm	589.8	589.8	589.8
cET, mm	627.4	608.5	585.2
cE, mm	170.8	147.5	113.9
cT, mm	456.6	461 0	471.3

one, three and seven day frequencies were 132, 108 and 71 mm respectively compared to 38.8, 39.5 and 43 mm during rest of the season. Therefore the difference in K_c and K_s occurred mainly during the incomplete canopy phase, while for the major part of the peak growing season, these coefficients were practically the same among all irrigation treatments. On the other hand transpiration was little changed due to differences in the irrigation treatments and K_p remained practically unchanged.

In the following discussion the effects of climate will be analyzed to determine what changes to expect in water use pattern and crop coefficients. To improve the clarity of graphical presentations all daily water loss components and crop coefficients were averaged over the interval between irrigations.

Temperature

The maximum and minimum daily temperatures were changed by ± 5 °C over the standard values. Examining Eqn. (5.3), the available net radiation increased with increase in temperature. To maintain the VPD constant at 7.5 mb, the dew point temperature and consequently vapor pressure at dew point temperature increased and reduced long wave thermal radiation. Therefore both ET and ET_p increased with temperature (Table 5.4). The change in temperature also influenced the sensible heat exchange between the canopy and the surrounding air. With a daily irrigation cycle, lower air temperature reduced leaf temperature and transpiration by 14% while an increase by the same amount caused a 17% higher transpiration (Table 5.4). The unequal change in transpiration was attributed to the non-linearity between temperature and saturated vapor pressure relationship.

TABLE 5.4 Cumulative reference crop evapotranspiration (cETr), simulated soybean evapotranspiration (cET), soil evaporation (cE) and transpiration (cT), for three combinations of Tmax and Tmin temperatures under daily, once every three days and weekly irrigation cycles.

	1 day cycle			3 day cycle			7 day cycle		
	<---------- Degree C ---------->								
Tmax --->	27	32	37	27	32	37	27	32	37
Tmin --->	17	22	27	17	22	27	17	22	27
cETr, mm	525	590	671	525	590	671	525	590	671
cET, mm	563	628	708	548	610	689	525	585	663
cE, mm	171	171	174	151	148	147	119	114	111
cT, mm	392	457	534	397	462	542	406	471	552

Similar behavior with 3 and 7 day frequencies was observed. At high LAI, increasing temperature caused higher leaf temperatures and higher vapor pressure gradient between leaves and canopy air causing more transpiration. This was illustrated by the shift between T and ET_r in Fig 5.3a. On the other hand, higher transpiration reduced soil evaporation.

The changes in K_c, K_p and K_s associated with temperature change are shown in Fig 5.3b. As net radiation increased, bare soil evaporation increased over a short time but soon became limited by available water. At low temperature and before plant emergence it exceeded ET_r, but with further rise in temperature and net radiation it failed behind ET_r. Therefore K_s decreased with temperature. On the otherhand, transpiration of the well-watered soybean increased proportionately and K_p were similar among all temperature simulations. Later, when the canopy reached its peak radiation absorption characteristics, vapor pressure deficits induced due to low soil evaporation and temperature brought additional transpiration. Hence K_p increased with temperature. Early in the growing cycle, the combination of relatively similar K_p among all treatments, but lowering K_s, caused a net reduction in K_c. While at high LAI, the increase in K_p was compensated by decrease in K_s and kept K_c constant. Therefore with changes in temperature K_c was almost constant, although K_p and K_s changed during the peak growing season

Vapor Pressure Deficit (VPD)

The Penman method is not very sensitive to changes in VPD in the humid climate. Low VPD is accompanied by low relative humidity, and according to Eqn. (5.3) lower net radiation. Due to these counteract-

Fig. 5.3 Effect of temperature on water use and crop coefficients

a) Variation in daily water use components under various combinations of maximum and minimum air temperature in °C. Top (27,17), middle (32,22), and bottom (37,27)

b) Comparison of crop coefficients due to changes in maximum and minimum air temperatures. Solid line (27,17), dotted line (32,22), and dot and dash combination (37,27).

EFFECT OF TEMPERATURE ON WATER USE AND CROP COEFFICIENTS

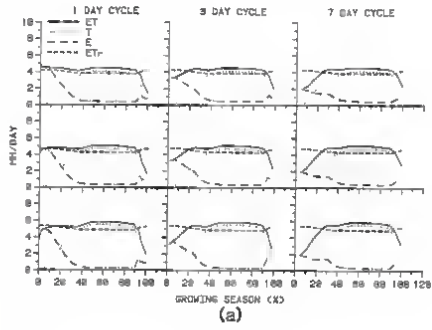

ing effects, the seasonal ET_c increased by merely 6% for a three fold increase in the VPD (Table 5.5) Changes in the VPD showed some interesting changes in the water use and crop coefficients (Fig 5.4). The soil evaporation increased more so than transpiration with increase in VPD. When the canopy was small, energy was not the limiting factor for soil evaporation and although VPD increased, it's influence was minor. However, as the canopy developed and energy became limiting, VPD was more important and caused increased soil evaporation. A three fold increase in VPD increased seasonal soil evaporation by 48% and T by 9% compared with the standard weather case. Most of this increase occurred during full canopy. For transpiration, on the otherhand at low LAI (high canopy stomatal resistance), VPD increased transpiration, while at high LAI it had very little influence Also at high LAI, the effect of the increase in VPD was neutralized by higher evaporation. Similar behevior was seen among all irrigation treatments.

The crop coefficients are shown in Fig. 5.4b. K_p remained relatively constant at high LAI under all three irrigation frequencies whereas K_s increased with VPD. At low LAI both K_p and K_s increased as transpiration and soil evaporation increased with VPD. The compensatory effect of soil evaporation on transpiration was neutralized by higher VPD. Therefore K_c was high for high VPD treatment by as much as 15 to 20 % throughout the growing period. These findings suggests that K_c determined under humid climatic conditions will underpredict water needs of a dry region and vice versa. However, if the surface wetting is minimized then adjustment in K_c or K_p may not be required.

TABLE 5.5 Cumulative reference crop evapotranspiration (cETr), simulated soybean evapotranspiration (cET), soil evaporation (cE) and transpiration (cT), for three VPD levels under daily, once every three days and weekly irrigation cycles.

	1 day cycle			3 day cycle			7 day cycle		
	<--- mb --->								
VPD --->	7.5	15	22.5	7.5	15	22.5	7.5	15	22.5
cETr, mm	590	611	623	590	611	623	590	611	623
cET, mm	627	688	752	611	667	725	585	635	684
cE, mm	171	209	254	148	182	221	114	142	173
cT, mm	456	479	498	463	485	504	471	493	511

Fig. 5.4 Effects of vapor pressure deficit on water use and crop coefficients

a) Variation in daily water use components under various vapor pressure deficits in mb. Top (7.5), middle (15), and bottom (22.5)

b) Comparison of crop coefficients due to changes in vapor pressure deficits. Solid line (7.5 mb), dotted line (15 mb), and dot and dash combination (22.5 mb)

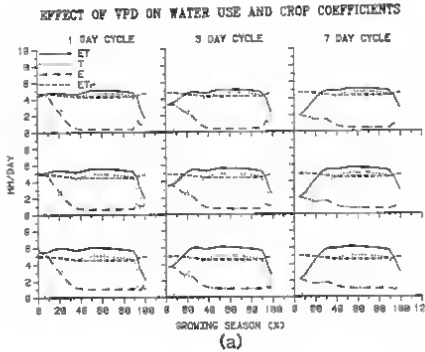
EFFECT OF VPD ON WATER USE AND CROP COEFFICIENTS
1 DAY CYCLE
3 DAY CYCLE
7 DAY CYCLE
ET
T
E
ETo
MM/DAY
GROWING SEASON (X)
(a)
1 DAY CYCLE
3 DAY CYCLE
7 DAY CYCLE
Ks
Kp
Ke
GROWING SEASON (X)
(b)

Radiation

Increases or decreases in radiation caused proportional rises and falls in daily and seasonal ET and ET_r (see Fig. 5.5b and Table 5.6). Soil evaporation during the incomplete canopy stage was also higher initially but decreased sharply under high radiation conditions. The effect of increased radiation on soil evaporation was less significant at longer irrigation intervals. Similariy, transpiration increased more rapidly with radiation and was little influenced by the irrigation frequency. At low LAI and high radiation, soil evaporation was limited by available water, while at high LAI it was limited by both the energy and the humid environment in the canopy. As a result Ks decreased with increasing radiation. On the other hand, lower evaporation at full canopy was compensated by increased transpiration. Therefore K_p was similar among all treatments early in the season while it was higher during the peak growing season. Due to the counteracting behavior of K_s and K_p at low LAI, K_c was lower for high radiation but at high LAI, radiation did not make any difference. Therefore from a practical point of view, changes in radiation could influence K_c considerably during the incomplete canopy stage but would have little effect during the peak growing season.

Wind Speed

Wind speed influenced the canopy to bulk air boundary layer resistance as well as the soil boundary layer resistance. The boundary layer resistance is inversely proportional to the wind speed, therefore both the soil evaporation and transpiration increased at higher wind speed (Table 5.7 and Fig 5.6). The effect of higher wind speed on soil evaporation was noticeable during full canopy stage when

Fig. 5.5 Effect of radiation on water use and crop coefficients

a) Variation in daily water use components under various radiation conditions, in cal/cm2/day. Top (222), middle (444), and bottom (722).

b) Comparison of crop coefficients due to changes in radiation. Solid line (222), dotted line (444), and dot and dash combination (722).

EFFECT OF RADIATION ON WATER USE AND CROP COEFFICIENTS

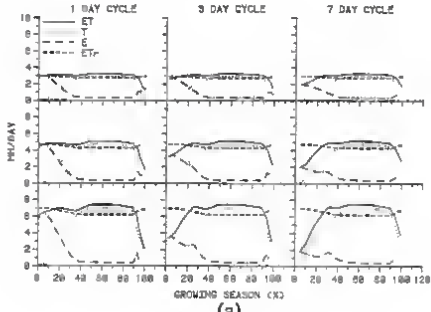

(a)

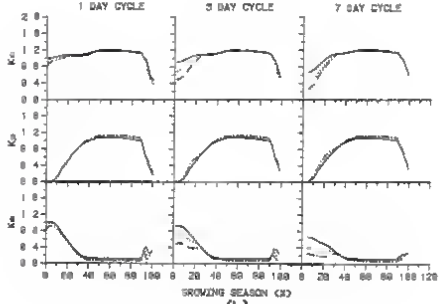

(b)

TABLE 5.6 Cumulative reference crop evapotranspiration (cETr), simulated soybean evapotranspiration (cET), soil evaporation (cE) and transpiration (cT), for three radiation levels under daily, once every three days and weekly irrigation cycles.

	1 day cycle			3 day cycle			7 day cycle		
	<---------- cal/cm^2-day ---------->								
RAD ---->	222	444	722	222	444	722	222	444	722
cETr, mm	374	590	860	374	590	860	374	590	860
cET, mm	406	627	904	402	611	863	389	585	833
cE, mm	121	171	224	117	148	164	100	114	120
cT, mm	284	456	680	285	463	699	289	471	713

TABLE 6.7 Cumulative reference crop evapotranspiration (cETr), simulated soybean evapotranspiration (cET), soil evaporation (cE) and transpiration (cT), for three wind speeds under daily, once every three days and weekly irrigation cycles.

	1 day cycle			3 day cycle			7 day cycle		
	<---------- Km/day ---------->								
WS ---->	86.4	259.2	518.4	86.4	259.2	518.4	86.4	259.2	518.4
cETr, mm	590	661	767	590	661	767	590	661	767
cET, mm	627	731	668	611	684	779	585	638	695
cE, mm	171	254	371	148	201	271	114	146	174
cT, mm	456	477	497	463	483	508	471	492	522

Fig. 5.6 Effect of wind sped on water use and crop coefficients

a) Variation in daily water use components under various wind speeds, in Km/day. Top (86.4), middle (259.2), and bottom (518.4).

b) Comparison of crop coefficients due to changes in wind speeds. Solid line (86.4), dotted line (259.2), and dot and dash combination (518.4).

EFFECT OF WIND SPEED ON WATER USE AND CROP COEFFICIENTS

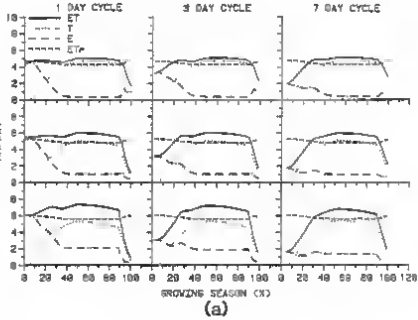

(a)

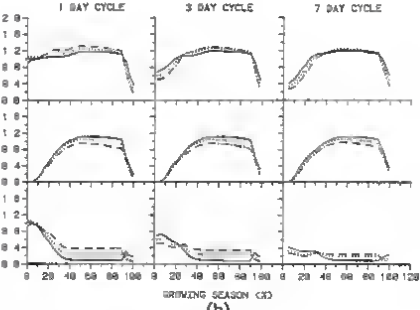

(b)

energy was limiting soil evaporation. With a daily irrigation cycle, seasonal soil evaporation was more than doubled at wind speeds of 518.4 Km/day while transpiration increased by merely 9%. The influence of wind speed on soil evaporation reduced with length of irrigation cycle as soil began to limit E. The feedback and compensatory effects between soil evaporation and transpiration was worth noting An increase in soil evaporation with wind speed increased K_s, but decreased K_p. However as the increase in K_s was greater than the decrease in K_p, K_c increased during the daily irrigation treatment. As the time between irrigation events increased, soil became the E limiting factor at low LAI, and K_c was lower.

In summary, radiation, VPD, and wind speed affected K_c. Radiation had large impact early in the season more so than VPD. Late in the season, K_c were insensitive to radiation but increased with VPD by as much as 15 to 20 %. Wind speed affected K_c throughout the growing season for 1 and 3 day cycles, where as during the 7 day cycle K_c was affected only early in the season.

Planting Dates

Management factors affecting the value of crop coefficient are mainly the crop characteristics, crop planting dates, rate of crop development, and length of growing season. In the earlier section the effects of climatic factors was considered. In this section results of using actual data with spring planting, summer planting and fall planting are analyzed to evaluate the effect of soybean development and length of growing season on water demand and crop coefficients.

Williams soybeans planted during March (maturity Group III) had slow vegetative growth due to relatively lower ambient temperatures. By contrast temperatures were high for the June and August plantings and the canopies attained maximum LAI within 50% of growing season compared to 65% for the March planting (Fig. 5.1). It is interesting to note that although both the June and August plantings dates reached maximum LAI at the same relative times, their magnitudes were significantly different due to the photoperiod response of the cultivar. Due to short days, soybeans planted on August 15 completed their life cycle in 110 days compared to 134 days for the June planting and 117 days for the March planting. The daily ET, E, T and ET_r for all three planting dates under the three irrigation frequencies is shown in Fig. 5.7a. The daily rate of transpiration increase was highest with the June planting date and slowest with the March planting date, while for the August planting it was intermediate, but it reached a lower peak value due to low LAI. The trend in the soil evaporation rates were opposite that of transpiration.

Under all planting dates seasonal soil evaporation decreased with the time between irrigations and transpiration increased (Table 5.8). Seasonal water use revealed that, with the August planting and daily irrigation, soil evaporation exceeded transpiration due to lower LAI development compared with the March and June planting. The incoming radiation increased with time during the March planting, while radiation decreased for the other two planting dates (see Table 5.2). As a result ET_r steadily increased for the March planting and decreased during the June and August planting dates.

The crop coefficients were significantly different among planting

Fig. 5.7 Effect of planting dates on water use and crop coefficients

a) Variation in daily water use rates under different planting dates: top (Mar 15), middle (Jun 26), and bottom (Aug 15).

b) Variation in crop coefficients under to different planting dates.

EFFECT OF PLANTING DATES ON WATER USE AND CROP COEFFICIENTS

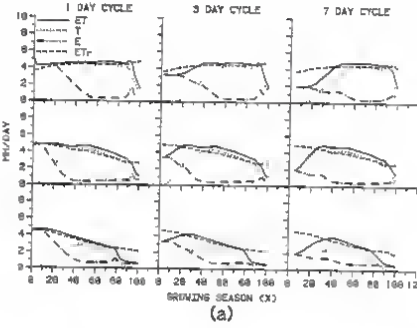

(a)

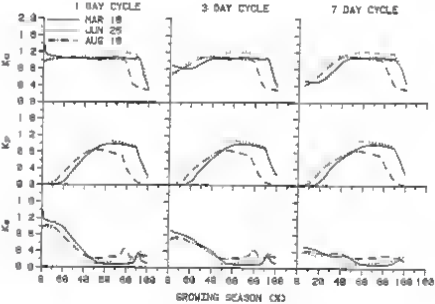

(b)

TABLE 5.8 Cumulative reference crop evapotranspiration (cETr), simulated soybean evapotranspiration (cET), soil evaporation (cE) and transpiration (cT), for three planting dates under daily, once every three days and weekly irrigation cycles.

	1 day cycle			3 day cycle			7 day cycle		
	MAR 15	JUN 26	AUG 15	MAR 15	JUN 26	AUG 15	MAR 15	JUN 26	AUG 15
cETr, mm	507	511	355	507	511	355	507	511	355
cET, mm	514	551	338	503	532	313	442	504	288
cE, mm	210	179	181	175	155	158	125	117	118
cT, mm	304	372	157	308	377	161	317	387	170

dates (Fig 5.7b). As the time between irrigations increased, E and consequently ET was reduced. Therefore according to Eqn (5.2) both the K_c and K_s varied with planting date. Since E was always less than ET_r, except for the first few days under the daily irrigation cycle, K_s was always less than 1. The relative magnitude of K_s before the time of maximum LAI among different planting dates was directly related to the soil evaporation rates (or inversely related to the rate of LAI development). K_s, for the August planting date, due to low LAI, exceeded the other two plantings. K_p for the June planting date was consistently higher than the other planting dates due to higher LAI and gradually decreasing ET_r. Peak T rates for the June and August planting occurred at the same time during the growing season, while it was delayed for the March planting. This behavior was duplicated by K_p values which also peaked at different times.

ET peaked at different times during each planting depending upon the magnitudes of T and E. Therefore K_c also varied accordingly. For the daily irrigation cycle K_c was almost constant between planting and physiological maturity irrespective of the planting dates. However as the time between irrigations increased, K_c increased gradually before attaining a relatively stable value. Therefore the magnitude of K_c was primarily governed by E during incomplete canopy state, while it depended more on T as the canopy attained full cover.

In summary, planting dates could change the magnitude and relative behavior of crop coefficients in the dynamic climate of Florida. The rate of development as well as variations in the ET_r governed the magnitude of K_c, K_p, and K_s.

Concluding Remarks

Most of the crop water requirements have been determined by specific field experiments (Doorenbos and Pruitt, 1977). These studies provided information on water required for ET when crop growth was not limited by soil water. Extrapolation of these published coefficients to different environments has been practiced repeatedly without knowing how valid they are for these different environments. In this paper, the model developed in Chapter III was used to study the effect of varying climate and management factors on water requirements and crop coefficients for a soybean crop growing on a sandy soil. A sensitivity analysis of crop coefficients to changes in temperature, radiation, vapor pressure deficit, and wind speed was performed. Since the method computes soil evaporation and transpiration separately, the overall crop coefficient K_c, was divided into soil evaporation coefficient K_s, and transpiration coefficient K_p. The analysis showed that K_p, the transpiration coefficient was insensitive to climatic changes when compared to K_c and K_s. K_c and K_s changed with variation in radiation, VPD, wind speed and irrigation management practice but were insensitive to temperature changes.

Simulation with actual weather data during three growing seasons, spring, summer and fall showed some interesting results. Due to changes in the ambient air temperature and photoperiod response of soybean cultivars, different canopy development rates occurred. As a result, K_c, K_p, and K_s all varied with planting date.

Irrigation frequency is a management practice that can have significant impact on water use and crop coefficients for the sandy soil. Seasonal water use for the daily irrigation was predicted to be

6 % higher than that for the 7-day interval (Table 5.1) irrigations. Crop coefficients near planting reduced from about 1.0 for the daily irrigation cycle to less than 0.4 for the 7-day cycle. This difference dissipated as LAI increased and K_c for all cycles were similar after full canopy. Therefore in planning for water needs of a crop, irrigation frequency is very important. Crop managers could perhaps conserve water for crops by developing strategies that maintain adequate water for transpiration but reduce soil evaporation. Possible methods include longer irrigation intervals, partial soil surface wetting, or irrigation below the soil surface.

There is growing evidence that computer models relating yield to transpiration are more sound than those relating yield to evapotranspiration (Hanks and Hill, 1980). Therefore the model used in this study when integrated with a crop growth model could enhance its application potential. The weather inputs required for the model are similar to many crop growth models, while the crop parameters are usually estimated during the simulation. However the time step needed by this model may be of some disadvantage. The model needed 1.8 CPU seconds to simulate one day on a PRIME 550 computer. When using this model with other models, the CPU requirements will be less since many of the inputs/outputs would become unnecessary. The entire model is less that 1000 lines of code and can be run on a micro-computer.

CHAPTER VI
SUMMARY AND CONCLUSIONS

The need to predict evaporation and transpiration components of a developing crop was identified as an important issue in determining appropriate water management strategies. Evapotranspiration for a specific crop is governed by prevailing climate, crop and stage of growth, and availability of soil water content. In this study a mechanistic model of evapotranspiration for well-watered crop, where the soil may go through cycles of wetting and drying, was developed based on the physical characteristics of soil, plant and atmosphere.

A physical model of soil evaporation was developed by assuming that soil evaporation was occurring from wet soil below a dry soil of increasing thickness. A ten- week soil evaporation study was conducted in outdoor controlled-environment chambers to determine an empirical function of soil resistance with drying. Cumulative soil evaporation over a 7-day period was less under high radiation, cloudless conditions than for cloudy conditions. This result demonstrated the importance of sensible heat transfer in forming a barrier to evaporation on the sandy soil.

The soil evaporation model was integrated with a two zone canopy model to form a comprehensive evapotranspiration model valid for any stage of crop growth. The canopy was divided into a zone of sun-lit leaves and a zone of shaded leaves. Algorithms to allow this distinction were presented. The proposed model included a number of rarely measured canopy and soil attributes, so solution schemes were develop-

ed using normally measured climate, crop and soil variable so that the model could be used for practical applications and evaluations.

Bragg soybeans were grown in 330, 660 and 990 CO_2 concentration levels in three outdoor, environmental controlled (temperature and humidity) chambers. Water use (evaporation and transpiration), plant growth characteristics, and weather inputs were monitored. The simulated results agreed well with the measurements. The average daily errors were less than 6% . The cumulative leaf area developed faster and water use decreased with increasing CO_2 levels. The sunlit and shaded leaf temperature increased with CO_2 levels.

Simulation studies were conducted to study the effect of CO_2 induced increases in stomatal resistance, leaf area development and air temperature on crop water use. Seasonal water use was reduced at high CO_2 concentration if the increase in air temperature projected for higher CO_2 environment was ignored. However, water use under high CO_2 conditions was predicted to increase under a combined effect of higher stomatal resistance, faster leaf area development, and a 5 °C higher air temperature.

In another simulation study, variation in soybean crop coefficient due to climatic changes were studied. Among the climate factors considered, water use and crop coefficients were most sensitive to increased radiation and lowering relative humidity. The overall crop coefficient, K_c was divided into a soil evaporation coefficient and a transpiration coefficient. For a fixed crop development, the transpiration coefficient was insensitive to changes in climate compared to soil evaporation and overall crop coefficient. However, all crop coefficients varied when soybeans were grown at different times of the year.

This study showed that K_c varied with climate and management factors. Use of published K_c values for varying climate and management may over or under predict crop water needs. The application model demonstrated how K_c values can be adjusted to more closely fit local weather and management conditions when better accuracy is needed.

The model developed in this study will provide an useful tool to study water use by a crop under a variety of climatic, soil, plant and management scenarios. The model can provide a useful research tool in identifying important and critical research needs by eliminating less important situations. Dynamic crop growth models are being developed to predict growth and yield of crops. These models are attractive because crop growth stresses due to pest, nutrient and or water can be included to provide a more comprehensive tool for crop production management. An evapotranspiration model such as the one developed here will greatly enhance application potentials of crop simulation models.

A model of this nature opens doors for the prospects of automated irrigation scheduling. A crop growth model integrated with this model will simulate plant growth and water requirements with inputs obtained from sensors in remote fields. With innovations in the integrated circuits, microprocessors and computer technology, a farmer can install an automated weather and crop reporting system for less than the cost of a garden tractor. Such self sustained systems are already providing weather, crop and soil information necessary for the model implementations.

APPENDIX A
DESCRIPTION OF SUBROUTINES

MAIN PROGRAM	This is the main driver program.
BLRRES	Computes soil boundary layer and canopy aerodynamic resistance to heat and vapor for bare soil and fully developed canopy. Main program uses these values and computes resistances for intermediate growth stages.
FIXEDI	Reads time invariant inputs needed by the model.
GAUSSJ	This routine is called repeatedly by subroutine SOLUTION to solve a system of three simultaneous linear equations.
INIT	Initializes variables each day
IRIGAT	Updates soil water content, and soil temperatures, following an irrigation.
MATADD	Matrix addition routine
MATPRO	Matrix product routine
OUTPUT	Routine to integrate diurnal fluxes of sensible, latent, and soil heat fluxes during the season and write diurnal and daily outputs.
SOILTEMP	Routine to compute soil temperature by layers.
SUNANG	Computes solar elevation as a function of geographical co-ordinates month, and time of day.
SOLUTION	Routine to compute sensible and latent heat fluxes, and soil surface temperatures.

TABEL	X-Y table look-up function
VPOF	Function to compute saturated vapor pressure of air at a given temperature

APPENDIX B
DEFINITION OF VARIABLES USED IN THE COMPUTER CODE

The variables in this list are described as follows

VARIABLE NAME [VARIABLE TYPE, LINKAGE (IF LOCAL VARIABLE) OR /COMMON STATEMENT NAME/,SUBROUTINE(S) IN WHICH VARIABLE IS USED, SUBROUTINE CODE] - DEFINITION OF VARIABLE

Concordance Codes

CODE VARIABLE TYPE

A - ASCII
I - SHORT INTEGER(INTEGER*2)
J - LONG INTEGER (INTEGER*4)
L - LOGICAL
R - REAL (REAL*4)

The following code appears after the subroutine name in the glossary

CODE SUBROUTINE CODE

A - VARIABLE IS CONTAINED IN THE ARGUMENT LIST OF THIS FUNCTION OR SUBROUTINE

D - VARIABLE IS DEFINED IN THIS FUNCTION OR SUBROUTINE

I - VARIABLE IS INITIALIZED IN THIS FUNCTION OR SUBROUTINE (DATA STATEMENT)

M - VARIABLE IS MODIFIED IN ONE OR MORE ASSIGNMENT STATEMENTS OF THIS FUNCTION OR SUBROUTINE

S - VARIABLE IS IN A DATA-MODE SPECIFICATION STATEMENT OF THIS FUNCTION OR SUBROUTINE

ALPHA R LINKAGE MAIN I - Constant in the soil resistance equation to compute effect of net radiation on soil resistance.

BETA R LINKAGE MAIN A - Solar elevation angle in radians

BITA R LINKAGE MAIN I - Constant in the soil resistance equation to compute effect of net radiation on soil resistance (day/mm).

CAP R LINKAGE/ FIXED1 M,TRIGET M SOILTEMP M - Heat capacity of soil at certain soil water content (J/m3- C)

CDL R LINKAGE MAIN M - Conductance of sunlit leaf (m/s)

CE R /MISC/ FIXEDI S M IRIGEI S M MAIN S M - Cumulative soil evaporation (mm)

CEC R /FIXI/ FIXEDI S M MAIN S - Critical magnitude of normalized cumulative evaporation after which soil resistance takes non-zero values (%).

CEM R /FIXI/ FIXEDI S M MAIN S - Maximum cumulative soil evaporation associated with an irrigation or rainfall event and antecedent soil water content (mm).

CEN R LINKAGE MAIN M - Ratio of CE/CEM in percentage

CHIGHT R /FIXI/ FIXEDI S M MAIN S A BLRRES S - Canopy height (m)

CMAX R /FIXI/ FIXEDI S M MAIN S Maximum stomatal conductance under non-limiting light conditions (m/s)

COND R LINKAGE SOLUTION M SOILTEMP M - Thermal conductivity of soil computed from a table look-up function (J/m-s-C)

CP R /SOL/ MAIN S I SOLUTION S - Specific heat of air at constant pressure (J/gm-C)

D R /SOL/ MAIN S M SOLUTION S A BLRRES M - Vapor pressure deficit in air (mb)

DAIR R /SOL/ MAIN S I SOLUTION S - Density of air (gm/m3)

DAPL R /FIXI/ FIXEDI S M MAIN S M OUTPUT S I - Days after planting

DAY R /MISC/ MAIN S I M OUTPUT S - Day number

DELG R LINKAGE SOLUTION M - Increment in soil heat flux computed during iterative calculations of soil temperatures.

DELTA R /SOL/ MAIN S M SOLUTION S - Slope of saturated vapor pressure vs. temperature curve (mb/C)

DELTOZ R LINKAGE SOILTEMP M - Distance between centers of two adjacent soil layers (m)

DG R /INI/ INIT S M OUTPUT S M Daily total of soil heat flux (in equivalent mm of water)

DLAYR R /IRR/ FIXEDI S M IRIGET S MAIN S SOLUTION S SOILTEMP S - Depth of a soil layer (m)

DRYDAY R /FIXI/ FIXEDI S M IRIGET S M MAIN S M - No. of dry days since last rain or irrigation.

[illegible] R /IRR/ FIXED1 S M IRIGET S Drained upper limit of soil water content, volume basis (m3/m3)

[illegible] R /SOL/ SOLUTION S M Mean vapor pressure in the canopy

EW R LINKAGE RLRRES M Crop specific velocity attenuation coefficient (unitless)

ERRBND R /FIX1/ FIXED1 S M SOLUTION S Acceptable absolute error between two subsequent computation of soil surface temperature

ERROR R LINKAGE SOLUTION M Computed error between two subsequent computation of soil surface temperature

ESESN R /MISC/ MAIN S I OUTPUT S M Evaporation for season, mm

ETA R LINKAGE MAIN I Constant in the soil resistance equation

ETSC R /IN1/ INIT S M OUTPUT S M Daily sum of canopy transpiration (mm)

ETSCL R /MISC/ MAIN S I OUTPUT S M Canopy transpiration from last simulation step (mm/hr)

ETSESN R LINKAGE MAIN I OUTPUT M Seasonal evapotranspiration, mm

ETSIM R /IN1/ INIT S M OUTPUT S M Daily sum of evapotranspiration, mm

ETSIML R /MISC/ MAIN S I OUTPUT S M Evapotranspiration from last time step (mm/hr)

ETSS R /IN1/ INIT S M OUTPUT S M Daily sum of evaporation, mm

ETSSL R /MISC/ MAIN S I OUTPUT S M evaporation from last simulation step (mm/hr)

EV2ONE R LINKAGE MAIN M Water lost from evaporation zone, mm

EXTINC R /FIX1/ FIXED1 S M MAIN S Light extinction coefficient

FLOW R LINKAGE SOILTEMP S M Heat flow between adjacent soil layers (J/s-C)

FRACTN R /FIX1/ FIXED1 S M MAIN S Fraction of above canopy net radiation and PPFD received by shaded canopy.

FREQNC R /FIX1/ FIXED1 S M MAIN S Frequency of irrigation, days

FTEZ R /FIX1/ FIXED1 S M MAIN S Fraction of transpiration coming from evaporation zone

G R /SOL/ MAIN S M OUTPUT S M SOLUTION S M Soil heat flux

GAMMA R /SOL/ MAIN S M SOLUTION S Psychrometric constant (mb/C)

GL R /MISC/ MAIN S I OUTPUT S M Soil heat flux from last simulation step

HCAP R /STMP/ FIXEDI S M A IRIGET S A SOILTEMP S A Soil heat capacity (J/m3-C)

HEC R /MISC/ MAIN S OUTPUT S M Hourly transpiration, mm/h

HES R /MISC/ MAIN S OUTPUT S M Hourly evaporation, mm/h

IERROR J ARGUMENT GAUSSJ S M SOLUTION A Error code

ITER J LINKAGE SOLUTION M Iteration number

JULIAN J /WETH/ MAIN S M WTHR S M A Julian day

KEY R /FIXI/ FIXEDI S M SOLUTION S KEY=1 soil surface temperature is an input. KEY=2 soil surface temperature need to be computed in the model

KK R LINKAGE SOLUTION M Error code

LAI R /MISC/ MAIN S M OUTPUT S Leaf area index

LAIDL R LINKAGE MAIN M LAI of shaded leaves

LAIMAX R /FIXI/ FIXEDI S M MAIN S LAI when canopy achieves full ground cover

LAISL R LINKAGE MAIN M LAI of sunlit leaves

LDAILY R /FIXI/ FIXEDI S M OUTPUT S Flag for daily output [LDAILY=1 i.e. YES, LDAILY=-1 i.e. NO]

LHOUR R /FIXI/ FIXEDI S M OUTPUT S Flag for hourly output [LHOUR=1 i.e. YES, LHOUR=-1 i.e. NO]

LHV R /MISC/ MAIN S M OUTPUT S WTHR S M Latent heat of vaporization of water (J/gm)

LL R /IRR/ FIXEDI S M MAIN S Lower limit of soil water extraction, volumetric basis.

NDATAP J /WETH/ MAIN S WTHR S M Time steps per day

NELAYR J /FIXI/ FIXEDI S M MAIN S Number of soil layers (counted from soil surface) from which water can be lost as soil evaporation.

NFLOW R LINKAGE SOILTEMP S M Net heat flow from a soil layer (J/s-C)

NHOUR J /SOL/ MAIN S M OUTPUT S I SOLUTION S I Simulation time step number

NMONTH J /WETH/ WTHR S M Month of the year

NR7 J /FIXI/ FIXED1 S M MAIN S Day when irrigations stopped

NTLAYR J /FIXI/ FIXED1 S M IRIGET S SOILTEMP S Total number of soil layers

NYR J /WETH/ WTHR S M A MONTH S Year

PPFD R /WETH/ MAIN S WTHR S M Photosynthetically active Photon Flux Density (micro Einstein/m2-s)

R R /SOL/ MAIN S M SOLUTION S I Mean aerodynamic resistance to heat and water vapor transfer from canopy to air (s/m),

RA R /FIXI/ FIXED1 S M MAIN S Boundary layer resistance of individual leaflet (s/m)

RB R /SOL/ MAIN S M SOLUTION S I Boundary layer resistance, s/m [RB(1)- sunlit leaves, RB(2)- shaded leaves, RB(3)- soil]

RC1 R ARGUMENT BLKRES S M MAIN A - Mean aerodynamic resistance to heat and water vapor from canopy to air (s/m), at LAI=0.

RC2 R ARGUMENT BLKRES S M MAIN A - Mean aerodynamic resistance to heat and water vapor from canopy to air (s/m), at LAI=LAIMAX.

RH R /SOL/ MAIN S M SOLUTION S A Resistance for sensible heat s/m, RH = R + RR (I) [RH(1)- sunlit leaves, RH(2)- shaded leaves, RH(3)- soil].

RMAX R /FIXI/ FIXED1 S M MAIN S Maximum boundary layer resistance of a leaf at LAI=0

RN R /SOL/ MAIN S M OUTPUT S I SOLUTION S H A I Net radiation absorbed [RN(1)- sunlit leaves, RN(2)- shaded leaves, RN(3)- soil].

RNO R /WETH/ MAIN S WTHR S M I Net radiation above the canopy

RNA R /MISC/ MAIN S H Average daily net radiation at soil surface from onset of drying cycle (mm/day)

RNAMIN R /FIXI/ FIXED1 S M MAIN S I Lower limit of RNA (mm/day)

RNNET R LINKAGE MAIN I M Total daily net radiation at soil surface, mm/day

RNTOT R /MISC/ IRIGET S M MAIN S I M Total net radiation at soil surface from onset of drying cycle.

RS R /SOL/ MAIN S M SOLUTION S Surface resistance, s/m [RS(1)- sunlit leaves, RS(2)- shaded leaves, RS(3)- soil]

RS1 R ARGUMENT RLRRES S M MAIN A Boundary layer resistance of soil surface at LAI=0

RS2 R ARGUMENT RLRRES S M MAIN A Boundary layer resistance of soil surface at LAI=LAIMAX

RV R /SOL/ MAIN S M SOLUTION S A Resistance to vapor transfer, s/m, RV = R + RB(I) + RS(I) [RV(1)- sunlit leaves, RV(2)- shaded leaves, RV(3)- soil]

S R /SOL/ OUTPUT S SOLUTION S A Sensible heat flux, J/m2-s [S(1)- sunlit leaves, S(2)- shaded leaves, S(3)- soil]

SAT R /IRR/ FIXED1 S M - Saturated soil water content by layers

SBNDRY R LINKAGE MAIN M - Soil surface boundary layer resistance, s/m

SHSC R /INI/ INIT S M OUTPUT S M Daily sum of sensible heat flux from canopy, mm/day

SHSCL R /MISC/ MAIN S I OUTPUT S M Sum of canopy sensible heat flux from previous time step, mm/h

SHSIM R /INI/ INIT S M OUTPUT S M Daily sum of sensible heat flux from canopy and soil, mm/day

SHSIML R /MISC/ MAIN S I OUTPUT S M Sum of canopy and soil sensible heat flux from previous time step, mm/hr

SHSS R /INI/ INIT S M OUTPUT S M Daily sum of sensible heat flux from soil, mm/day

SHSSL R /MISC/ MAIN S I OUTPUT S M Sum of soil sensible heat flux from previous time step, mm/h

SLOPE R /FIXI/ FIXED1 S M, MAIN S Initial slope of leaf conductance vs PPFD (m3/ micro Einstein)

SUMH R /SOL/ OUTPUT S M SOLUTION S M Sum of sensible heat flux from canopy and soil at each simulation step (mm/h)

SUMRN R LINKAGE OUTPUT M Net radiation at each time step (mm/h)

SUMV R /SOL/ OUTPUT S M SOLUTION S M Sum of latent heat flux from canopy and soil at each simulation step (mm/h)

SW R /IRR/ FIXED1 S M A IRIGET S A M MAIN S M SOLUTION S A SOILTEMP S A Soil water content by layers, volume basis

TA R /WETH/ IRIGET S MAIN S A OUTPUT S SOLUTION S

	WTHR	S	M	Air temperature, C			
TAVG	R	LINKAGE	MAIN	M	A	Average of soil and air temperature to compute slope of saturated vapor pressure vs temperature curve.	
TC	R	/SOL/	OUTPUT	S	SOLUTION	S	M Mean canopy temperature, C
TD	R	/WETH/	MAIN	S	A SOLUTION	S	A WTHR S M Dew point temperature, C
TEMP	R	/STMP/	FIXED1	S	M IRIGET	S	M SOLUTION S SOILTEMP S M Temperature of soil by layers, C
THCOND	R	/STMP/	FIXED1	S	M SOLUTION	S	A SOILTEMP S A Thermal conductivity of soil, J/m-s-C.
THETA	R	/STMP/	FIXED1	S	M A IRIGET	S	A SOLUTION S A SOILTEMP S A Water content of soil at which HCAP values are specified.
TIME	R	/WETH/	MAIN	S	A OUTPUT	S	WTHR S M Time of day, h
TOTAL	R	/WETH/	MAIN	S	WTHR	S	M Total daily incoming net radiation, mm
TS	R	/SOL/	MAIN	S	M OUTPUT	S	SOLUTION S M Computed surface temperatures, C [TS(1)- sunlit leaves, TS(2)- shaded leaves, TS(3)- soil surface]
TS3MAX	R	/SOL/	INIT	S	OUTPUT	M	Maximum soil surface temperature
TS3MN	R	/SOL/	INIT	S	OUTPUT	M	Minimum soil surface temperature
TSESN	R	/MISC/	MAIN	S	1 OUTPUT	S	M Transpiration for season, mm
TSS	R	/WETH/	MAIN	S	WTHR	S	M Soil surface temperature, C
TSTEP	R	/STMP/	OUTPUT	S	M SOILTEMP	S	Time step of simulation, h
TSURF	R	/SOL/	SOLUTION	S	M SOILTEMP	S	Intermediate value of soil surface temperature
U	R	/WETH/	WTHR	S	M	Wind speed, m/s	
UAVG	R	/FIX1/	FIXED1	S	M MAIN	S	A BLRRES S Average wind speed between LAI=0 and LAI=LAIMAX, m/s
V	R	/SOL/	OUTPUT	S	SOLUTION	S	A Latent heat flux, J/m2-s [S(1)- sunlit leaves, S(2)- shaded leaves, S(3)- soil]
VHCAP	R	/STMP/	FIXED1	S	M IRIGET	S	M SOILTEMP S M Volumetric heat capacity of soil, (J/m3)

XLAT R /FIXI/ FIXEDI S M MAIN S A SUNANG S Latitude of the site, degrees

XLONG R /FIXI/ FIXEDI S M MAIN S A SUNANG S Longitude of the site, degrees

XLST R ARGUMENT SUNANG S Time of day

XTRACT R LINKAGE MAIN M Amount of water extracted from evaporation zone, mm

Z0 R LINKAGE BLOCKES M - Crop roughness height, m

ZI R LINKAGE BLOCKES M - Soil roughness height, m

APPENDIX C

SOURCE CODE OF SUBROUTINES

```
C*** MAIN PROGRAM
$STORAGE 2
$NOFLOATCALLS
$INCLUDE  'COMMON.DAT'
      DATA ALPHA,BITA,ETA/1.0942E-3,2.0197E-3,1.35757/
C
C=====================================================================
C              INPUT SECTION                                          C
C=====================================================================C
C
      OPEN (UNIT = 6 ,FILE = 'INPUT.DAT',STATUS = 'OLD')
      OPEN (UNIT = 7 ,FILE = 'WEATHER.DAT',STATUS = 'OLD')
      OPEN (UNIT = 8 ,FILE = 'PLANT.DAT',STATUS = 'OLD')
      OPEN (UNIT = 9 ,FILE = 'OUTPUT1.DAT',STATUS = 'NEW')
      OPEN (UNIT = 10,FILE = 'OUTPUT2.DAT',STATUS = 'NEW')
C     gm/m3
      DAIR = 1.1400E3
C     J/gm-C
      CP = 1.00488
C     mb
      P = 1013.
      BSILON = 0.622
      DAY = 1
      RNTOT = 0.
      TSESN = 0.
      ESESN = 0.
      FTSESN = 0.
      RNNET = 0.
      CALL FIXEDI
      CALL BLRRES(CHIGNT,UAVG,RS1,RS2,RC1,RC2)
C
C***  NEW DAY
C
  100 READ (8,*  ,END = 1000) JULIAN,LAI
      CALL JTHR
      IF (DAY .GT. 1) GO TO 200
      TS(3,1) = TA(1)
      G       = RND(1)*EXP(-EXTINC*LAI)
  200 RNTOT = RNTOT+RNNET
      IF (DRYDAY .LE. FREQNC .OR. DAPL .GE. NR7) GO TO 300
      CALL IRIGAT
  300 IF (LAI .GT. LAIMAX) GO TO 400
      SBNDRY = RS1+(RS2-RS1)*LAI/LAIMAX
      R      = RC1+(RC2-RC1)*LAI/LAIMAX
  400 RNNET  = TOTAL*EXP(-EXTINC*LAI)
      RNA    = (RNTOT + RNNET)/ DRYDAY
      IF (RNA .LT. RNAMIN) RNA = RNAMIN
```

```
      CALL INIT
C
C-----------------------------------------------------------------------
C     DAILY CALCULATIONS
C-----------------------------------------------------------------------
C
      TLAST  = TIME(1)
           DO 900 NHOUR = 1,NDATAP
           LHV    = 2500.9 - 2.345*TA(NHOUN)
           GAMMA  = P*CP/(LHV*BSILON)
           TAVG   = (TS(3,1)+TA(NHOUR))*0.5
           DELTA  = VPDF(TAVG+1.)-VPDF(TAVG)
           CALL SUNANG(XLAT,XLONG,NMONTH,TIME(NHOUR),BETA,AZANGL)
           SBETA  = SIN(BETA)
           IF (SBETA .LE. 0) SBETA = 1.
           XK     = EXTINC/SBETA
           LAISL  = (1./XK)*(1. - EXP(-XK*LAI))
           LAIOL  = LAI - LAISL
           RB(1)  = RMAX
           RB(2)  = RMAX
           RB(3)  = SUNDRY
           IF (LAISL .GT. 0.0001) RS(1) = RA/LAISL
           IF (LAIOL .GT. 0.0001) RS(2) = RA/LAIOL
           RS(1) = RMAX
           RS(2) = RMAX
           CSL    = CMAX*(1.-EXP(SLOPE*PPFD(NHOUR)/CMAX))
           COL    = CMAX*(1.-EXP(SLOPE*PPFD(NHOUR)*FRACTN/CMAX))
           IF (LAISL .GT. 0.001 .AND. CSL .GT. 0) RS(1) =
     +        1./(CSL*LAISL)
           IF (LAIOL .GT. 0.001 .AND. COL .GT. 0) RS(2) =
     +        1./(COL*LAIOL)
           RS(3) = 0.
           CEN    = (CE/CEM)*100.
           IF (CEN .GT. 100) CEN = 100.
            IF (CEN .GT. CEC) RS(3) = 154*(EXP((ALPHA+R1TA*RNA)*(CEN-
     +                                        CEC)**ETA)-1.)
           IF (RS(3) .LT. 0) RS(3) = 0.
           IF (FREQNC .GT. 99) RS(3) = RMAX
           RN(1,1) = RNO(NHOUR)*XK*LAISL
           RN(2,1) = RNO(NHOUR)*FRACTN *XK*LAIOL
           RN(3,1) = RNO(NHOUR)*EXP(-XK*LAI)-RN(2,1)
           IF (RN(3,1) .LT. 0) RN(3,I) = 0.
           TS(3,1) = TSS(NHOUR)-TA(NHOUR)
                DO 600 I = 1,3
                     DO  500 J = 1,3
                     NH(I,J) = R
                     RV(I,J) = R
                     IF (I .NE. J) GO TO 500
                     RH(I,J) = R +RB(I)
                     RV(I,J) = R +RB(I)+RS(I)
  500                CONTINUE
                O(I,1) = VPDF(TA(NHOUN))-VPDF(TO(NHOUR))
  600           CONTINUE
C
```

```
C*** SOLVE THE THREE ZONE SOIL-PLANT MODEL AT THIS TIME
C
          CALL SOLUTION
          CALL OUTPUT(1)
          CALL SOILTEMP
C
C     UPDATE SOIL WATER
          EVZONE = MES + FTEZ*NEC
          CE     = CE + EVZONE
          EVZONE = EVZONE*0.001
               DO 800 IJ = 1,NELAYR
               IF (EVZONE .LE. 0) GO TO 800
               IF (SW(IJ) .LE. LL(IJ)) GO TO 800
               XTRACT = (SW(IJ)-LL(IJ))*DLAYR(IJ)
               IF (EVZONE .LE. XTRACT) GO TO 700
               SW(IJ) = LL(IJ)
               EVZONE = EVZONE-XTRACT
               GO TO 800
  700          SW(IJ) = SW(IJ) - EVZONE/DLAYR(IJ)
               EVZONE = 0.
  800          CONTINUE
  900     CONTINUE
      CALL OUTPUT(2)
      NAPL  = NAPL+1
      NAY   = DAY + 1
      DRYDAY = DRYDAY+1
      GO TO 100
 1000 CLOSE (6)
      CLOSE (7)
      CLOSE (8)
      CLOSE (9)
      CLOSE (10)
      STOP
      END
```

```
$STORAGE=2
$NOFLOATCALLS
      SUBROUTINE ALARRES (CHIGHT,UAVG,RS1,RS2,RC1,RC2)
      EN = 3.
      Z1 = 0.01
      X = 2.
      D = 0.7*CHIGHT**0.979
      Z0 = 0.13*CHIGHT**0.997
      E1 = EXP(EN*(1.-(D+Z0)/CHIGHT))
C     E2=EXP(EN*(CHIGHT-Z1))
      E2 = EXP(EN)
      E3 = CHIGHT/(EN*(CHIGHT-D))
      E4 = ALOG((X-D)/Z0)
      E5 = 0.4*0.4*UAVG
      RS2 = E4*E3*(E2-E1)/E5
      E6 = ALOG((X-D)/(CHIGHT-D))
      RC2 = E4*(E6+E3*(E1-1))/E5
      RS1 = ALOG(X/Z1)*ALOG((D+Z0)/Z1)/E5
      RC1 = (ALOG(X/Z1)**2)/E5
      RC1 = RC1-RS1
      RETURN
      END
```

```
$STORAGE 2
$NOFLOATCALLS
      SUBROUTINE FIXEDI
$INCLUDE   COMMON.DAT'
      READ (6,*) DAPL,ORYDAY,CE,LOAILY,LHOUR,FREQNC,CHIGHT,LATMAX,
     +           UAVG,RA,ERRBND,RMAX,RNAMIN,XLAT,XLONG,KEY
      READ (6,*) EXTINC,FRACTN,CMAX,SLOPE,NR7
      READ (6,*) NELAYR,NTLAYR,CEM,CEC,FTEZ
      READ (6,*) (DLAYR(I),I = 1,NTLAYR)
      READ (6,*) (TEMP(I) ,I = 1,NTLAYR)
      READ (6,*) (SW(I)   ,I = 1,NTLAYR)
      READ (6,*) (SAT(I)  ,I = 1,NTLAYR)
      READ (6,*) (OUL(I)  ,I = 1,NTLAYR)
      READ (6,*) (LL (I)  ,I = 1,NTLAYR)
      READ (6,*) (THCOND(I),I = 1,3)
      READ (6,*) (  HCAP(I),I = 1,3)
      READ (6,*) ( THETA(I),I = 1,3)
           DO 100 I  = 1,NTLAYR
           XSW       = SW(I)
           CAP       = TABEL(HCAP,THETA,XSW,3)
 100       VHCAP(I)  = TEMP(I)*CAP*DLAYR(I)
      RETURN
      END
```

```
$STORAGE 2
$NOFLOATCALLS
      SUBROUTINE GAUSSJ(B, W, NROW,MAXD,IERROR)
C
C     MATRIX INVERSION BY THE GAUSS JORDAN METHOD.
C
C     B       COEFFICIENT MATRIX BECOMES INVERSE MATRIX
C     INDEX   WORK ARRAY, NEEDS THREE COLUMNS.
C     NROW    CURRENT MATRIX SIZE.
C     MAXD    DIMENSION MATRIX SIZE.
C     IERROR LOGICAL ERROR FLAG .TRUE. IF MATRIX SINGULAR
C
      DIMENSION INDEX(15,3)
      INTEGER NROW,MAXD,I,J,K,L,IROW,ICOL,LI
      REAL  B(MAXD,MAXD), W(MAXD,MAXD),BIG,SUM,T,PIVOT,OFTERM
      IERROR = .FALSE.
           DO 100 I = 1, NROW
           INDEX(I,3) = 0
  100      CONTINUE
      DETERM = 1.0
           DO 900 I = 1, NROW
C  SEARCH FOR LARGEST ELEMENT.
           BIG = 0.0
                DO 300 J = 1, NROW
                IF (INDEX(J,3) .EQ. 1) GO TO 300
                     DO 200 K = 1, NROW
                     IF (INDEX(K,3) .GT. 1) GO TO 1300
                     IF (INDEX(K,3) .EQ. 1) GO TO 200
                     IF (ABS(B(J,K)) .LE. BIG) GO TO 200
                     IROW = J
                     ICOL = K
                     BIG = ABS(B(I,K))
  200                CONTINUE
  300           CONTINUE
           INDEX(ICOL,3) = INDEX(ICOL,3) + 1
           INDEX(I,1) = IROW
           INDEX(I,2) = ICOL
C
C  INTERCHANGE ROWS TO PUT PIVOT ON DIAGONAL.
C
           IF (IROW .EQ. ICOL) GO TO 500
           DETERM = -DETERM
                DO 400 L = 1, NROW
                CALL SWAP(B(IROW,L), B(ICOL,L))
  400           CONTINUE
C
C  DIVIDE PIVOT ROW BY PIVOT ELEMENT
C
  500      PIVOT = B(ICOL,ICOL)
           DETERM = DETERM * PIVOT
           B(ICOL,ICOL) = 1.0
                DO 600 L = 1, NROW
                B(ICOL,L) = B(ICOL,L) / PIVOT
  600           CONTINUE
```

```
C  REDUCE NON PIVOT TERMS.
C
                DO 800 L1 = 1, NROW
                IF (L1 .EQ. ICOL) GO TO 800
                T = B(L1,ICOL)
                B(L1,ICOL) = 0.0
                     DO 700 L = 1, NROW
                     B(L1,L) = B(L1,L) - B(ICOL,L) * T
  700                CONTINUE
  800           CONTINUE
  900      CONTINUE
C  END OF I LOOP.
C  INTERCHANGING COLUMNS.
           DO 1100 I = 1, NROW
           L = NROW - I + 1
           IF (INDEX(L,1) .EQ. INDEX(L,2)) GO TO 1100
           IROW = INDEX(L,1)
           ICOL = INDEX(L,2)
                DO 1000 K = 1, NROW
                CALL SWAP(B(K,IROW), B(K,ICOL))
 1000           CONTINUE
 1100      CONTINUE
           DO 1200 K = 1, NROW
           IF (INDEX(K,3) .NE. 1) GO TO 1300
 1200      CONTINUE
      RETURN
 1300 IERROR = 1
      RETURN
      END
C
      SUBROUTINE SWAP(A,B)
C  INTERCHANGE TWO VALUES.
      NOLD = A
      A = B
      B = NOLD
      RETURN
      END
```

```
$STORAGE 2
$NOFLOATCALLS
      SUBROUTINE INIT
$INCLUDE  'COMMON.DAT'
      OG     = 0.
      ETSIM  = 0.
      ETSC   = 0.
      ETSS   = 0.
      SHSC   = 0.
      SHSS   = 0.
      SHSIM  = 0.
      ETSIML = 0.
      ETSCL  = 0.
      ETSSL  = 0.
      SHSCL  = 0.
      SHSSL  = 0.
      SHSIML = 0.
      GL     = 0.
      TACMN  = 100.
      TACMX  = 0.
      TS3MN  = 100.
      TS3MX  = 0.
      RETURN
      END
```

```
$STORAGE 2
$NOFLOATCALLS
      SUBROUTINE IRIGAT
$INCLUDE: 'COMMON.DAT'
            DO 100 I = 1,NTLAYR
            CAP       = TABEL(HCAP,THETA,SW(I),3)
            VHCAP(I) = ( CAP*TEMP(I) + 4.187E6*(DUL(1)-SW(I))*TA(1) )*
     +            DLAYR(I)
            SW(I)     = DUL(1)
            CAP       = TABEL(HCAP,THETA,SW(I),3)
            TEMP(1)   = VHCAP(I)/(CAP*DLAYR(I))
  100       CONTINUE
        CE = 0.
        RNTOT = 0.
        DRYDAY = 1.
        RETURN
        END
```

```
$STORAGE 2
$NOFLOATCALLS
      SUBROUTINE MATADD(A, B, C, IX, IY)
      IMPLICIT REAL*8(A-H,O-Z)
      REAL A(IX,IY),B(IX,IY),C(IX,IY)
            DO 100 IROW = 1,IX
                  DO 100 JCOL = 1,IY
                  C(IROW,JCOL) = A(IROW,JCOL) + B(IROW,JCOL)
  100             CONTINUE
      RETURN
      END
```

```
$STORAGE 2
$NOFLOATCALLS
      SUBROUTINE MATPRO(A, B, C, IX, IY,IZ)
      REAL A(IX,IY),B(IY,IZ),C(IX,IZ)
            DO 300 NCOL = 1,IZ
                DO 200 IROW = 1,IX
                SUM = 0.
                     DO 100 JCOL = 1,IY
                     SUM = SUM + A(IROW,JCOL) * B(JCOL,NCOL)
  100                CONTINUE
                C(IROW,NCOL) = SUM
  200           CONTINUE
  300       CONTINUE
      RETURN
      END
```

```
$STORAGE:2
$NOFLOATCALLS
      SUBROUTINE OUTPUT(rII)
$INCLUDE: 'COMMON.DAT
C
C     Integrate & convert from J/m2-s to mm H2o
C
      IF (III .EQ. 2) GO TO 300
      TSTEP = (TIME(NHOUR)-TLAST)*3600.
      HEC   = (ETSCL+V(1,1)+V(2,1))*0.5*TSTEP/(1000.*LHV)
      HES   = (ETSSL+V(3,1))*0.5*TSTEP/(1000.*LHV)
      ETSC  = ETSC  +(V(1,1)+V(2,1)+ETSCL) * 0.5*TSTEP/(1000.*LHV)
      ETSS  = ETSS  +(V(3,1)+ETSSL)*0.5*TSTEP/(1000.*LHV)
      SHSC  = SHSC  +(S(1 1)+S(2,1)+SHSCL) * 0.5*TSTEP/(1000.*LHV)
      SHSS  = SHSS  +(S(3,1)+SHSSL)*0.5*TSTEP/(1000.*LHV)
      OG    = OG +(G+GL)*0.5*TSTEP/(1000.*LHV)
      ETSIM = ETSIM+(V(1,1)+V(2,1)+V(3,1)+ETSIML)*0.5*
     +        TSTEP/(1000.*LHV)
      SHSIM = SHSIM+(S(1,1)+S(2,1)+S(3,1)+SHSIML)*0.5*
     +        TSTEP/(1000.*LHV)
      GL    = G
      ETSIML = V(1,1)+V(2,1)+V(3,1)
      SHSIML = S(1,1)+S(2,1)+S(3,1)
      ETSCL = V(1,1)+V(2,1)
      ETSSL = V(3,1)
      SHSCL = S(1,1)+S(2,1)
      SHSSL = S(3,1)
      TLAST = TIME(NHOUR)
C
C*** CONVERT OIURNAL VALUES TO MM/HR
C
      SUMV    = SUMV*3600./(LHV*1000.)
      SUMH    = SUMH*3600./(LHV*1000.)
      G       = G*3600./(LHV*1000.)
      SUMRN   = (RN(1,1)+RN(2,1)+RN(3,1))*3600./(LHV*1000.)
           DO 100 IJ = 1,3
           V(IJ,1)     = V(IJ,1)*3600./(LHV*1000.)
           S(IJ,1)     = S(IJ,1)*3600./(LHV*1000.)
           RN(I1,1)  = RN(IJ,1)*3600./(LHV*1000.)
  100      CONTINUE
      IF (TS(3,1) .LT. TS3MN)    TS3MN = TS(3,1)
      IF (TS(3,1) .GT. TS3MX)    TS3MX = TS(3,1)
      IF (TC .LT. TACMN)         TACMN = TC
      IF (TC .GT. TACMX)         TACMX = TC
      IF(TIME(NHOUR).GT.9.75.AND.TIME(NHOUR).LT.10.25)
     +   TCTA=TC-TA(NHOUR)
C
C***  OIURRAL OUTPUT
C
      RADNET = RN1T + RN2T + RN3T
      VPRES  = VPOF(TO(NHOUR))
      IF (LHOUR .LE. 0) RETURN
      WRITE (9,200) DAY,DAPL,TIME(NHOUR),RN(1,1),V(1,1),S(1,1),
     + RN(2,1),V(2,1),S(2,1),RN(3,1),V(3,1),S(3,1),G,TC,TS(1,1),
```

```
     + TS(2,1),TS(3,1),VPRES,EC
  200 FORMAT(2F5.0,1X,F5.1,1X,10(F5.2 ,1X),6(F5.2,1X))
      RETURN
C
C
C*** DAILY OUTPUT
C
  300 IF (LDAILY .LE. 0) RETURN
      TSESN  = TSESN + ETSC
      ESESN  = ESESN + ETSS
      ETSESN = ETSESN+ ETSC + ETSS
      WRITE (10,400) DAPL,LAI,ETSIM,ETSC,ETSS,ETSESN,TSESN,ESESN,
     +               TGTA,TS3MX,TS3MN,DAPL
  400 FORMAT(F4.0,1X ,F3.1,1X,3(F6.3,1X),3(F6.1,1X),3(F5.1,1X),F4.0)
      RETURN
      END
```

```
$STORAGE:2
$NOFLOATCALLS
      SUBROUTINE SOILTEMP
$INCLUDE: 'COMMON.DAT'
      REAL FLOW(20),NFLOW(20)
      CONO       = TABEL(THCOND,THETA,SW(1),3)
      DELTOZ     = (TSURF-TEMP(1))/(0.5*DLAYR(1))
      FLOW(1)    = DELTDZ*CONO
           DO 100 I   = 2,NTLAYR
           COND1      = TABEL(THCOND,THETA,SW(I-1),3)
           COND2      = TABEL(THCOND,THETA,SW(I)  ,3)
           THICK      = (DLAYR(I-1)+DLAYR(I))*0.5
           DELTOZ     = (TEMP(I-1)-TEMP(I))/THICK
           FLOW(I)    = DELTDZ * (COND1+COND2)*0.5
           NFLOW(I-1) = (FLOW(I-1)-FLOW(I))*TSTEP
           VHCAP(I-1) = VHCAP(I-1)+NFLOW(I-1)
           IF (VHCAP(I-1) .LT. 0) VHCAP(I-1) = 0.
  100      CONTINUE
      NFLOW(NTLAYR) = FLOW(NTLAYR)*TSTEP
      VHCAP(NTLAYR) = VHCAP(NTLAYR) + NFLOW(NTLAYR)
           DO 200 I = 1,NTLAYR
           CAP       = TABEL(HCAP,THETA,SW(I),3)
  200      TEMP(I) = VHCAP(I)/(DLAYR(I)*CAP)
      RETURN
      END
```

```
C
C*****************************************************************
C   This program does following
C   1. Finds solar angle elevation for a location at a given time, and
C   2. Solar azimuthal angle measured from N-S direction.
C
C   Theory  Refer to 1977 ASHARAE FUNDAMENTALS HANDBOOK
C           Ch, 26 pages 26.2, 26.3 & Table 1.
C
C   Gainesville location 29.7 North latitude & 82.4 West Longitude
C
C   Eastern Standard Time Longitude = 75 Deg.
C
C    XLAT = Latitude in Deg.
C    XLONG= Longitude in Deg.
C    XLSM  = Local standard time meridian, Deg.
C    AST   = Apparent solar time
C    ET    = Equation of time(MINUTES)
C    DECLIN = Declination   (DEGREES)
C    LST   = Local standard time
C    AZANGL = AZIMUTHAL ANGLE IN RADIANS MEASURED FROM SOUTH
C    BETA = SOLAR ELEVATION IN RADIANS
C*****************************************************************
**
C
$STORAGE 2
$NOFLOATCALLS
      SUBROUTINE SUNANG(XLAT,XLONG,MONTH,XLST,BETA,AZAHGL)
      DIMENSION ET(12),DECLIH(12)
      DATA ET/-11.2,-13.9,- 7.5,1.1,3.3,-1.4,-6.2,-2.4,7.5,15.4,13.8,
     +1.6/
        DATA DECLIH/-20.,-10.8,0.,11.6,20.,23.45,20.6,12.3,0.,-10.5,-
     + 19.8,-23.45/
      DATA FACTOR,XLSM/0.017453277,75./
      AST = XLST +(ET(MONTH) + 4.*(XLSM-XLONG))/60.
      H   = 0.25 * (AST-12.)*60.* FACTOR
      IF (AST .LE. 12.) H = 0.25 * (12.-AST) * 60. * FACTOR
      D   = DECLIH(MONTH) * FACTOR
      BETA=ASIN(COS(XLAT*FACTOR)*COS(H)*COS(D)+
     +     SIN(XLAT*FACTOR)*SIN(D))
      AZANGL = ASIN(COS(D) * SIN(H)/COS(BETA))
      RETURN
      END
```

```
$STORAGE 2
$NOFLOATCALLS
      SUBROUTINE SOLUTION
$INCLUDE: 'COMMON.OAT'
      DIMENSION A(3,3),W(3,3),RHC1(3,3),RVC2(3,3),ARV(3,3),AVPO(3,1),
     +ARN(3,1),TSC1(3,1),TSC2(3,1),RVVPO(3,1),RVTSC2(3,1)
      N      = 3
      C1     = DAIR*CP
      C2     = C1*DELTA/GAMMA
      C3     = C1/GAMMA
      RN3    = RN(3,1)
      CALL GAUSSJ(RN,W,N,N,IERROR)
      IF (IERROR .LT. 0) GO TO 100
      KK   = 1
      GO TO 1600
  100 CONTINUE
      CALL GAUSSJ(RV,W,N,N,IERROR)
      IF (IERROR .LT. 0) GO TO 200
      KK   = 2
      GO TO 1600
  200       DO 300 I = 1,N
                DO 300 J = 1,N
                RHC1(I,J) = RN(I,J) * C1
                RVC2(I,J) = RV(I,J) * C2
  300           A(I,J) = RHC1(I,J) + RVC2(I,J)
      CALL GAUSSJ(A,W,N,N,IERROR)
      IF (IERROR .LT. 0) GO TO 400
      KK   = 3
      GO TO 1600
  400 CALL MATPRO(RV,0,RVVPO,N,N,1)
          DO 500 I = 1,N
          RVVPO(I,1) =  RVVPO(I,1)*C3
  500     CONTINUE
      CALL MATPRO(A,RVVPO,AVPO,N,N,1)
      GO TO (600,900),KEY
  600 SUM  = 0
          DO 700 J = 1,2
          SUM  = SUM + A(N,J) * RN(J,1)
  700     CONTINUE
      RN(N,1) = ( TS(N,1) - ( SUM ) + AVPO(N,1) ) / A(N,N)
      CALL MATPRO(A,RN,ARN,N,N,1)
          DO 800 IJ = 1,N
          TS(IJ,1) = ARN(IJ,1)-AVPO(IJ,1) + TA(NHOUR)
  800     CONTINUE
      GO TO 1300
  900 ITER = 0
 1000 RN(3,1) = RN3 - G
      CALL MATPRO(A,RN,ARN,N,N,1)
          DO 1100 Id = 1,N
 1100     TS(IJ,1)  = ARN(IJ,I)-AVPO(IJ,1)+TA(NHOUR)
      COND = TABEL(THCOND,THETA,SH(1),3)
      TSURF = TEMP(1) + DLAYR(1)*0.5*G/COND
      ERROR = ABS(TS(3,1)-TSURF)
      ITER = ITER + 1
```

```
      IF (ERROR .LE. ERRBND) GO TO 1200
      DENOM1 = DLAYR(1)*0.5/COND
      RV3    = RS(3) + R + RS(3)
      RB3    = RB(3) + R
      DENOM2 = (-GAMMA/C1)*RB3*RV3/(GAMMA*RV3+DELTA*RB3)
      DENOM = DENOM1 - DENOM2
      DELG  = (TS(3,1)-TSURF)/DENOM
      G     = G + DELG
      GO TO 1000
 1200 TSURF = TS(3,1)
      RN(3,1) = RN3
 1300 CONTINUE
           DO 1400 I = 1,N
           TSC1(I,1) =  (ARN(I,1) - AVPD(I,1))  * C1
           TSC2(I,1) =  (ARN(I,1) - AVPD(I,1))  * C2
 1400      CONTINUE
      CALL MATPRD(RH,TSC1,S,N,N,1)
      CALL MATPRD(RV,TSC2,RVTSC2,N,N,1)
      CALL MATADD(RVTSC2,RVVPD,V,N,1)
      SUMH = 0
      SUMV = 0
           DO 1500 I = 1,N
           SUMH = SUMH + S(I,1)
           SUMV = SUMV + V(I,1)
 1500      CONTINUE
      EC = (R*SUMV/C3) + VPDF(IO(NHOUR))
      TC = (R*SUMH/C1) + TA(NHOUR)
      IF (KEY .EQ. 2) GO TO 1700
      G = RN3 - RN(3,1)
      RN(3,1) = RN3
      GO TO 1700
 1600 WRITE (*,*) 'ERROR CODE ', KK
      STOP
 1700 CONTINUE
      RETURN
      END
```

```
$STORAGE 2
%NOFLOATCALLS
      FUNCTION TABEL(VAL,ARG,DUMMY,K)
      DIMENSION VAL(K),ARG(K)
            DO 100  J = 2,K
            IF (DUMMY .GT. ARG(J)) GO TO 100
            GO TO 200
  100       CONTINUE
      J = K
  200 TABEL = (DUMMY-ARG(J-1))*(VAL(J)-VAL(J-1))/(ARG(J)-
     +        ARG(J-1))+VAL(J-1)
      END
```

```
$STORAGE 2
$NOFLOATCALLS
      FUNCTION VPDF(T)
      IMPLICIT REAL*4(A-H,O-Z)
      VPDF = 2.7489 * 1.E8 * EXP(-4274.6/(T + 242.79))
      RETURN
      END
```

```
$STORAGE=2
$NOFLOATCALLS
      SUBROUTINE 4THR
$INCLUDE: 'COMMON.DAT'
      REAL LHV
      TOTAL  = 0.
      RNLAST = 0.
      I      = 1
  100 READ (7,200,END = 400) NYR,JULIAN,TIME(I),PPFD(I),RNO(I),
     +      TA(I),TO(I),TSS(I),U(I)
  200 FORMAT(I3,1X,I3,1X,7(F8.2,1X))
      IF (TIME(I) .LT. 0) GO TO 400
      IF (I       .GT. 1) GO TO 300
      TLAST  = TIME(I)
      NMONTH = MONTH(JULIAN,NYR)
C
C J/m2-sec to cm H2O
C
  300 LHV    = 2500.8 - 2.345*TA(I)
      TSTP   = TIME(I)-TLAST
      TOTAL  = TOTAL +(RNO(I)+RNLAST)*0.5*(TIME(I)-TLAST)*3.600/LHV
      RNLAST = RNO(I)
      TLAST  = TIME(I)
      I      = I + 1
      GO TO 100
  400 CONTINUE
      NDATAP = I - 1
      REWIND 7
      RETURN
      END
C
      FUNCTION MONTH(JULIAN,NYR)
      DIMENSION MON(12)
      DATA MON/31,29,31,30,31,30,31,31,30,31,30,31/
      MON(2) = 28
      IF ((NYR/4)*4 .EQ. NYR) MON(2) = 29
      NSUM = 0
           DO 100 J = 1,12
           IF (JULIAN-NSUM .LE. MON(J)) GO TO 200
  100      NSUM = NSUM+MON(J)
  200 MONTH = J
      RETURN
      END
```

```
C
C
C*********************************************************************
C     COMMON BLOCK
C*********************************************************************
C
      IMPLICIT REAL (L)
      COMMON/WETH/TIME(50),PPFD(50),RNO(50),TA(50),TD(50),
     2       TSS(50), U(50),TOTAL,JULIAN,NYR,NMONTH,NOATAP
      COMMON/SOL/NHOUR,R,RH(3,3),RV(3,3),RN(3,1),G,TS(3,1),D(3,1),
     2       DAIR,CP,GAMMA,DELTA,RB(3),RS(3),S(3,1),V(3,1),EC,TC,
     3       SUMH,SUMV,TSURF
      COMMON/STMP/TSTEP,THCOND(3),THETA(3),HCAP(3),TEMP(20),VHCAP(20)
      COMMON/IRR/SAT(20),OUL(20),LL(20),DLAYR(20),SW(20)
      COMMON/INI/DG,ETSIM,ETSC,ETSS,SHSC,SHSS,SHSIM,TACMN,TS3MN,
     2       TACMX,TS3MX
      COMMON/FIXI/DAPL,DRYDAY,FREQHC,CHIGHT,LAIMAX,UAVG,RA,ERRBND,
     2       RMAX,RNAMIN,XLAT,XLONG,KEY,EXTINC,FRACTN,CMAX,SLOPE,
     3       NR7,NELAYR,NTLAYR,CEM,CEC,FTEZ,LOAILY,LHOUR
      COMMON/MISC/TSESN,ESESN,CE,RNTOT,TLAST,LHV,DAY,LAI,RNA,ETSIML
     2       SHSIML,ETSCL,ETSSL,SHSCL,SHSSL,GL,HES,HEC
```

APPENDIX D
LISTING OF INPUT/OUTPUT FILES

FILE INPUT.DAT - contains fixed inputs needed by the model

```
001 01 00 +1 -1 001 0.5 03.50 01.5 10. 0.02 1.E10 02.00 29.4 02.2 2
0.50 0.05 0.0180 -38.14E-6 119                    EXPNT,FRACTN,CMAX,SLOPE,NR7
3 8 18.5 15 0.30                                  NELAYR,NTLAYR,CEM,CEC,FTEZ
0.1 0.1 0.1 0.3 0.3 0.4 0.4 0.4                   (DLAYR(I),I=1,NTLAYR)
22.5 22.5 22.5 22.5 22.5 22.5 22.5 22.5           (TEMP(I) ,I=1,NTLAYR)
0.10 0.10 0.10 0.10 0.10 0.10 0.10 0.10           (SW(I)   ,I=1,NTLAYR)
0.25 0.25 0.25 0.25 0.25 0.25 0.25 0.25           (SAT(I)  ,I=1,NTLAYR)
0.10 0.10 0.10 0.10 0.10 0.10 0.10 0.10           (OUL(I)  ,I=1,NTLAYR)
0.05 0.05 0.05 0.05 0.05 0.05 0.05 0.05           (LL (I)  ,I=1,NTLAYR)
0.574 04.522 04.522                               (THCOND(I),I=1,3)
01.126E6 02.663E6 02.663E6                        (  HCAP(I),I=1,3)
00 0.13 0.30                                      ( THETA(I),I=1,3)
```

FILE= WEATHER.DAT contains weather data for a day. This data was used to create output file OUTPUT2.DAT.

86 180	1.00	0.00	-50.72	17.00	15.00	17.50	1.50
86 180	1.50	0.00	-48.19	17.00	15.00	17.50	1.50
86 180	2.00	0.00	-45.65	17.00	15.00	17.50	1.50
86 180	2.50	0.00	-45.65	16.90	15.00	17.50	1.50
86 180	3.00	0.00	-45.66	16.80	15.00	17.50	1.50
86 180	3.50	0.00	-43.14	16.25	15.00	17.25	1.50
86 180	4.00	0.00	-40.63	15.70	15.00	17.00	1.50
86 180	4.50	0.00	-33.01	15.60	15.00	16.75	1.50
86 180	5.00	0.00	-25.40	15.50	15.00	16.50	1.50
86 180	5.50	0.00	-17.78	15.25	15.00	16.45	1.50
86 180	6.00	0.00	-10.16	15.00	15.00	16.40	1.50
86 180	6.50	57.25	20.30	16.50	17.00	16.70	1.50
86 180	7.00	114.50	50.67	18.00	19.00	17.00	1.50
86 180	7.50	206.10	91.10	19.25	19.00	17.75	1.50
86 180	8.00	297.70	131.44	20.50	19.00	18.50	1.50
86 180	8.50	463.72	204.45	22.00	19.00	19.25	1.50
86 180	9.00	629.75	277.24	23.50	19.00	20.00	1.50
86 180	9.50	727.07	319.75	24.50	19.00	20.80	1.50
86 180	10 00	824.40	362.24	25.50	19.00	21.60	1.50
86 180	10.50	916.00	402.20	26.26	19.00	22.30	1.50
86 180	11.00	1007.60	442.10	27.00	19.00	23.00	1.50
86 180	11.50	1030.50	451.93	27.50	19.00	24.00	1.50
86 180	12.00	1053.40	461.75	28.00	19.00	25.00	1.50
86 180	12.50	1053.40	461.64	28.25	19.00	25.10	1.50
86 180	13.00	1053.40	461.53	28.50	19.00	25.20	1.50
86 180	13.50	984.70	431.53	28.25	19.00	25.72	1.50
86 180	14.00	916.00	401.52	28.00	19.00	26.25	1.50
86 180	14.50	801.50	351.30	28.10	19.00	25.63	1.50
86 180	15.00	687.00	301.08	28.20	19.00	25.00	1.50
86 180	15.50	515.25	226.00	27.35	19.00	24.25	1.50
86 130	16.00	343.50	150.79	26.50	19.00	23.50	1.50
86 180	16.50	200.38	88.04	25.50	19.00	23.25	1.50
86 180	17.00	57.25	25.18	24.50	19.00	23.00	1.50
86 180	17.50	28.63	-12.60	23.75	19.00	22.40	1.50
86 180	18.00	0.00	-50.43	23.00	19.00	21.80	1.50
86 180	18.50	0.00	-50.50	21.50	19.00	21.40	1.50
86 180	19.00	0.00	-50.58	20.00	19.00	21.00	1.50
86 180	19.50	0.00	-46.53	19.75	19.00	20.75	1.50
86 180	20.00	0.00	-40.48	19.50	19.00	20.50	1.50
86 180	20.50	0.00	-40.49	19.25	19.00	20.15	1.50
86 180	21.00	0.00	-40.50	19.00	19.00	19.80	1.50
86 180	21.50	0.00	-40.48	19.15	19.00	19.70	1.50
86 180	22.00	0.00	-40.49	19.30	19.00	19.60	1.50
86 180	22.50	0.00	-35.42	19.55	19.00	19.60	1.50
86 180	23.00	0.00	-30.35	19.80	19.00	19.60	1.50
86 180	23.50	0.00	-30.36	19.40	19.00	19.60	1.50
86 180	24.00	0.00	-30.38	19.00	19.00	19.60	1.50
86 180	-1.00	0.00	-30.38	19.00	19.00	19.60	1.50

FILE OUTPUT2.DAT

DAY	LAI	ETSIM	ETSC	ETSS	ETSESN	TSESN	ESESN	TCTA	TS3MX	TS3MN
1.	.0	4.181	.000	4.181	4.2	.0	4.2	.2	30.4	17.9
2.	.0	4.021	.000	4.021	8.2	.0	8.2	.2	30.4	17.6
3.	.0	4.040	.000	4.040	12.2	.0	12.2	.2	30.4	17.7
4.	.0	4.049	.000	4.049	16.3	.0	16.3	.2	30.4	17.7
5.	.0	4.056	.000	4.056	20.3	.0	20.3	.2	30.4	17.7
6.	.0	4.061	.000	4.061	24.4	.0	24.4	.2	30.4	17.7
7.	.0	4.064	.000	4.064	28.5	.0	28.5	.2	30.4	17.7
8.	.0	4.068	.000	4.068	32.5	.0	32.5	.2	30.4	17.7
9.	.0	4.063	.099	3.964	36.6	.1	36.5	.3	30.4	17.7
10.	.1	4.066	.123	3.943	40.7	.2	40.4	.3	30.4	17.7
11.	.1	4.067	.147	3.920	44.7	.4	44.4	.3	30.4	17.7
12.	.1	4.068	.172	3.896	48.8	.5	48.3	.3	30.4	17.8
13.	.1	4.067	.219	3.848	52.9	.8	52.1	.3	30.4	17.8
14.	.1	4.067	.266	3.801	56.9	1.0	55.9	.3	30.4	17.8
15.	.1	4.066	.312	3.754	61.0	1.3	59.7	.3	30.4	17.8
16.	.2	4.064	.381	3.684	65.1	1.7	63.3	.3	30.4	17.9
17.	.2	4.061	.470	3.592	69.1	2.2	66.9	.3	30.3	17.9
18.	.2	4.060	.556	3.503	73.2	2.7	70.4	.3	30.3	17.9
19.	.3	4.058	.641	3.417	77.2	3.4	73.9	.3	30.2	18.0
20.	.3	4.056	.723	3.333	81.3	4.1	77.2	.4	30.2	18.0
21.	.4	4.052	.842	3.210	85.4	4.9	80.4	.4	30.1	18.1
22.	.4	4.051	.938	3.113	89.4	5.9	83.5	.4	30.1	18.1
23.	.5	4.048	1.067	2.981	93.5	7.0	86.5	.4	30.0	18.2
24.	.6	4.047	1.208	2.839	97.5	8.2	89.3	.4	29.9	18.2
25.	.7	4.047	1.341	2.705	101.5	9.5	92.0	.5	29.8	18.3
26.	.7	4.046	1.468	2.578	105.6	11.0	94.6	.5	29.7	18.3
27.	.8	4.047	1.575	2.472	109.6	12.5	97.1	.5	29.6	18.4
28.	.9	4.047	1.676	2.371	113.7	14.2	99.5	.5	29.5	18.4
29.	1.0	4.048	1.787	2.261	117.7	16.0	101.7	.6	29.3	18.5
30.	1.0	4.049	1.867	2.182	121.8	17.9	103.9	.6	29.2	18.5
31.	1.1	4.050	1.956	2.094	125.8	19.8	106.0	.6	29.1	18.6
32.	1.2	4.052	2.078	1.974	129.9	21.9	108.0	.7	28.9	18.6
33.	1.3	4.055	2.181	1.874	133.9	24.1	109.9	.7	28.8	18.7
34.	1.3	4.057	2.247	1.810	138.0	26.3	111.7	.7	28.7	18.7
35.	1.4	4.059	2.332	1.727	142.1	28.7	113.4	.7	28.5	18.8
36.	1.5	4.063	2.442	1.621	146.1	31.1	115.0	.8	28.3	18.8
37.	1.6	4.067	2.537	1.531	150.2	33.7	116.5	.8	28.2	18.9
38.	1.8	4.073	2.643	1.430	154.3	36.3	118.0	.9	27.9	18.9
39.	1.9	4.079	2.759	1.321	158.3	39.1	119.3	.9	27.7	19.0
40.	2.0	4.086	2.866	1.220	162.4	41.9	120.5	1.0	27.4	19.1
41.	2.2	4.094	2.973	1.121	166.5	44.9	121.6	1.0	27.2	19.1
42.	2.3	4.101	3.071	1.030	170.6	48.0	122.7	1.1	26.9	19.2
43.	2.5	4.109	3.168	.941	174.7	51.1	123.6	1.2	26.6	19.2
44.	2.7	4.117	3.258	.860	178.8	54.4	124.5	1.2	26.3	19.3
45.	2.8	4.125	3.341	.784	183.0	57.7	125.2	1.3	26.1	19.3
46.	3.0	4.133	3.422	.711	187.1	61.2	126.0	1.3	25.8	19.3
47.	3.1	4.142	3.493	.649	191.3	64.6	126.6	1.4	25.5	19.3
48.	3.3	4.152	3.567	.585	195.4	68.2	127.2	1.5	25.3	19.4
49.	3.5	4.160	3.628	.532	199.6	71.8	127.7	1.5	25.0	19.4
50.	3.7	4.186	3.693	.493	203.7	75.5	128.2	1.6	24.8	19.4
51.	3.8	4.206	3.753	.453	208.0	79.3	128.7	1.6	24.5	19.3

DAY	LAI	ETSIM	ETSC	ETSS	ETSESN	TSESN	ESESN	TCTA	TS3MX	TS3MN
52.	4.0	4.225	3.806	.419	212.2	83.1	129.1	1.6	24.3	19.3
53.	4.2	4.243	3.857	.386	215.4	86.9	129.5	1.6	24.1	19.2
54.	4.3	4.261	3.902	.359	220.7	90.9	129.8	1.6	23.9	19.2
55.	4.5	4.277	3.942	.335	225.0	94.8	130.2	1.7	23.7	19.1
56.	4.6	4.292	3.982	.320	229.2	98.8	130.5	1.7	23.7	19.1
57.	4.7	4.290	3.983	.307	233.5	102.7	130.8	1.7	23.6	19.1
58.	4.8	4.305	4.012	.293	237.8	106.7	131.1	1.7	23.5	19.0
59.	4.9	4.323	4.043	.280	242.2	110.8	131.4	1.7	23.4	19.0
60.	5.0	4.344	4.073	.271	245.5	114.9	131.6	1.7	23.4	19.0
61.	5.2	4.376	4.108	.267	250.9	119.0	131.9	1.7	23.4	19.0
62.	5.3	4.406	4.140	.265	255.3	123.1	132.2	1.7	23.4	19.0
63.	5.5	4.429	4.165	.264	259.7	127.3	132.4	1.8	23.4	19.0
64.	5.5	4.428	4.165	.263	264.1	131.4	132.7	1.8	23.4	19.0
65.	5.5	4.440	4.180	.261	268.6	135.6	133.0	1.8	23.4	19.0
66.	5.6	4.445	4.186	.259	273.0	139.8	133.2	1.8	23.4	19.0
67	5.6	4.441	4.183	.258	277.5	144.0	133.5	1.8	23.4	19.0
68.	5.5	4.435	4.179	.256	281.9	148.2	133.7	1.8	23.4	19.0
69.	5.5	4.429	4.175	.254	286.3	152.3	134.0	1.8	23.4	19.0
70.	5.5	4.424	4.173	.251	290.8	156.5	134.2	1.8	23.4	18.9
71.	5.5	4.418	4.169	.249	295.2	160.7	134.5	1.8	23.4	18.9
72.	5.5	4.415	4.167	.248	299.6	164.9	134.7	1.8	23.4	18.9
73.	5.5	4.411	4.165	.246	304.0	169.0	135.0	1.8	23.4	18.9
74.	5.5	4.409	4.165	.245	308.4	173.2	135.2	1.8	23.4	18.9
75.	5.4	4.405	4.163	.243	312.8	177.3	135.5	1.8	23.4	18.9
76.	5.4	4.402	4.160	.241	317.2	181.5	135.7	1.8	23.4	18.9
77.	5.4	4.400	4.160	.240	321.6	185.7	135.9	1.8	23.3	18.9
78.	5.4	4.399	4.160	.238	326.0	189.8	136.2	1.8	23.3	18.9
79.	5.4	4 395	4.158	.237	330.4	194.0	136 4	1.7	23.3	18.9
80.	5.4	4.394	4.158	.236	334.8	198.1	136.7	1.7	23.3	18.9
81.	5.4	4.393	4.158	.235	339.2	202.3	136.9	1.7	23.3	18.9
82.	5.4	4 392	4.158	.234	343.6	206.5	137.1	1.7	23.3	18.9
83.	5.4	4.391	4.158	.233	348.0	210.6	137.4	1.7	23.3	18.9
84.	5.4	4.390	4.158	.232	352.4	214.8	137.6	1.7	23.3	18.9
85.	5.4	4.389	4.158	.231	356.8	218.9	137.8	1.7	23.3	18.9
86.	5.4	4.388	4.158	.230	361.1	223.1	138.1	1.7	23.3	18.9
87.	5.4	4.387	4.158	.229	365.5	227.3	138.3	1.7	23.3	18.9
88.	5.4	4.387	4.158	.229	369.9	231.4	138.5	1.7	23.3	18.9
89.	5.4	4.386	4.158	.228	374.3	235.6	138.7	1.7	23.3	18.9
90.	5.4	4.385	4.158	.227	378.7	239.7	139.0	1.7	23.3	18.9
91.	5.4	4.370	4.143	.227	383.1	243.9	139.2	1.7	23.3	18.8
92.	5.3	4.354	4.128	.225	387.4	248.0	139.4	1.7	23.3	18.8
93.	5.2	4.335	4.111	.224	391.8	252.1	139.6	1.7	23.3	18.8
94.	5.1	4.318	4.096	.222	396.1	256.2	139.9	1.7	23.2	18.8
95.	5.1	4.300	4.080	.220	400.4	260.3	140.1	1.7	23.2	18.8
96.	5.0	4.285	4.066	.219	404.7	264.4	140.3	1.7	23.2	18.8
97.	4.9	4.270	4.050	.220	408.9	268.4	140.5	1.7	23.2	18.8
98.	4.9	4.255	4.034	.222	413.2	272.4	140.7	1.7	23.2	18.8
99.	4.8	4.242	4.017	.225	417.4	276.5	141.0	1.7	23.2	18.8
100.	4.7	4.230	4.002	.228	421.7	280.5	141.2	1.7	23.2	18.8
101.	4.7	4.218	3.985	.233	425.9	284.4	141.4	1.7	23.3	18.8
102.	4.6	4.208	3.970	.238	430.1	288.4	141.7	1.6	23.3	18.8
103.	4.5	4.196	3.952	.244	434.3	292.4	141.9	1.6	23.4	18.8
104.	4.5	4.185	3.936	.249	438.5	296.3	142.2	1.6	23.4	18.8

DAY	LAI	ETSIM	ETSC	ETSS	ETSESN	TSESN	ESESN	TCTA	TS3MX	TS3MN
105.	4.4	4.176	3.920	.256	442.6	300.2	142.4	1.6	23.5	18.8
106.	4.4	4.167	3.904	.263	446.8	304.1	142.7	1.6	23.6	18.8
107.	4.3	4.156	3.885	.271	451.0	308.0	143.0	1.6	23.6	18.8
108.	4.2	4.147	3.868	.279	455.1	311.9	143.2	1.6	23.7	18.8
109.	4.2	4.138	3.851	.288	459.2	315.7	143.5	1.6	23.7	18.8
110.	4.1	4.129	3.830	.298	463.4	319.6	143.8	1.6	23.8	18.8
111.	4.0	4.121	3.812	.308	467.5	323.4	144.1	1.6	23.9	18.9
112.	4.0	4.113	3.794	.319	471.6	327.2	144.4	1.6	24.0	18.9
113.	3.9	4.105	3.775	.329	475.7	330.9	144.8	1.5	24.0	18.9
114.	3.9	4.096	3.756	.340	479.8	334.7	145.1	1.5	24.1	18.9
115.	3.8	4.089	3.737	.352	483.5	338.4	145.5	1.5	24.2	18.9
116.	3.8	4.088	3.730	.359	488.0	342.2	145.8	1.5	24.2	18.9
117.	3.7	4.080	3.710	.370	492.1	345.9	146.2	1.5	24.3	18.9
118.	3.7	4.074	3.693	.382	496.1	349.6	146.6	1.5	24.4	18.9
119.	3.6	4.118	3.674	.444	500.3	353.2	147.0	1.5	24.7	19.1
120.	2.9	4.038	3.381	.657	504.3	356.6	147.7	1.3	26.1	18.8
121.	2.3	3.943	3.051	.893	508.2	359.7	148.6	1.2	27.5	18.6
122.	1.8	3.840	2.724	1.117	512.1	362.4	149.7	1.0	29.0	18.6
123.	1.4	3.673	2.410	1.262	516.8	364.8	151.0	.9	30.8	18.7
124.	1.1	3.430	2.149	1.281	519.2	367.0	152.2	.9	32.6	18.8
125.	.9	3.162	1.934	1.228	522.3	368.9	153.5	.9	34.5	19.3
126.	.7	2.859	1.735	1.125	525.2	370.6	154.6	1.0	36.3	19.7
127.	.6	2.541	1.553	.988	527.7	372.2	155.6	1.1	37.9	20.1
128.	.5	2.235	1.367	.868	530.0	373.5	156.4	1.3	39.4	20.4
129.	.4	2.038	1.195	.844	532.0	374.7	157.3	1.5	40.5	20.7
130.	.3	1.868	1.009	.858	533.9	375.7	158.1	1.7	41.2	20.9
131.	.2	1.713	.884	.829	535.6	376.5	159.0	1.8	41.9	21.1
132.	.2	1.547	.743	.804	537.2	377.4	159.8	2.0	42.6	21.2
133.	.2	1.397	.617	.779	538.5	378.0	160.6	2.2	43.1	21.4
134.	.1	1.269	.515	.754	539.8	378.5	161.3	2.3	43.6	21.6

REFERENCES

Al-Khafaf, S., P. J. Wiarenga, and R. C. Williams. 1978. Evaporative flux from irrigated cotton as related to leaf area index, soil water, and evaporative demand. Agron. J. 70 912-917.

Allen, L. H., Jr. 1979. Potentials for carbon dioxide enrichment. In "Modification of the Aerial Environment of Crops", Ed. by B. J. Barfield and J. F. Gerber, ASAE Monogr. 2, American Society of Agricultural Engineers, St. Joseph, MI.

Baldocchi, D. D., S. B. Verma, N. J. Rosenberg, B. L. Blad, A. Garay, and J. E. Specht. 1983. Influence of water stress and diurnal exchange of mass and energy between the atmosphere and a soybean canopy. Agron. J. 75 643-648.

Black, T. A., W. R. Gardner, and G. W. Thurtell. 1969. The prediction of evaporation, drainage and soil water storage for a bare soil. Soi. Sci. Soc. Amer. Proc. 33 655-660.

Black, T. A., C. B. Tanner, and W. R. Gardner. 1970. Evapotranspiration from a snap bean crop. Agron. J. 62 66-69.

Blad, B. L. 1982. Atmospheric demand for water. In "Crop Water Relations", Ed. by I. D. Teare and M. M. Peet. John Wiley and sons, New York, NY.

Blomm, Th. J. M., and S. R. Troelstra. 1972. A simulation model of the combined transport of water and heat produced by a thermal gradient in porous media. Report no. 6. Dept. of Theoretical Production Ecology, Agricultural University, Wageningen, The Netherlands.

Burman, R. D., P. R. Nixon, J. L. Wright, and W. O. Pruitt. 1981. Water requirements. In "Design and Operation of Farm Irrigation Systems", Ed. by M. E. Janson. ASAE Monograph No. 3, St. Joseph, MI.

Cary, J. W. 1965. Water flux in moist soil Thermal versus suction gradients. Soil Sci. 100 168-175.

Cary, J. W., and S. A. Taylor. 1962. The influence of simultaneous diffusivity of heat and water vapor. Soil Sci. Soc. Amer. Proc. 26 413-416.

Chan, J. 1984. Uncoupled multi-layer model for the transfer of sensible and latent heat flux densities from vegetation. Boundary Layer Meteorol., 28 213-225.

Clark, G. A. 1982a. Simulation of the sensitivity of water movement and storage in sandy soils to irrigation application rate and

depth. ME thesis, university of Florida, Gainesville, FL.

Clark, W. C. 1982b. Carbon Dioxide Review. Oxford University Press, New York.

Conaway, J., and C. H. M. van Bavel. 1967. Evaporation from a wet soil surface calculated from radiometrically determined surface temperatures. J. Appl. Meteorol. 6 650-655.

Covey, W., and M. E. Bloodworth. 1966. Evaporativity and the second stage of drying of soil. J. Appl. Meteorol. 5 364-365.

Denmead, O. T. 1976. Temperate Cereals. In "Vegetation and the atmosphere", Ed. by J. L. Monteith, volume 2, pp. 1-30, Academic Press, New York, NY.

Denmead, O. T., and R. H. Shaw. 1962. The effect of soil moisture stress at different stages of growth on the development and yield of corn. Agron. J. 54 385-390.

De Wit, C. T., and H. Van Keulen. 1972. Simulation of transport processes in soil. Center for agricultural publishing and documentation, Wageningen, The Netherlands.

Doorenbos, J., and A. H. Kassam. 1979. Yield Response to Water. FAO Irrigation and drainage paper No. 33 Rome, Italy.

Doorenbos, J., and W. O. Pruitt. 1977. Guidelines for Predicting Crop Water Requirements. FAO Irrigation and drainage paper No. 24, Rome, Italy.

Ehrler, W. L. 1973. Cotton leaf temperatures as related to soil water depletion and meteorological factors. Agron. J. 65 404-409.

FAO. 1979. The on-farm use of water. Com. on Agr., 8th session, 22p.

Fritton, D. D., D. Kirkham, and R. H. Shaw. 1970. Soil water evaporation, isothermal diffusion, and heat and water transfer. Soil Sci. Soc. Am. J. 42 32-39.

Gardner, H. R., and W. R. Gardner. 1969. Relation of water application to evaporation and storage of soil water. Soil Sci. Soc. Amer. Proc. 33 192-196.

Gardner, W. R. 1959. Solution of the flow equation for the drying of soil and other porous media. Soil Sci. Soc. Amer. Proc. 23 183-187.

Gardner, H. R., and R. J. Hanks. 1966. Evaluation of the evaporation zone in soil by measurement of heat flux. Soil Sci. Soc. Amer. Proc. 30 425-428.

Gardner, W. R., and D. Hillel. 1962. The relation of external evaporative conditions to the drying of soils. J. Geophys.

Res. 67 4313-4325.

Gifford, R. M. 1979. Growth and yield of Co2-enriched wheat under water-limited conditions. Aust. J. Plant Physiol. 6 367-78.

Goudriaan, J. 1977. Crop micrometeorology A simulation study. Center for agricultural publishing and documentation. Wageningen, The Netherlands.

Grover, C. C. 1972. A mathematical simulation of water movement in unsaturated soil during drying. Ph. D. thesis. Dept. of Biological and Agricultural Engineering, North Carolina State University, Raleigh, NC.

Hanks, R. J. 1985. Crop coefficients for transpiration. In "Advances in Evapotranspiration", Proceedings of the National Conference on Advances in Evapotranspiration. ASAE, St. Joseph, MI.

Hanks, R. J. and H. R. Gardner. 1965. Influence of different diffusivity-water content relations on evaporation of water from soils. Soil Sci. Soc. Am. Proc. 29 495-498.

Hanks, R. J. and R. W. Hill. 1980. Modeling Crop Responses to Irrigation in Relation to Soils, Climate and salinity. International Irrigation Information Center Pub. No. 6. Pergamon Press Inc., New York, NY.

Hillel, D., 1975. Simulation of evaporation from bare soil under steady and diurnal fluctuating evaporativity. Soil Sci. 120 230-237

Hillel, D , 1980. Application of Soil Physics. Academic Press, New York, NY.

Jackson, R. D., R. A. Campbell, R. J. Reginato, and F. S. Nakayama. 1973. Diurnal soil water evaporation; Time-depth flux pattern. Soil Sci. Soc. Amer. Proc. 37 505-509.

Jackson, R. D. 1982. Canopy temperatures and crop water stress. In "Advances in Irrigation", Ed. by D. Hillel. Academic Press, New York, NY.

Jagtap, S. S., J. W.Jones, R. Zur, and J. M.Bennett. 1983. A quasi steady state model of transpiration and crop water status. ASAE paper no.83-2095. ASAE, St. Joseph, MI.

Jansen, M. E., D. C. N. Robb, and C. E. Franzoy. 1970. Scheduling irrigation using climate-soil data. J Irrig. and Drain. Div., Am. Soc. Civil Engr. 96 25-38.

Jones, J. W. and A. G. Smajstrla. 1980. Application of modeling to irrigation management of soybeans. Proceedings of the World Soybean Research Conference - II. Raleigh, North Carolina.

Jones, J. W., L. H. Allen, Jr., S. F. Shih, J. S. Rogers, L. C. Hammond, A. G. Smajstrla, and J. D. Martsolf. 1984a. Estimated and Measured Evapotranspiration for Florida Climate, Crops, and soils. Technical Bulletin 840. Agricultural Experiment Stations, Institute of Food and Agricultural Sciences, University of Florida, Gainesville.

Jones, P., J. W. Jones, L. H. Allen, Jr. and J. W. Hilshoe. 1984b. Dynamic computer control of closed environmental plant growth chambers. Trans. ASAE 27:879-883.

Jones, P., L. H. Allen, Jr., J. W. Jones. 1985a. Response of soybean canopy photosynthesis and transpiration to whole day temperature changes in different CO2 environments. Agron. J. 77:242-249.

Jones, P., J. W. Jones, L. H. Allen, Jr. 1985b. Seasonal Carbon and Water balances of soybeans grown under stress treatments in sunlit chambers. Transactions of ASAE, 28:2021-2028.

Kanemasu, E. T., L. R., Stone, and H. L. Powers, 1976. Evapotranspiration model tested for soybean and sorghum. Agron. J. 68:569-572.

Kijne, J. H., 1975. Evaporation from bare soils. In "Physical aspects of soil water and salts in ecosystem", Ed. by A. Hadas, D. Swartzendruber, P. E. Rijtema, M. Fuchs and B. Yaron. Springer-Verlag, New York, NY.

Kimball, B. A. and S. B. Idso. 1983. Increasing atmospheric CO2 effects on crop yield, water use and climate. In "Plant Production and Management Under Drought Conditions", Ed. by J. F. Stone and H. D. Willis, Elsevier Science Publisher, B. V, New York, NY.

Kramer, P. J. 1981. Carbon dioxide concentrations, photosynthesis, and dry matter production. Bioscience 31:29-33.

Lemon, E. R., 1956. The potential for decreasing soil moisture evaporation loss. Soil Sci. Soc. Amer. Proc. 20:120-125.

Lemon, E. R. 1965. Microclimatology and the physiology of plants F. C. Steward. Volum 4A:203-209

Lemon, E. R. 1966. Plant factors and transpiration - The plant community. In "Evapotranspiration and its role in water resources management", Ed. by M. E. Jensen. ASAE St. Joseph, MI.

McGowan, M, 1973. Depth of water extraction by roots. In "Radiation techniques in soil physics and irrigation studies". IAEA, Vienna, Austria.

McNaughton, K. G. and P. G. Jarvis. 1983. Predicting effect of vegetation changes on transpiration and evaporation. In "Water Deficits and Plant Growth", Ed. by T. T. Kozlowski, volume 7, pp. 1-47. Academic Press, New York, NY.

Nerva, G., P. 1975. Physioengineering Principles. The AVI publishing company, Inc., Westport, Connecticut.

Monteith, J. M. 1963. Gas exchange in plant communities. In "Environmental Control of Plant Growth", Ed. by L. T. Evans, pp. 95-113, Academic Press, New York, NY.

Monteith, J. M. 1965. Evaporation and environment. Symp. Soc. Expl. Biol. 19:205-234.

Morison, J. L. and R. M. Gifford. 1984. Plant growth and water use with limited water supply in high CO_2 concentrations. I. Leaf area, water use and transpiration. Aust. J. Plant Physiol. 11:361-74.

Norman, J. M., and G. Campbell. 1983. Application of a plant-environment model to problems in Irrigation. In "Advances in Irrigation, Vol. 2.", Ed. by D. Hillel. Academic Press, New York, NY.

Novak, M. D., and T. A. Black. 1985. Theoretical determination of the surface energy balance and thermal regimes of bare soil. Boundary Layer Meteorol. 33: 313-333.

Pearse, J. F., T. R. Oliver, and D. M. Newitt. 1949. The mechanism of the drying of solids Part I. The forces giving rise to movement of water in granular beds during drying. Trans. Inst. Chem. Eng. (London) 27: 1-8.

Penman, H. L. 1941. Experiments on evaporation from fallow soil. J. Agri. Sci. 31:454-465.

Penman, H. L. 1948. Natural evaporation from open water, bare soil and grass. Proc. Royal Soc. London, Ser. A, 193:120-145

Phene, C. J., D. W. Meek, K. R. Davis, R. L. McCormick, and R. B. Hutmacher. 1985. Real time crop evapotranspiration and determination of crop coefficients. In "Advances in Evapotranspiration", Proceedings of the National Conference on Advances in Evapotranspiration. ASAE, St. Joseph, MI.

Philip, J. R. 1957. Evaporation, and moisture and heat fields in the soil. J. Meteorol. 14:354-366.

Philip, J. R., and D. A. De Vries. 1957. Moisture movement in porous material under temperature gradients. Amer. Geophys. Union Trans. 38:222-232.

Reddy, S. J. 1963. A simple method of estimating the soil water balance. Agric. Meteorol. 1 1-17.

Ritchie, J. T. 1972. A model for predicting evapotranspiration from a row crop with incomplete cover. Water Resour. Res. 8 1204-1213.

Ritchie, J. T. and E. Burnett, 1971. Dryland evaporative flux in subhumid climate. 2 Plant influences. Agron. J. 62 56-62.

Rosenberg, N. J. 1982. The increasing CO_2 concentration in the atmosphere and its implications on agricultural productivity, II. Effects through CO_2-induced climatic changes. Climatic Change 4 239-254.

Shawcroft, R. W., E. R. Lemon, L. H. Allen, Jr., D. W. Stewart, and S. E. Jenson. 1974. The soil plant - atmosphere model and some of its predictions. Agric. Meteorol. 14 287-307.

Shuttleworth, W. J. 1976. A one dimentional theoretical description of the vegetation - atmosphere interaction. Boundary Layer Meteorol. 10 273-302.

Shuttleworth, W. J. and J. S. Wallace. 1985. Evaporation from sparse crops. Quart. J. Royal Meteorol. Soc. 111 839-855.

Sinclair, T. R., C. E. Murphy, Jr., and K. R. Knoerr. 1976. Development and evaluation of simplified models for simulating canopy photosynthesis and transpiration J. Appl. Ecol. 13 813-826.

Smajstrla, A. G. 1982. Irrigation Management for the Conservation of Limited Water Resources. Project Completin Report. Agricultural Engineering Department. University of Florida, Gainesville, FL.

Smajstrla, A. G., G. A. Clark, S. F. Shih, F. S. Zazueta and D. S. Harrison. 1984. Characteristics of potential evapotranspiration in Florida. ASAE Paper No. FCS-84-003, St. Joseph, MI.

Stanhill, G. 1969. A simple instrument for field measurement of turbulent diffusion flux. J. Appl. Meteorol. 8 509-513.

Stewart, D. W. 1970. A simulation of net photosynthesis of field corn. Ph. D. Dissertation, Cornell University, Ithaca, New York. Dissertation abstracts number 70-17,101. University microfilms, Ann Arbor, Michigan, 132 pp.

Szeicz, G., G. Endredim and S. Tajchman. 1969. Aerodynamic and surface factors in evaporation. Water Resources Res. 5 380-394.

Tanner, C. B., and M. Fuchs. 1968. Evaporation from unsaturated surfaces A generalized combination method. J. Geotech. Res. 73 1299-1304.

Tanner, C. B. and W.A. Jury. 1976. Estimating evaporation and transpiration from a row crop during incomplete cover. Agron. J. 68 239-243.

Ting. I. P. 1982. Plant Physiology. Addison-Wesley Publishing Company, Menlo Park, CA.

Valle, R., J. W. Mishoe, W. J. Campbell, J. W. Jones, and L. H. Allen, Jr. 1985. Photosynthatic response of 'Bragg' soybean leaves adapted to different CO_2 environments. Crop Sci. 25:333-339.

Van Bavel, C. H. M., and D. Hillel, 1976. Calculating potential and actual evaporation from a bare soil surface by simulation of concurrent flow of water and heat. Agri. Meteorol. 17 453-476.

Van Keulen, H. 1975. Simulation of water use and herbage growth in arid regions. Center for agricultural Publishing and Documentation, Wageningen, The Netherlands.

Van Loon, L., and H. Wosten, 1979. A model to simulate evaporation of bare soils in arid regions. Internal Report No. 10. Dept. of Theoretical Production Ecology, Agricultural University, Wageningen, The Netherlands.

Waggoner, P. E. and W. E. Raifsnyder, 1968. Simulation of the temperature, humidity and evaporation profiles in a leaf canopy. J. Appl. Meteorol. 7 400-409.

Wallings, S. R., and J. P. Bell. 1980. Movement of water and nitrate in the unsaturated zone of chalk near Winchester. J. Hydrol. 48 119-136.

Wiegand, C. L., and S. A. Taylor. 1961. Evaporative drying of porous media: Influential factors, physical phenomena, mathematical analysis. Utah State University, Agricultural Experiment Station, Special Report 15, Logan, Utah.

Wilkerson, G. G., J. W. Jones, K. J. Boote, K. T. Ingram, and J. W. Mishoe. 1983. Modeling soybean growth for management. Transactions of ASAE. 26:63-73.

Wright, J. L. 1982. New evapotranspiration crop coefficients. J. of Irrig. and Drain. Div., Proceedings of the ASCE. 108. No. IR1 57-74.

Zur, B., J. W. Jones. 1982. A model for the water relations, photosynthesis, and expansive growth of crops. Water Resour. Res. 17:311-320.

BIOGRAPHICAL SKETCH

The author, Shrikant Shankar Jagtap, was born in Bombay, India, on November 23, 1957. He graduated from the King George English School with First Class in 1973. In June 1975, he was admitted in the five year Bachelor of Technology (B. Tech.) programm in agricultural engineering at the Indian Institute of Technology (I. I. T.), Kharagpur. He graduated at the top of his class with honors in June 1980. During his final year at I. I. T. he researched low cost technology to improve subsurface drainage.

He completed the Master of Science degree in agricultural engineering at the University of Georgia, Athens, in June 1982 with distinction. While at the University of Georgia, he developed simulation models of container nursery operations.

In June 1982, he chose to attend the Graduate school of the University of Florida in Gainesville, Florida, and became a candidate for the degree of Doctor of Philosophy in June 1984.

He has been recognized in the 'International Who's Who in Engineering" and is a member of several other organizations. He intends to continue basic and applied research in crop modeling, water management, and expert systems for technology transfer. He is married to former Miss Rekha Dadasaheb Sawant and they have one son, Sanjiv.

I certify that I have read this study and that in my opinion it conforms to acceptable standards of scholarly presentation and is fully adequate, in scope and quality, as a dissertation for the degree of Doctor of Philosophy.

James W. Jones, Chairman
Professor of Agricultural
Engineering

I certify that I have read this study and that in my opinion it conforms to acceptable standards of scholarly presentation and is fully adequate, in scope and quality, as a dissertation for the degree of Doctor of Philosophy.

Kenneth J. Boote
Professor of Agronomy

I certify that I have read this study and that in my opinion it conforms to acceptable standards of scholarly presentation and is fully adequate, in scope and quality, as a dissertation for the degree of Doctor of Philosophy.

Wayne C. Huber
Professor of Environmental
Engineering Sciences

I certify that I have read this study and that in my opinion it conforms to acceptable standards of scholarly presentation and is fully adequate, in scope and quality, as a dissertation for the degree of Doctor of Philosophy.

P. S. C. Rao
Professor of Soil Science

I certify that I have read this study and that in my opinion it conforms to acceptable standards of scholarly presentation and is fully adequate, in scope and quality, as a dissertation for the degree of Doctor of Philosophy.

Allen G. Smajstrla
Associate Professor of
Agricultural Engineering

This dissertation was submitted to the Graduate Faculty of the College of Engineering and to the Graduate School and was accepted as partial fulfillment of the requirement of the degree of Doctor of Philosophy.

December 1986

Herbert A. Beaver
Dean, College of Engineering

Dean, Graduate School